THE ROLE OF HEPATIC ARYL HYDROCARBON RECEPTOR IN METABOLIC HOMEOSTASIS AND HEPATIC CARCINOGENESIS

By

Peipei Lu

Master of Science, Xi'an Jiaotong University, 2011

Submitted to the Graduate Faculty of

School of Pharmacy in partial fulfillment

of the requirements for the degree of

Doctor of Philosophy University of Pittsburgh

University of Pittsburgh

2016

UNIVERSITY OF PITTSBURGH

School of Pharmacy

This thesis was presented

By

Peipei Lu

It was defended on

July 11, 2016

and approved by

Song Li, MD., PhD., Professor, Pharmaceutical Sciences

Thomas Kensler, PhD., Professor, Pharmacology and Chemical Biology

Regis R. Vollmer, PhD., Professor, Pharmaceutical Sciences

Xiaochao Ma,PhD., Associate Professor, Pharmaceutical Sciences

Dissertation Advisor: Wen Xie, MD., PhD., Professor, Pharmaceutical Sciences

THE ROLE OF HEPATIC ARYL HYDROCARBON RECEPTOR IN METABOLIC HOMEOSTASIS AND HEPATIC CARCINOGENESIS

Peipei Lu

University of Pittsburgh, 2016

THE ROLE OF HEPATIC ARYL HYDROCARBON RECEPTOR IN METABOLIC HOMEOSTASIS AND HEPATIC CARCINOGENESIS

Peipei Lu, PhD

University of Pittsburgh, 2016

The aryl hydrocarbon receptor (AHR), also known as the dioxin receptor, was originally characterized as a xenobiotic receptor that senses xenotoxicants. In the first part of my thesis research, I have uncovered an unexpected endobiotic and hepatic role of AHR in fatty liver and energy metabolism. Despite causing severe fatty liver, transgenic activation of AHR protected mice from diet-induced obesity and type 2 diabetes. The endocrine hormone fibroblast growth factor 21 (FGF21) was established as a novel transcriptional target of AHR and mediates the metabolic benefit of AHR. Moreover, the transactivation of FGF21 by AHR contributed to both hepatic steatosis and systemic insulin hypersensitivity, both of which were largely abolished upon FGF21 knockdown. Results from this study may help to establish AHR as a pivotal environmental modifier that integrates signals from chemical exposure in the regulation of lipid and energy metabolism.

The second part of my thesis research is to investigate the function of AHR in promoting hepatic carcinogenesis and to study the mechanisms of its tumor-promoting effect. 2,3,7,8-tetrachlorodibenzo-*p*-dioxin (TCDD), or dioxin, is a potent liver cancer promoter through sustained activation of AHR in rodents, but its carcinogenic effect in human has been controversial. This inter-species difference is largely due to different ligand affinity and distinct gene transactivation selectivity and potency. Here I report the oncogenic potential of human AHR in promoting hepatic carcinogenesis. Constitutive activation of human AHR was as

efficiently as mouse Ahr in promoting diethylnitrosamine (DEN)-initiated hepatic carcinogenesis in transgenic mice. The growth arrest and DNA damage-inducible gene 45 beta (Gadd45b), a signal molecule inducible to external stress and UV irradiation, is highly induced upon AHR activation and acts as a transcriptional target of AHR. In addition, as an intrinsic coactivator, Gadd45b facilitates the AHR transcription activity, which might play a role in potentiating the tumor promoting effect of AHR.

Taken together, my work has revealed critical functions of AHR in energy homeostasis and hepatic carcinogenesis. It is hoped that understandings of the functions of AHR may help develop AHR-based novel therapeutics in the treatment of metabolic diseases and hepatic carcinogenesis.

TABLE OF CONTENTS

PREFACE ..... **XII**

ABBREVIATIONS ..... **XIII**

1.0 CHAPTER I: INTRODUCTION **1**

1.1 ARYL HYDROCARBON RECEPTOR AS A XENOBIOTIC SENSOR **1**

1.2 MECHANISMS OF AHR ACTIVATION **3**

1.2.1 AHR Ligands **3**

1.2.2 Mechanisms of AHR Action **4**

2.0 CHAPTER II: ENDOBIOTIC FUNCTION OF AHR IN LIPID AND ENERGY METABOLISM **7**

2.1 OVERVIEW OF LIPID AND ENERGY METABOLISM **7**

2.1.1 Fatty Acid and Triglyceride Metabolism **7**

2.1.2 Glucose and Insulin Metabolism **8**

2.2 AHR IN LIPID AND ENERGY METABOLISM **9**

2.2.1 AHR in NAFLD and NASH **9**

2.2.2 AHR in Type 2 Diabetes and Insulin Resistance **11**

2.3 SPECIFIC AIMS **14**

2.4 METHODS **15**

2.5 RESULTS **20**

2.5.1 Creation and Characterization of the Constitutively Activated AHR (CA-AHR) Construct 20

2.5.2 Generation of Conditional Tetracycline Inducible Transgenic Mice Expressing CA-AHR in the Liver 22

2.5.3 Activation of AHR Exacerbated High-Fat Diet (HFD)-Induced Steatosis 28

2.5.4 AHR Transgenic Mice Were Protected from Diet-induced Obesity and Insulin Resistance 31

2.5.5 The Pleotropic Effects of AHR in Improving Metabolic Function 31

2.5.6 Activation of AHR Induced the Expression of FGF21 37

2.5.7 Knockdown of FGF21 Abolished the Metabolic Benefits of AHR 39

2.5.8 FGF21 Knockdown Ameliorated Hepatosteatosis by AHR Activation 42

2.5.9 FGF21 Knockdown Exacerbated Liver Damage in CA-AHR Mice 43

2.5.10 FGF21 is a Direct Transcriptional Target of AHR 44

2.6 DISCUSSION 46

3.0 CHAPTER III: FUNCTION OF AHR IN PROMOTING HEPATIC CARCINOGENESIS 50

3.1 THE ROLE OF AHR IN HEPATIC CARCINOGENESIS 50

3.1.1 AHR in Liver Carcinogenesis 50

3.1.2 Species Difference of AHR in Promoting Hepatic Carcinogenesis 52

3.2 SPECIFIC AIMS 54

3.3 METHODS 55

3.4 RESULTS 59

3.4.1 Activation of Human AHR Promoted DEN-initiated Liver Tumor 59

3.4.2 Activation of Human AHR Increased Inflammation and Impaired Liver Function after DEN Treatment 63

3.4.3 Growth Arrest and DNA-Damage-Inducible beta (Gadd45b) is Induced by AHR Activation 66

3.4.4 Gadd45b is An AHR Target Gene 68

3.4.5 Gadd45b Coactivates AHR-mediated Transcription 71

3.5 DISCUSSION 75

4.0 CHAPTER IV: SUMMARY AND PERSPECTIVES 79

APPENDIX A 84

BIBLIOGRAPHY 86

LIST OF TABLES

Table 1. Liver tumors in DEN-treated male and female WT, CA-Ahr, and CA-AHR mice. 60

LIST OF FIGURES

Figure 1. Mechanism of classical Aryl hydrocarbon receptor (AHR) action. 1

Figure 2. Characterization of the constitutively activated AHR (CA-AHR) construct. 21

Figure 3. Generation of transgenic mice expressing CA-AHR in the liver and intestine. ... 23

Figure 4. Characterization of the liver-specific expression of the CA-AHR. 25

Figure 5. Activation of AHR in CA-AHR mice was not associated with obvious hepatotoxicity. 26

Figure 6. CA-AHR TG mice developed spontaneous steatosis. 27

Figure 7. Activation of AHR exacerbated high-fat diet induced steatosis. 29

Figure 8. Decreased VLDL-triglyceride secretion and decreased fatty acid oxidation in TG mice..... 30

Figure 9. AHR transgenic mice were protected from diet-induced obesity. 32

Figure 10. AHR transgenic mice were protected from diet-induced insulin resistance. 33

Figure 11. The pleotropic effects of AHR in improving metabolic function. 34

Figure 12. The pleotropic effects of AHR in improving metabolic function. 35

Figure 13. The metabolic benefits of the transgene were normalized upon DOX treatment. 37

Figure 14. Activation of AHR induced the expression of FGF21. 38

Figure 15. The AHR responsive induction of FGF21 was abolished upon DOX treatment. 39

Figure 16. Knockdown of FGF21 abolished the metabolic benefits of AHR. 40

Figure 17. Knockdown of FGF21 abolished the metabolic benefits of AHR in extrahepatic tissues. 41

Figure 18. FGF21 knockdown ameliorated hepatosteatosis by AHR activation. 42

Figure 19. FGF21 knockdown exacerbated liver damage in CA-AHR mice. 43

Figure 20. FGF21 is a direct transcriptional target of AHR..... 46

Figure 21. Schematic representation of the two-stage initiation-promotion liver tumor model. 59

Figure 22. Representative gross tumor appearance of DEN-treated mice after 9 months. . 62

Figure 23. Activation of AHR induced mitosis and increased DNA proliferation..... 63

Figure 24. Activation of AHR induced TNF-α expression and increased liver injury after DEN treatment. 65

Figure 25. AHR activation induced expression of Gadd45b..... 67

Figure 26. AHR activation induced expression of Gadd45b in an AHR-dependent manner. 69

Figure 27. Gadd45b is a direct transcriptional target of AHR..... 70

Figure 28. Gadd45b coactivates AHR-mediated transcription. 72

Figure 29. Physical interaction of AHR and Gadd45b..... 74

Figure 30. Model of the AHR-FGF21 axis in lipid and energy metabolism. 79

Figure 31. Model of AHR-Gadd45b regulation in hepatic carcinogenesis. 81

PREFACE

This thesis is dedicated to my loving husband Zhaohui Wu, who inspired me in every aspect of my life; to my parents Zeshu Lu and Rongzhen Zhang, who have always given me your unconditional love and been proud of your daughter.

ABBREVIATIONS

3-MC, 3-methylcholanthrene; **ABC**, ATP-binding cassette; **ACC-1**, acetyl coenzyme A carboxylase 1; **AHR**, aryl hydrocarbon receptor; **AHRKO**, AHR knockout; **AMPK**, AMP-activated protein kinase; **ApoB**, Apolipoprotein B; **ARNT**, AHR nuclear translocator; **ATGL**, adipocyte triglyceride hydrolase; **BAT**, brown adipose tissue; **CA-AHR**, constitutively activated AHR; **CAR**, constitutive androstane receptor; **CPT1**, carnitine palmitoyltransferase 1; **CYP**, cytochrome P450; **DEN**, diethylnitrosamine; **DOX**, doxycycline; **DREs**, dioxin response elements; **ER**, estrogen receptor; **FABP**, fatty acid binding protein; **FAS**, fatty acid synthase; **FAT/CD36**, fatty acid translocase; **FATP**, fatty acid transport protein; **FFA**, free fatty acid; **FGF21**, fibroblast growth factor 21; **FICZ**, 6-formylindolo[3,2-b]carbazole; **Gadd45b**, growth arrest and DNA-damage-inducible beta; **G6Pase**, glucose 6-phosphatase; **GLUT4**, glucose transporter 4; **GST**, glutathione *S*-transferase; **HAHs**, halogenated aromatic hydrocarbons; **HFD**, high-fat diet; **HMGCS**, 3-hydroxy-3-methylglutarate-CoA synthase; **HSP90**, heat shock protein 90; **IDO**, indoleamine 2,3-dioxygenase; **LDL**, low-density lipoprotein; **LDLR**, low-density lipoprotein receptor; **LPL**, lipoprotein lipase; **MCD**, methionine and choline deficient diet; **NAFLD**, nonalcoholic fatty liver disease; **NASH**, non-alcoholic steatohepatitis; **Nqo1**, NAD(P)H:quinone oxidoreductase 1; **Nrf2**, nuclear factor erythroid 2 related factor 2; **GTT**, glucose tolerance test; **PGC1α**, peroxisome proliferative activated receptor-γ co-activator 1α; **PPARα/γ**, peroxisome proliferator-activated receptor α/γ; **PXR** , pregnane X receptor; **ROS**,

reactive oxygen species; **SCD-1**, stearoyl CoA desaturase 1; **SOD**, superoxide dismutase; **SREBP-1c**, sterol regulatory element binding protein 1c; **SULT**, sulfotransferase; **TCDD**, 2,3,7,8-Tetrachlorodibenzo-p-dioxin; **TCPOBOP**, 1,4-Bis[2-(3,5-dichloropyridyloxy)]benzene; **TDO**, tryptophan 2,3-dioxygenase; **TiPARP**, TCDD-inducible poly (ADP-ribose) polymerase; **TK**, thymidine kinase; **TRE,** tetracycline responsive element; **tTA**, tetracycline transcriptional activator; **UGT**, UDP-glucuronosyltransferase; **VLDL**, very-low-density lipoproteins; **WAT**, white adipose tissue; **XAP2**, X–associated protein 2

1.0 CHAPTER I: INTRODUCTION

1.1 ARYL HYDROCARBON RECEPTOR AS A XENOBIOTIC SENSOR

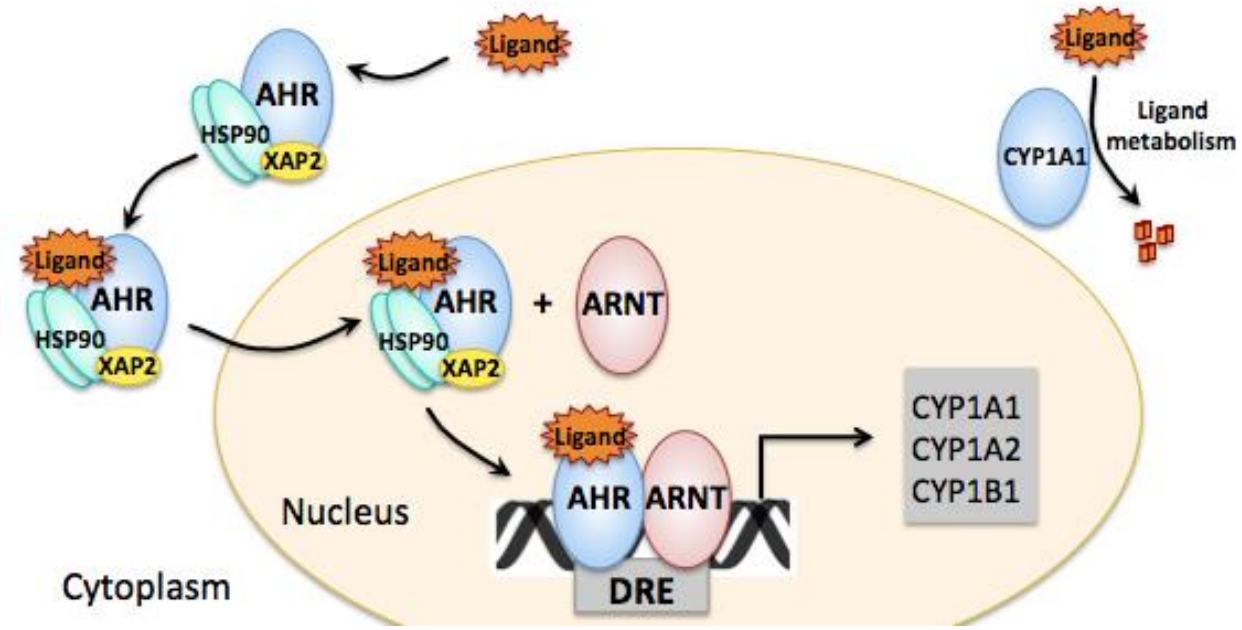

Figure 1. Mechanism of classical Aryl hydrocarbon receptor (AHR) action.
AHR is retained in the cytoplasm in a complex with X-associated protein 2 (XAP2) and two heat shock protein 90 (HSP90) molecules in the absence of AHR ligands. Ligand binding triggers their nuclear translocation and causes conformational change and as a result, the AHR nuclear translocator (ARNT) binds to AHR and forms a functional heterodimer. This heterodimer binds to the dioxin response element (DRE) located in the promoter regions of AHR targets, such as CYP1s, therefore inducing their transcription and causing drug metabolism.

Exposures to xenobiotics such as environmental chemicals and drugs have profound influence on human health. The induction of xenobiotic metabolizing enzymes in response to chemical insults is an adaptive response found in most organisms. The detoxification and clearance of these

xenobiotics are accomplished by the concerted action of Phase I cytochrome P450 (CYP) enzymes, Phase II conjugating enzymes, and drug transporters (1). The P450 enzymes catalyze the monooxygenase reactions of lipophilic compounds facilitated by the reducing power of the NADPH P450 oxidoreductase (2, 3). Phase II enzymes are several large group of transferases, such as sulfotransferase (SULT), glutathione *S*-transferase (GST), and UDP-glucuronosyltransferase (UGT), which conjugate polar functional groups onto xenobiotics (4). Finally, the members of ABC transporter proteins and solute carrier family act to mediate the excretion process (5). Although in most cases, the biotransformation of xenobiotics leads to pharmacologically inactive metabolites, it may also activate so-called pro-drugs to pharmacologically active products or even to toxic metabolites (6).

Most drug-metabolizing enzymes are inducible in response to xenobiotics (7, 8). However, the molecular basis underlying this drug-induced metabolism remained largely unknown for a long time. Discovery of xenobiotic receptors stemmed from the concept that xenobiotic induction was mediated by a receptor through a transcriptional machinery, which is so called "induction-receptor" hypothesis. The plausibility of this hypothesis took a great leap forward with the discovery of the dioxin receptor or the aryl hydrocarbon receptor (AHR) in 1976 (9). AHR is a ligand-activated transcription factor that belongs to the basic helix–loop–helix-PER-ARNT-SIM (bHLH-PAS) subgroup of the bHLH superfamily (10). It is widely expressed in the body and evolutionarily conserved from invertebrates onwards, but its activity is tightly regulated (11). Upon binding to its agonists, such as 2,3,7,8-tetrachlorodibenzo-*p*-dioxin (TCDD) or 3-methylcholanthrene (3-MC), AHR dissociates from its cytoplasmic complex and translocates into the nucleus, forms a heterodimer with its partner AHR nuclear translocator (ARNT), binds to dioxin response elements (DREs) located in the promoter of its target genes,

and activates their transcription (Fig. 1). The sustained hyperactivation of AHR can result in a myriad of toxicological outcomes (12). Examples of AHR target genes include several P450 enzymes that are important in drug metabolism and bioactivation, such as CYP1As and CYP1B1, and Phase II UGT1As (8, 13).

Although AHR was identified as a xenobiotic receptor, emerging evidence has pointed to an equally important role of AHR as an endobiotic receptor. DNA microarray studies have established a large number of genes that are regulated in an AHR-dependent manner. These gene products are involved in a wide variety of biochemical pathways, including energy metabolism, lipid and cholesterol synthesis, and transportation pathways (14). The evidence that AHR null mice showed impairment in normal development of liver, immune system, heart, and vascular tissues also provide insights into the physiological functions of AHR beyond mediating xenobiotic metabolism (15-18).

1.2 MECHANISMS OF AHR ACTIVATION

1.2.1 AHR Ligands

The characterization of high-affinity ligands for AHR, including xenobiotics such as persistent planar halogenated polycyclic hydrocarbons (HAHs) (dioxins, dibenzofurans, and biphenyls) and polycyclic aromatic hydrocarbons (PAHs) (benzo[a]pyrene (BaP) and benzanthracene), has been the focus for many years. HAHs, the best-characterized and highest affinity prototype ligands (with binding affinities in the pM to nM range) of the AHR, are poorly metabolized. In contrast,

PAHs and PAH-like chemicals are readily metabolized by the action of CYPs, which may convert them into reactive metabolites (19).

The evidence that AHR signaling pathway is active in the absence of exogenous ligands suggests the existence of endogenous physiological AHR ligands (20, 21). Diet contains the greatest source of AHR agonists or products that can be readily converted to agonists, and this could substantially contribute to our AHR action levels (15). For example, extracts of vegetables and several dietary plant compounds (such as curcumin, 7,8-dihydrorutacarpine, dibenzoylmethanes, and carotinoids) were reported to exert AHR activation potential (15). Tryptophan derivatives are a major group of endogenous AHR ligands. UV illumination can convert tryptophan to its photoproduct 6-formylindolo[3,2-b]carbazole (FICZ), which exhibits a more potent AHR agonist activity (22). Bacteria in the intestinal tract can metabolize tryptophan into indole metabolites (such as indole-3-carbinol, indolo [3,2-b]-carbazole, indole-3-acetate, etc.) with AHR-inducing activities (15, 23, 24). The tryptophan metabolite kynurenine, which can be generated by the enzymes indoleamine 2,3-dioxygenase (IDO) and tryptophan 2,3-dioxygenase (TDO), were shown to be present in large amounts in human brain tumors with AHR-activating effect (25). Indigo and indirubin, which are also tryptophan-derived metabolites by P450 enzymes action, were identified in human urine as a potent activator of the AHR (15). Other endogenous ligands such as tetrapyroles and arachidonic acid derivatives have also been shown to activate the AHR (26, 27).

1.2.2 Mechanisms of AHR Action

Classical AHR- and DRE-dependent mechanisms mediate most of the toxic and biological effects caused by TCDD and other AHR ligands. In the absence of ligands, AHR exists in a

multi-protein complex comprising of two heat shock protein 90 (HSP90) molecules and a HBV X–associated protein 2 (XAP2) (Fig. 1) (8, 28). Upon ligand binding, the AHR complex undergoes a conformational change and translocates into the nucleus. Once in the nucleus, the dimerization between AHR and its partner ARNT results in the dissociation of other binding proteins from the AHR complex (15). The AHR/ARNT heterodimer binds to the DREs (their consensus sequence being "GCGTG") located on the promoters of AHR responsive genes, leading to coactivator recruitment and transcriptional activation of genes. Nuclear export of AHR into the cytosol is mediated by its N-terminal nuclear export sequence followed by ubiquitin-mediated AHR proteosomal degradation (29).

Although the AHR responsive genes for its xenobiotic and biological effects remain to be identified, studies using mice with deletion of AHR or ARNT clearly demonstrated that the AHR/ARNT functional heterodimer was required for TCDD-induced phenotypic changes in mice (30). In addition, mice were found resistant to the TCDD-induced toxicity when carrying the mutation in the nuclear localization sequence or in the DNA-binding domain of the AHR, demonstrating that both the AHR nuclear localization and DRE binding are required for the toxic and biological effects of TCDD (31, 32).

As a transcription factor, AHR can crosstalk with other nuclear receptors through protein-protein interaction and/or DNA-protein interaction. The best understood example is the crosstalk between the AHR and estrogen receptor (ER) signaling pathways (33). Several mechanisms account for the AHR-ER crosstalk. For example, AHR/ARNT complex could bind to the inhibitory DREs, leading to the blockade of ER binding to its estrogen response element (ERE) on the gene and resulting in repressed estrogen response. AHR can also compete with ER in recruiting common coactivators (such as p300/CBP, SRC1/2, and RIP140) for both receptors,

leading to reduced available coactivators for ER transcriptional activity (33). Similar mutual repressive crosstalk has also been observed between AHR and intracellular signaling pathways. For example, the inhibitory crosstalk between AHR and NF-κB pathway can be caused by the formation of transcriptionally inactive AHR/RelA dimer, as well as competition for common coactivators (19). CYP1s-induced metabolism of exogenous and endogenous chemicals can lead to generation of reactive oxygen species and oxidative stress, which alters cellular responses via activating intracellular kinases (19).

The TCDD-induced effects in an AHR-independent manner could be achieved through increasing the intracellular calcium levels. This induction of calcium influx by TCDD could cause the activation of a variety of signaling pathways including protein kinase C (PKC), epidermal growth factor receptor (EGFR), mitogen-activated protein kinase (MAPK), etc., all of which contribute to the complexity and diversity of the nongenomic action of TCDD (19).

2.0 CHAPTER II: ENDOBIOTIC FUNCTION OF AHR IN LIPID AND ENERGY METABOLISM

2.1 OVERVIEW OF LIPID AND ENERGY METABOLISM

2.1.1 Fatty Acid and Triglyceride Metabolism

The liver is the hub of fatty acid synthesis and triglyceride storage. The liver integrates incoming signals to control triglyceride production for use by other tissues and for storage in adipose tissues. Triglycerides are the preferred storage nutrient to buffer against fluctuations in energy demands and availability. Hepatic steatosis, or fatty liver, is defined as the presence of cytoplasmic triglyceride droplets in more than 5% of hepatocytes (34). Fatty liver is commonly associated with metabolic syndromes including obesity and type 2 diabetes and can lead to inflammation, fibrosis, and even cirrhosis and cancer.

Steatosis may develop as a consequence of multiple dysfunctions. The fatty acids used for hepatic triglyceride formation originate from *de novo* synthesis, diet, and adipose tissue. Carbohydrate feeding promotes *de novo* lipogenesis by inducing the key enzymes involved in this pathway such as the fatty acid synthase (FAS), stearoyl CoA desaturase 1 (SCD-1), and acetyl coenzyme A carboxylase 1 (ACC-1), all of which are under the transcriptional control of the master lipogenic transcriptional factor sterol response element binding protein-1c (SREBP-

1c). Lipoprotein lipase (LPL) and adipocyte triglyceride hydrolase (ATGL) catalyze the hydrolysis of the triglyceride in the chylomicrons and adipocytes, respectively; thereby releasing free fatty acids into the circulation. The liver takes up free fatty acids via the fatty acid transport protein (FATP) or fatty acid translocase (FAT/CD36) when there is an excess of circulating fatty acids. Once in the liver, fatty acids can be oxidized to produce energy and ketone bodies, re-esterified to triglyceride, or exported as very-low-density lipoproteins (VLDL). Carnitine palmitoyltransferase 1 (CPT1) and mitochondrial 3-hydroxy-3-methylglutarate-CoA synthase (HMGCS) are two key enzymes in β-oxidation and ketogenesis. Apolipoprotein B100 (ApoB100) is the key component that controls the overall rate of VLDL production and secretion (35). In summary, steatosis may arise from an imbalance between triglyceride acquisition and removal due to increased fatty acid synthesis and uptake, decreased fatty acid β-oxidation, and reduced triglyceride secretion.

2.1.2 Glucose and Insulin Metabolism

Plasma glucose levels are strictly regulated in normal individuals, which process is controlled by the actions of insulin and glucagon. Circulating glucose is derived from three sources: intestinal absorption, gluconeogenesis, and glycogenolysis, and its levels are maintained by glucose appearance and removal. Insulin is the only pancreatic β-cell hormone that can lower the glucose levels. Following feeding, insulin is secreted and acts on skeletal muscle through binding to the insulin receptor and increases glucose uptake through the action of glucose transporters such as glucose transporter 4 (GLUT4). On the other hand, insulin exerts its effect on liver to trigger glycogenesis, in which glucose molecules are added to chains of glycogen for storage. Finally,

insulin represses the secretion of glucagon from pancreatic α-cells, thus blocking gluconeogenesis and glycogenolysis in the liver.

Abnormal action of insulin is the foundation of the pathophysiology in diabetes. Type 1 diabetes is characterized by the dysfunction of pancreatic β-cells in producing insulin, whereas Type 2 diabetes is associated with peripheral insulin resistance in the early stage followed by progressive β-cell failure during the late stage. Insulin resistance, a pathological condition in which cells fail to respond to the normal actions of insulin, is a major feature of Type 2 diabetes.

Particularly, insulin resistance can lead to nonalcoholic fatty liver disease (NAFLD) by increasing lipolysis in adipose tissue and facilitating fatty acid uptake into the liver, inducing hepatic *de novo* lipogenesis, and decreasing the fatty acid β-oxidation (36). Liver fat accumulation, on the other hand, is believed to generate elevated levels of free fatty acids and pro-inflammatory lipid intermediates that can disrupt the insulin signaling cascade and cause insulin resistance (37). However it remains uncertain whether a causal relationship exists.

2.2 AHR IN LIPID AND ENERGY METABOLISM

2.2.1 AHR in NAFLD and NASH

It has long been suggested that the systemic TCDD toxicity involves an overall perturbation of energy homeostasis (38). Earlier work associated exposures to AHR agonists with dyslipidemia by reporting that TCDD and related halogenated aromatic hydrocarbons (HAHs) produced marked fatty liver in several species (39-41). In agreement with these animal results, dioxin exposure in human populations has also been reported to be associated with increased incidence

of fatty liver (42). The accumulation of hepatic triglycerides was accompanied by an increase in liver weight and liver to body weight ratios (43). Increased *de novo* fatty acid synthesis (44), decreased fatty acid oxidation (45), and increased half-life of liver lipid moieties (43) have been suggested to account for the hepatic steatosis in AHR agonist-treated rats. In contrast, some other studies have shown decreased hepatic fatty acid synthesis in both animal models and primary human hepatocytes upon TCDD treatment, which was associated with reduced expressions of key lipogenic genes including FAS, SCD-1, and acetyl-CoA carboxylase (46-48).

One needs to be cautious when interpreting these phenotypes because TCDD itself is toxic to the cells and animals. AHR function has also been studied by overexpressing a constitutively active AHR in which the ligand-binding domain has been deleted. Recently, we showed that mice overexpressing a constitutively activated mouse Ahr (CA-Ahr) in the liver developed a spontaneous steatosis without causing a general hepatotoxicity. The steatosis in CA-Ahr transgnenic mice was manifested by increased fatty acid uptake and decreased VLDL-triglyceride secretion. CD36, the fatty acid translocase, was identified as a novel AHR target gene that mediated the steatotic effect (49). In another independent study, mice fed with the AHR ligand 3-MC, an AHR agonist less toxic than TCDD, showed a hepatosteatotic phenotype through a similar mechanism (50).

Using the same CA-Ahr transgenic mice, we showed that activation of Ahr also sensitized mice to non-alcoholic steatohepatitis (NASH), an advanced stage of NAFLD with the hallmarks of inflammation and progressive fibrosis (51). The CA-Ahr transgenic mice showed heightened sensitivity to methionine and choline deficient diet (MCD)-induced NASH by decreasing the activity of superoxide dismutase 2 (SOD2) and increasing mitochondrial reactive oxygen species (ROS) production in the liver. Mechanistically, the mitochondrial sirtuin

deacetylase Sirt3, which could enhance the scavenging of superoxide through activating the mitochondrial SOD2, was inhibited by Ahr. The Ahr-responsive inhibition of Sirt3, a NAD+ dependent deacetylase, was likely due to the depletion of the cellular concentration of NAD+ because of the activation of TiPARP by Ahr (52). Sensitization of mice to the MCD diet-induced NASH was also demonstrated in WT mice treated with TCDD. Interestingly, the anti-oxidative role of Ahr has also been reported. For example, the nuclear factor erythroid 2 related factor 2 (Nrf2), a master regulator of anti-oxidative responses, was directly induced by AHR activation, which in turn protected against the oxidative stress (53). Other reported AHR inducible cytoprotective genes include the NAD(P)H:quinone oxidoreductase 1 (Nqo1), GSTs, and UGTs (54). These results suggested that AHR might have a rather complex role in liver's handling of oxidative stress.

2.2.2 AHR in Type 2 Diabetes and Insulin Resistance

Dyslipidemia is a well-known predisposing factor for the development of type 2 diabetes. With the potential effects of AHR on dyslipidemia, it is reasonable to hypothesize that AHR can affect the pathogenesis of diabetes as well. Indeed, both animal models and human studies suggested an association between TCDD exposure and increased incidence of diabetes (55-57), but the underlying mechanism is poorly defined. TCDD-induced reduction in glucose uptake has been reported in adipose tissue, liver, and pancreas (58-60), primarily through the decreased expression of GLUT4 (61). Another suggested mechanism was the inhibition of hepatic phosphoenolpyruvate carboxykinase (PEPCK) and glucose 6-phosphatase (G6Pase), which resulted in an impairment of gluconeogenesis (62). In a human study, non-diabetic veterans with high blood TCDD levels were found to more likely develop insulin resistance (63). TCDD-

treated animals showed β cell dysfunction, including reduced insulin production and secretion (59, 64). Based on the fact that loss of PPARγ is diabetogenic, and the PPARγ agonists thiazolidinediones sensitize tissues to the insulin actions, it was also suggested that the diabetogenic effects of TCDD might be through antagonizing the PPARγ functions (55). The direct link between AHR and diabetes and insulin resistance has been reported using the AHR-null mice, which displayed enhanced insulin sensitivity and improved glucose tolerance in both normal chow diet- and high fat diet-fed conditions (65, 66). But the mechanisms underlying its metabolic effects in insulin resistance need to be evaluated.

The AHR heterodimerization partner ARNT, also known as hypoxia-inducible factor 1β (HIF1β), is a ubiquitously expressed nuclear protein that also belongs to the bHLH/PAS family of transcription factors (67). Recent findings showed that the expression of ARNT was reduced in both liver and β cells of obese individuals with type 2 diabetes (68, 69), suggesting an important role of ARNT in the development of metabolic disease. Further studies demonstrated that the deficiency of ARNT activity in β cells and liver contributed to impaired insulin secretion and dysregulation of glucose homeostasis, respectively (68, 69).

Insulin resistance is associated with elevated plasma levels of very-low-density lipoprotein (VLDL) and low-density lipoprotein (LDL) (70, 71). Subsequent atherosclerotic lesion is a serious cause for the cardiovascular complications arisen in the patients with type 2 diabetes. A significant positive correlation between high serum TCDD and plasma cholesterol and triglyceride levels was observed in subjects exposed to chloracne, and among US Vietnam war veterans who had been exposed to high levels of TCDD (72-74). A follow-up study on a cohort of former TCDD workers showed that exposure to TCDD caused atherosclerotic plaques and ischemic heart disease (75). Animal studies confirmed that TCDD induced a marked

dyslipidemia characterized by increased total cholesterol, VLDL, LDL, and triglyceride levels (76-78). Mechanistically and of particular relevance to triglyceride metabolism, the adipose activity of LPL, which hydrolyses triglyceride and promotes its cellular uptake, was reduced in both animals and adipocyte cultures after TCDD treatment (60, 79). As for the cause of hypercholestenolemia, TCDD caused a down-regulation of LDLR on the plasma membrane of hepatocytes, leading to a decreased cholesterol internalization and elevated levels of plasma cholesterol (80). However, it remains to be determined whether the effect of TCDD on the expression of adipose LPL and liver LDLR is AHR dependent. The effects of AHR on energy metabolism are summarized in Figure 2.

Particularly, having known that activation of AHR causes spontaneous fatty liver (49), it is paradoxical to note that TCDD seemed to induce the expression of fibroblast growth factor 21 (FGF21) (81), a systemic insulin sensitizer. FGF21 is an atypical member of the FGF family produced predominantly in the liver (82). FGF21 is induced in the liver by fasting through the activation of the peroxisome proliferator-activated receptor α (PPARα) (83, 84). FGF21 exhibits many metabolic benefits, ranging from reducing body weight to alleviation of hyperglycemia and insulin resistance, and improvement of lipid profiles (85). In hepatocyte and adipocyte, FGF21 directly regulates metabolism through interactions with FGF receptor 1 (FGFR1) and βKlotho (86). Adiponectin plays an important role in coupling FGF21 actions in adipocytes to liver and skeletal muscle, thereby mediating the systemic effects of FGF21 on energy metabolism and insulin sensitivity (87). Although FGF21 was shown to be regulated by TCDD, the pathophysiological relevance of this regulation remains undefined. Therefore, the experiments described in this chapter were designed to investigate the endobiotic and hepatic

function of AHR in lipid and energy homeostasis, and to identify the potential contribution of FGF21 in these processes.

2.3 SPECIFIC AIMS

Although we know that AHR activation in transgenic mice induces spontaneous fatty liver, the metabolic effects of AHR in dietary induced fatty liver and associated metabolic syndromes such as obesity and insulin resistance has not been addressed. Meanwhile, having noticed that TCDD induced FGF21 production, it is interesting to study the relative contribution of FGF21-dependent pathways in AHR-induced metabolic phenotypes. Therefore, we aim to investigate the metabolic outcomes of AHR activation using the gain-of function CA-AHR transgenic mouse model, and determine the metabolic changes by using loss-of function of FGF21.

Aim 1: To determine the role of human AHR in dietary induced fatty liver and associated metabolic syndromes such as obesity and insulin resistance.

Aim 2: To explore the transcription regulation of FGF21 by AHR activation in the context of both chow diet- and high fat diet-fed conditions.

Aim 3: To investigate the contribution of FGF21 transactivation in AHR-mediated metabolic effects using FGF21 knockdown.

2.4 METHODS

Mice and Diets

AHR knockout (AHRKO) mice in C57BL/6 background were purchased from Taconic (Hudson, NY). Mice were fed with standard chow from PMI Nutrition (St. Louis, MO) or high fat diet (HFD) (S3282) from Bio-serv (Frenchtown, NJ). In the HFD model, 6-week-old mice (N=5 for each group) received HFD for 12 weeks in most of the experiments, except that when adenovirus were used, mice were treated with HFD for 6 weeks before viral infection. Body weights were monitored during HFD feeding and tissues were collected and analyzed at the end of the feeding. When necessary, doxycycline (DOX; 1 mg/ml) was given in drinking water. The food intake was measured for 7 days after 10 weeks of HFD feeding, and the data was normalized to lean content of body weight. Body composition was analyzed using EchoMRI-100TM from Echo Medical Systems (Houston, TX). The use of mice in this study complied with relevant federal guidelines and institutional policies.

Short Hairpin Adenoviral Production

Entry clones targeting either FGF21 or LacZ were gifts from Dr. Eleftheria Maratos-Flier (Beth Israel Deaconess Medical Center) (83). To generate shRNA expression clones, FGF21 and LacZ entry vectors were used to perform LR recombination with the E1- and E3-deleted pAd/BLOCK-iT-DEST vector from Invitrogen. Adenoviruses were generated by transfecting 293A cells with vectors digested with PacI. After plaque selection and amplification, viruses were purified on a discontinuous CsCl gradient. Mice received adenovirus intravenously at the dose of 2×10^9 viral particle/g body weight.

H&E and Oil Red O staining

For H&E staining, tissues were fixed in 10% buffered formalin, embedded in paraffin, sectioned at 5 μm, and stained with hematoxylin and eosin. For Oil Red O staining, snap-frozen liver tissues were sectioned at 8 μm, fixed in 10% buffered formalin, and stained in 0.5% Oil Red O in propylene glycerol. The histology was determined under microscopy.

Serum and Tissue Biochemical Analysis

Serum levels of triglyceride and cholesterol (Stanbio Laboratory, Boerne, TX), ALT and AST (Stanbio Laboratory, Boerne, TX), insulin (Crystal Chem, Downers Grove, IL), IL-6, FGF21, and Adiponectin (R&D Systems, Minneapolis, MN) were measured by using commercial assay kits. To measure serum lipid levels, 75 μl of methanol was mixed with 25 μl of serum and centrifuged at 15,000 *g* for 20 min. To measure hepatic lipid contents, liver tissues were homogenized and lipids were mixed with chloroform/methanol (3:1, v/v) and centrifuged at 3,000 *g* for 10 min. The organic phase was transferred to a glass tube and dried under a gentle stream of nitrogen. The residue was reconstituted by acetonitrile: water (1:1, *v/v*) and subject to measurement. Triglyceride and cholesterol levels were measured at 500 nm using a PerkinElmer plate reader. Free fatty acid (FFA) levels were analyzed using the UPLC-QTOFMS methods. 1.0 μg/ml of internal standards of different species of FFAs-d31 (myristic acid, palmitic acid, palmitoleic acid, steric acid, oleic acid, linoleic acid, linolenic acid, arachidonic acid, eicosapentaenoic acid, docosahexaenoic acid, and eicosanoic acid) were added into serum or tissue homogenates before lipid extraction. Chromatographic separation of metabolites was performed on an Acquity UPLC BEH C18 column (2.1 × 100 mm, 1.7 μm, Waters). The mobile phase A was 0.1% formic acid in acetonitril: water (6:4, *v/v*), and mobile phase B was 0.1%

formic acid in acetonitrile: isoproponal (1:9, *v/v*). The gradient for aqueouse extraction began at 35% MPB and held for 1 min, followed by 10-min linear gradient to 95% MPB, held for 3 min and decreased to 35% MPB for column equilibration. The flow rate of mobile phase was 0.40 ml/min and the column temperature was maintained at 50 °C. The Waters Synapt G2-S QTOFMS system (Milford, MA) was operated in high resolution mode (resolution ~ 20,000) with electrospray ionization. The source and desolvation temperatures were set at 150 and 500 °C, respectively. Nitrogen was applied as the cone gas (50 l/h) and desolvation gas (800 l/h). Argon was applied as collision gas. The capillary and cone voltages were set at 0.8 kV and 40 V. The data were acquired in both positive and negative ionization mode. QTOFMS was calibrated with sodium formate and monitored by the intermittent injection of lock mass leucine encephalin (*m/z* = 556.2771) in real time. Product ion scans with collision energy ramping from 15 to 50 eV were used for structural elucidations of metabolites.

Indirect Calorimetry, Glucose Tolerance Test (GTT), and Insulin Tolerance Test (ITT)

Indirect calorimetry was performed using the Oxymax Indirect Calorimetry System (Columbus, OH). Mice were individually housed in the chamber with a 12 h light and 12 h dark cycle and monitored over a 48 h period. For GTT, mice were fasted for 12 h before receiving an intraperitoneal injection of D-glucose at 2 g/kg body weight. For ITT, mice were fasted for 6 h before receiving an intraperitoneal injection of insulin at 0.5 units/kg body weight. Blood glucose concentrations were measured by sampling from the tail.

Western Blotting Analysis

Tissues were lysed in RIPA buffer supplemented with protease inhibitors. Protein samples were

resolved by SDS-PAGE gel, transferred to a polyvinylidene fluoride membrane, and blotted with antibodies. The primary antibodies used include those against AHR (N-19, Santa Cruz), pThr172AMPKα (cat# 2535, Cell Signaling) and total AMPKα (cat# 260, Cell Signaling), FGF21 (cat# 171941, Abcam), ApoB100 (H-15, Santa Cruz), and β-actin (A1978, Sigma).

Electrophoretic Mobility Shift Assay (EMSA), Chromatin Immunoprecipitation (ChIP) Assay, Transient Transfection and Luciferase Reporter Assay

EMSA was performed using ^{32}P-labeled oligonucleotides and receptor proteins prepared by the TNT method (88). ChIP assays for the human and mouse FGF21 promoters were performed on 293 cells transfected with pCMX-Flag-CA-AHR plasmid for 24 h and WT mice whose livers were transfected with the pCMX-Flag-CA-AHR plasmid by a hydrodynamic gene delivery method for 8 h (88), respectively. Cells or liver lysates were immunoprecipitated with the anti-Flag antibody (Sigma). The recovered DNA was assayed for enrichment of the FGF21 promoters by PCR. For luciferase reporter assay, the human FGF21 reporter plasmids (-2124/+29, -1836/+29, and -1562/+29) were PCR-amplified. The mouse FGF21 reporter plasmids (-98/+5 and -66/+5) were gifts from Dr. Steven A. Kliewer (UT Southwestern Medical Center) (84). HepG2 cells were transfected with the reporter construct and AHR or CA-AHR expression vector in triplicate groups in 48-well plates. When necessary, cells were treated with 3-MC (4 μM) or TCDD (10 nM) for 24 h before reporter assay. The transfection efficiency was normalized against the β-galactosidase activities from a co-transfected CMX-β-galactosidase vector.

VLDL Secretion Assay

Mice were fasted for 4 h before receiving an intravenous injection of tyloxapol, a lipoprotein lipase inhibitor at 500 mg/kg body weight. Tail vein blood samples were collected at 0, 60, and 90 min after the tyloxapol injection, and plasma triglyceride levels were measured at 500 nm using a PerkinElmer plate reader.

Tissue Mitochondrial Fatty Acid Oxidation

Liver and skeletal muscle mitochondrial fatty acid oxidation was measured as described previously (89). Fresh tissues were excised and placed in ice-cold modified Chappell-Perry buffer. Tissues were homogenized and mitochondria were isolated using differential centrifugation. Oxidation assays were performed using 0.2 mM [^{14}C]-oleate. Reactions were terminated by adding 100 µl of 70% perchloric acid, and [^{14}C]-CO_2 was trapped in 200 µL of 1 N NaOH. [^{14}C]-CO_2 and [^{14}C]-labeled acid-soluble metabolites (ASM) were assessed by liquid scintillation counting.

Quantitative RT-PCR

Total RNA was extracted using TRIzol and subjected to reverse transcription with random hexamer primers and Superscript RT III enzyme (Invitrogen). SYBR Green-based qRT-PCR was performed with the ABI7500 System. Data were normalized against the cyclophilin control.

Statistical Analysis

When applicable, results are presented as means ± standard error of the mean (SEM). Statistical significance between the means of two groups was analyzed using an unpaired Student *t* test, and

analysis of variance (ANOVA) for the comparison among the means of three or more groups. Differences were considered statistically significant at $P < 0.05$. Repeated-measures ANOVA was used to compare means of two or more groups across multiple time points (body weight monitoring study).

2.5 RESULTS

2.5.1 Creation and Characterization of the Constitutively Activated AHR (CA-AHR) Construct

Previous study has shown that CA-mAhr is constitutively activated if it lacks the region of the ligand-binding domain (amino acids 287-422) (90). To study the function of human AHR, we constructed a constitutively activated human AHR (CA-AHR) by similarly deleting the minimal ligand-binding domain (amino acids 273-432) of AHR (Fig. 2A). Functionality of the CA-AHR construct was determined in CV-1 cells (normal African green monkey kidney fibroblast cells) transiently transfected with the DRE-driven luciferase reporter construct pGud-Luc, together with expression constructs of AHR or CA-AHR and ARNT. As shown in Figure 2B, CA-AHR dramatically increased the pGud luciferase activity in the absence of an AHR ligand, and addition of the agonist ligand 3-MC had no further effect. In contrary, the wild type AHR exhibited ligand-dependent activation effect as shown by Fig. 2B. When mice liver were transfected with CA-AHR construct by a hydrodynamic gene delivery system, hepatic mRNA expression of AHR-responsive genes including CYP1A1 and CYP1B1 was significantly induced

without a ligand treatment (Fig. 2C). Thus, CA-AHR transgene is transcriptionally active with ligand-independent manner in both *in vitro* and *in vivo*.

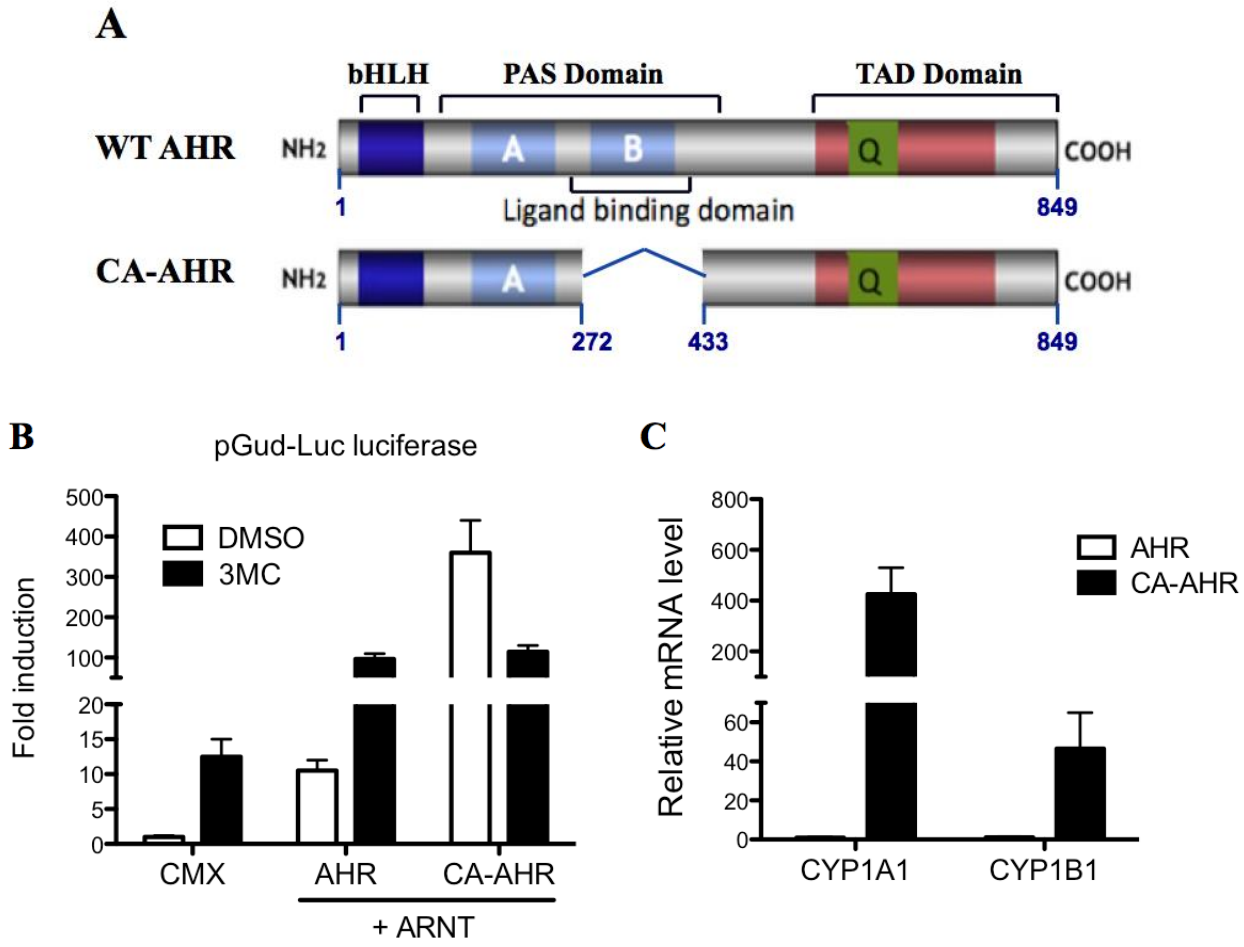

Figure 2. Characterization of the constitutively activated AHR (CA-AHR) construct.
(A) Schematic representation and domain structure of the wild type (WT) AHR and constitutively activated AHR (CA-AHR). bHLH, helix-loop-helix; PAS, PER-ARNT-SIM; TAD, transactivation domain. (B) CA-AHR activates the AHR-responsive pGud-Luc reporter in a ligand independent manner. CV-1 cells cultured in 48-well plates were transfected with CMX (cytomegalovirus-based)-PL2 empty vector or AHR, CA-AHR, and ARNT (AHR nuclear translocator) expressing plasmids at 50ng/well concentrations for 6 hours before the treatment with 3-methylchoranethrene (3-MC) (4 μM). After 24 hours, cells were lysed and subject to luciferase reporter assay in triplicate groups. (C) Eight week-old CD-1 male mice were hydrodynamically delivered with 5μg of the AHR or CA-AHR plasmids. Mice were sacrificed 16 h later, the livers were collected and the expressions of CYP1A1 and CYP1B1 were measured by RT-PCR. N=5 for each group. Results are presented as means ± standard error of the mean (SEM).

2.5.2 Generation of Conditional Tetracycline Inducible Transgenic Mice Expressing CA-AHR in the Liver

To study the *in vivo* function of human AHR, we generated the "Tet-off" tetracycline inducible FABP-tTA/TetRE-CA-AHR transgenic mice overexpressing the CA-AHR in the liver under the control of the fatty acid binding protein (FABP) gene promoter (Fig. 3A). Our "Tet-off" transgenic system is composed of two transgenic lines: TetRE-CA-AHR and FABP-tTA lines. To generate the TetRE-CA-AHR transgenic line, CA-AHR was placed downstream of a minimal cytomegalovirus promoter fused to the tetracycline responsive element (TetRE). The functionality of TetRE-CA-AHR construct was analyzed by reporter assay, in which TRE-CA-AhR and pGud-Luc constructs were transiently transfected, together with CMX-tTA that express the tTA in CV-1 cells (Fig. 3B). Coexpression of tTA with TRE-CA-AHR resulted in induction of pGud luciferase activity in the absence of doxycycline (DOX), however with DOX treatment there was no stimulation of luciferase activity (Fig. 3B). Pronuclear microinjection of the TetRE-CA-AHR into the C57BL/6 embryos was performed at the University of Pittsburgh Transgenic Core Facility. The genotyping for TetRE-CA-AHR mice was performed by PCR using primers for TRE1-5'- (GAGCTCGTTTAGTGAACCGTCA) and CA-AHR-3'-(AGACCAGTGGCTTC TTCAATTCC). The liver-specific FABP-CA-AHR mice in C57BL/6 background were generated by crossbreeding TetRE-CA-AHR mice with the FABP-tTA mice (88).

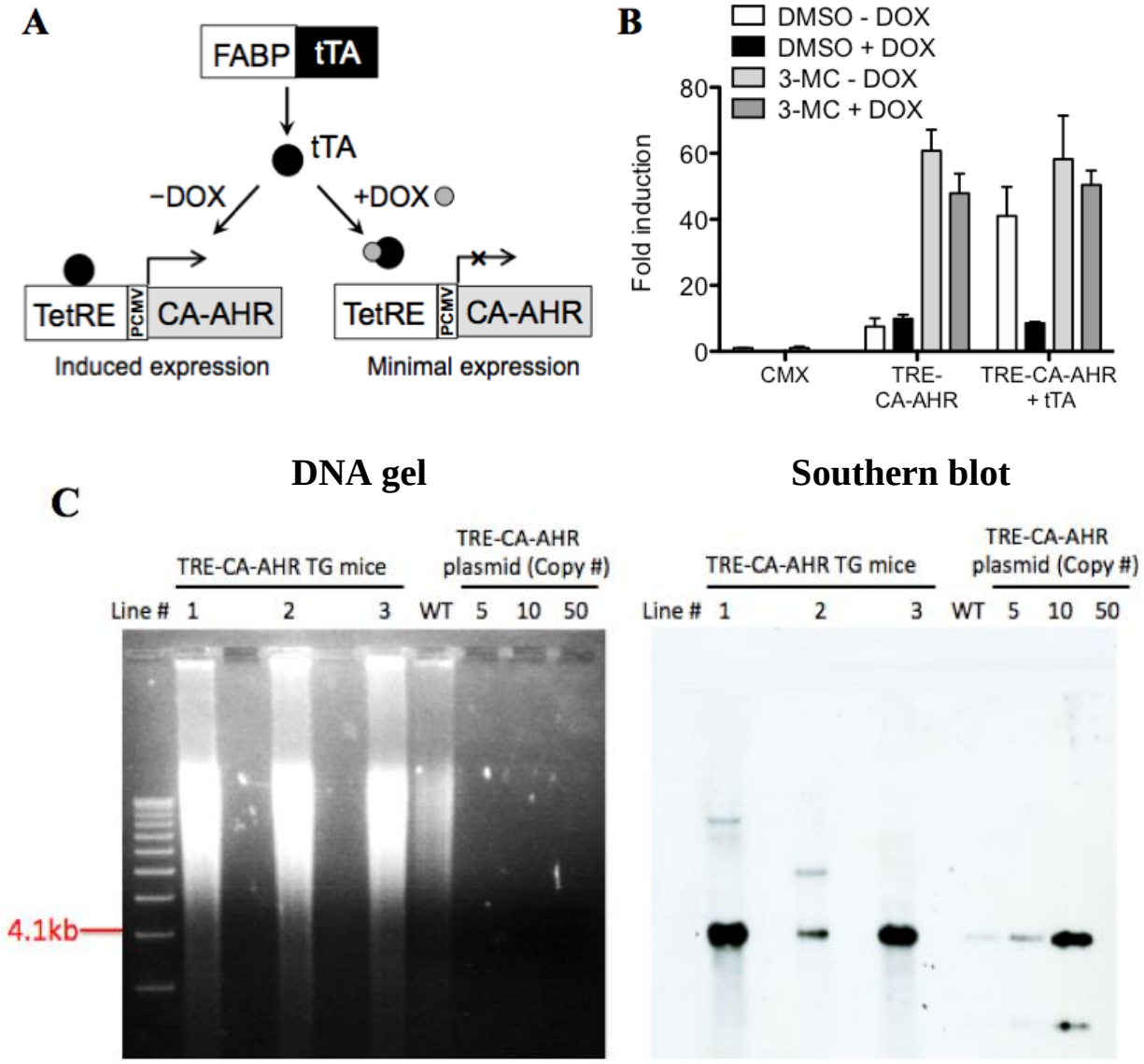

Figure 3. Generation of transgenic mice expressing CA-AHR in the liver and intestine.
(A) Schematic representation of the Tet-off FABP-tTA/TRE-CA-AhR transgenic system. CMX, cytomegalovirus; DOX, doxycycline; FABP, fatty acid binding protein; PCMV, minimal CMV promoter; TRE, tetracycline responsive element; tTA, tetracycline transcriptional activator. (B) CV-1 cells in 48-well plates were transiently transfected with pGud-Luc and TRE-CA-AHR together with expression vectors of tTA followed by DOX (1mg/mL) treatment for 24 hours before the luciferase reporter assay in triplicate groups. (C) Generation of TRE-CA-AHR transgenic mice. Shown are DNA gel (left) and integration and copy number of transgene (right) verified by Southern blot analysis of genomic DNA from mouse tails. Results are presented as means ± standard error of the mean (SEM).

Three founders were obtained and evaluated for the integration and copy numbers of the transgene as shown by Southern blot analysis (Fig. 3C). Crossbreeding of the TRE-CA-AHR founders with FABP-tTA mice yielded one bi-transgenic line, which was chosen for further characterization and most of the subsequent experiments. The liver-specific expression of CA-AHR was confirmed at both mRNA and protein levels, without affecting the expression of endogenous AHR (Fig. 4A). The expression of typical AHR target genes was induced in TG livers, and abolished when mice were given DOX-contained drinking water for one week (Fig. 4B). The gene regulatory effect appeared to be AHR specific and did not affect the activity of other partners of AHR nuclear translocator (ARNT), because the expression of VEGF, a typical target gene of the HIF1α-ARNT heterodimers, was not affected (Fig. 4C).

Although AHR mediates most of the toxic and biological effects of TCDD, the ability of TCDD to produce effects in an AHR-independent manner has also been observed and likely contributes to the overall adverse effects of these compounds. Therefore, we checked the liver injury and inflammatory status in the AHR TG mice. Unlike the TCDD model of AHR activation, the transgene was not associated with obvious hepatotoxicity, because neither the serum levels of liver injury markers (ALT, AST, and ALP) (Fig. 5A) nor the expression of hepatic inflammatory cytokines or marker genes (Fig. 5B) were increased in the TG mice.

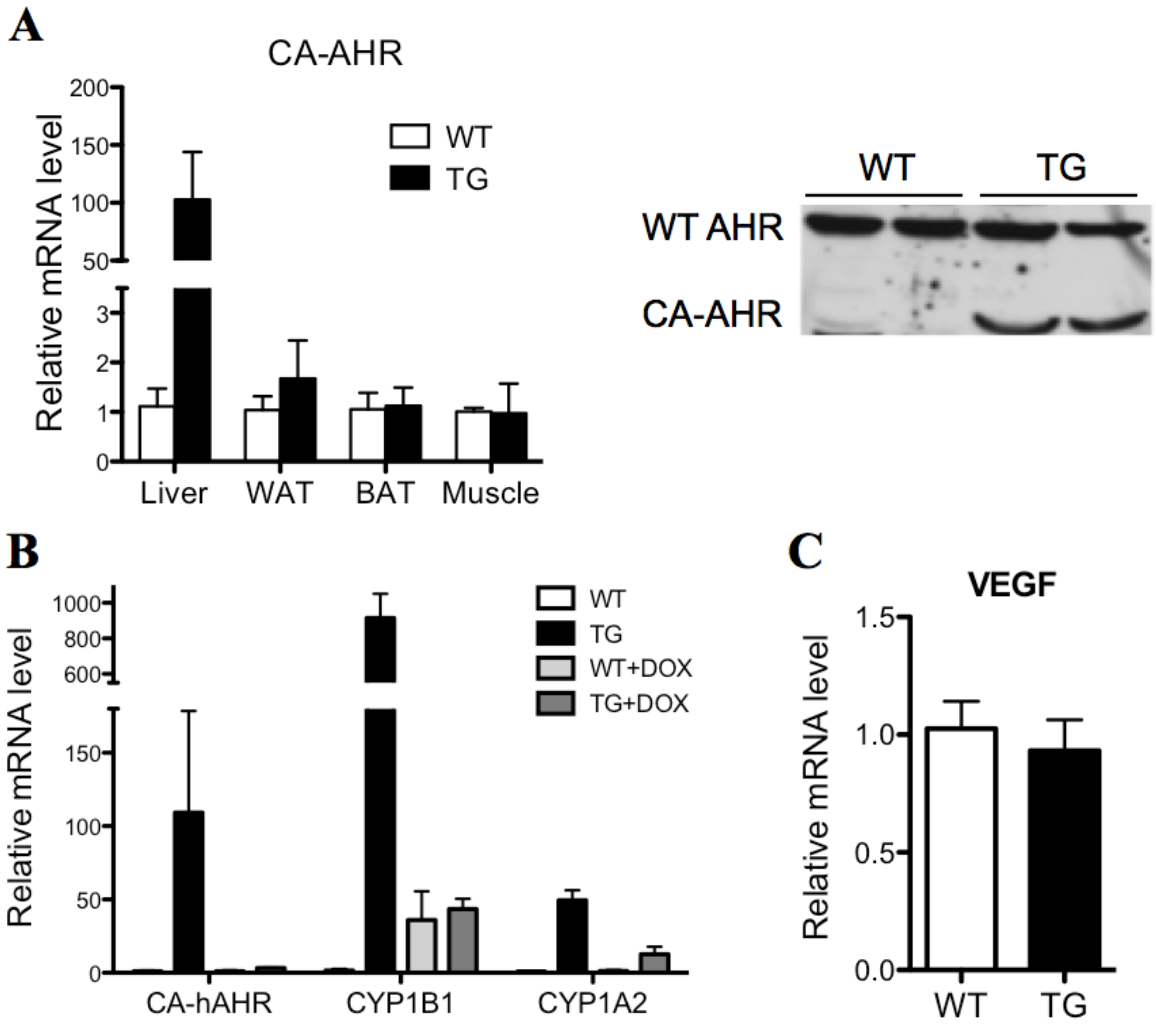

Figure 4. Characterization of the liver-specific expression of the CA-AHR.
Wild-type (WT) and transgenic (TG) mice were 6 weeks old and maintained on chow diet. (A) The mRNA expression of the transgene in a panel of tissues (left) and Western blotting of hepatic wild type (WT) AHR and CA-AHR (right). (B) Hepatic mRNA expresssion of CA-AHR transgene and CYP1 genes. DOX (1mg/ml) was given in drinking water for 2 weeks starting at 4-week old when necessary. (C) Hepatic mRNA expresssion of ARNT target gene VEGF. N=5 for each group. Results are presented as means ± standard error of the mean (SEM).

The TG mice showed apparent hepatomegaly. At 6 weeks, the liver accounted for 4.38±0.23% of total body weight in WT mice, but 5.35±0.26% in TG mice with an increase of 22% (Fig. 6A). Consistent with the previous study that transgenic mice overexpressing CA-mAhr developed spontaneous steatosis at the age of 6 weeks old (49), lipid analysis in the CA-AHR TG livers showed a significantly increased hepatic and cholesterol levels (Fig. 6B) as well as free fatty acid contents (Fig. 6C) as compared to WT livers. Oil-red O staining confirmed the lipid droplet accumulation in hepatocytes of TG mice (Fig. 6D).

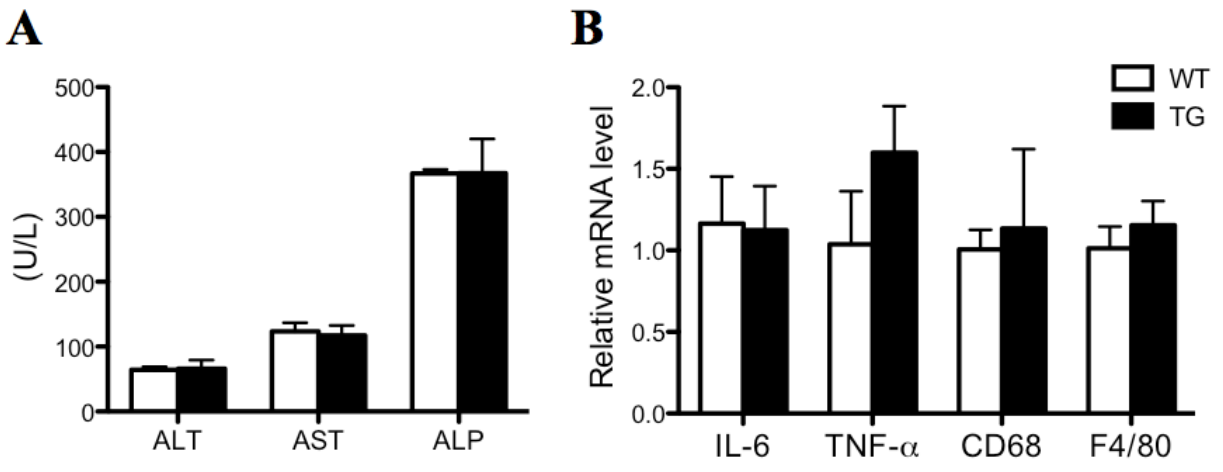

Figure 5. Activation of AHR in CA-AHR mice was not associated with obvious hepatotoxicity.
Mice were 6 weeks old and maintained on chow diet. (A) Serum levels of ALT, AST, and ALP. (B) Hepatic mRNA expression of inflammatory cytokines and macrophage markers. N=5 for each group. Results are presented as means ± standard error of the mean (SEM).

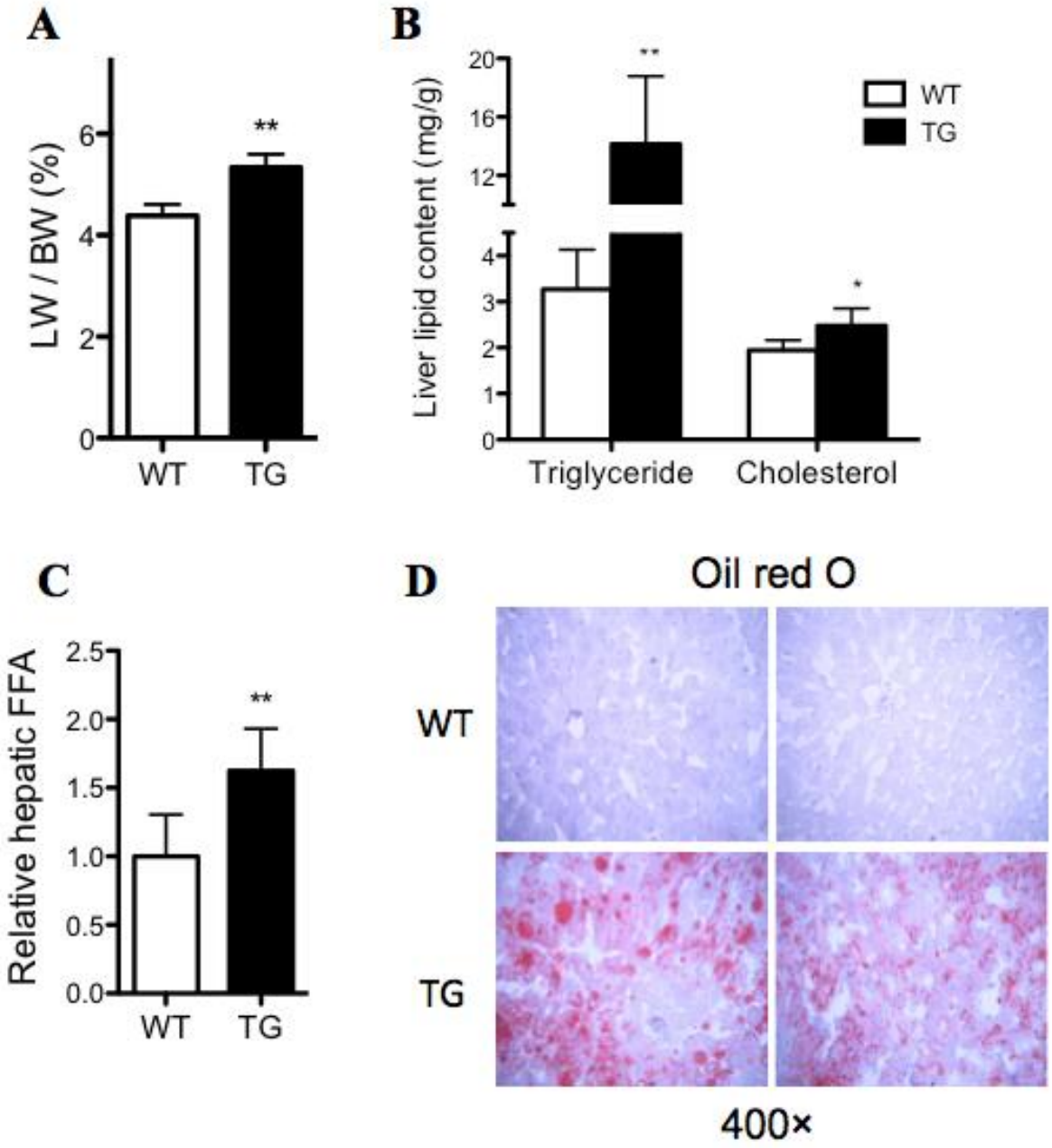

Figure 6. CA-AHR TG mice developed spontaneous steatosis.
Mice were 6 weeks old and maintained on chow diet. (A) The liver weight (LW) was measured as percentage of the total body weight (BW). (B) Hepatic triglyceride and cholesterol contents in liver homogenates were measured at 500 nm. (C) Hepatic free fatty acid (FFA) levels were measured using LC-MS method, and the data was presented as the summation of all FFA species. (D) Liver sections were stained with oil red o dye, and examined microscopically (400×). N=5 for each group. *, $P<0.05$; **, $P<0.01$, TG vs. WT. Results are presented as means ± standard error of the mean (SEM).

2.5.3 Activation of AHR Exacerbated High-Fat Diet (HFD)-Induced Steatosis

To determine whether AHR played a role in diet-induced fatty liver and associated metabolic syndrome, we challenged TG mice with HFD. Upon HFD feeding, the TG livers were larger and appeared paler and fattier compared to the WT livers (Fig. 7A). Hepatic triglyceride and cholesterol contents were higher (Fig. 7B, left panel), whereas serum levels of triglyceride and cholesterol were lower in TG mice (Fig. 7B, right panel). Interestingly, HFD feeding alone resulted in the accumulation of small lipid droplets within the hepatocytes of WT mice, whereas AHR activation caused formation of large lipid droplets as shown by H&E and Oil-red O staining (Fig. 7C). Additionally, the small lipid droplets in WT liver were mainly localized in the central vein areas and were formed in almost all hepatocytes in that area, whereas the large lipid droplets in TG liver were mostly restricted to the portal vein areas and developed only in certain hepatocytes (Fig. 7C).

Hepatosteatosis is a result of imbalanced triglyceride secretion, *de novo* lipogenesis, fatty acid oxidation, or fatty acid uptake (34). The secretion of VLDL, which indicates the capacity of triglyceride secretion, was inhibited in HFD-fed TG mice (Fig. 8A). The protein level of ApoB100, the main structural component of VLDL, was reduced in TG liver (Fig. 8B). Interestingly, the TG liver showed an unchanged rate of complete fatty acid (FA) oxidation (Fig. 8C) and a decreased rate of incomplete FA oxidation (Fig. 8D), in which FAs entering the mitochondria are partially degraded and may generate toxic metabolites that contribute to insulin resistance. The expression of FA oxidation genes including Pparα and its targets Cpt1α, Lcad, and Mcad was decreased in TG liver (Fig. 8E), which was consistent with previous report in CA-Ahr transgenic mice (49). Despite their exacerbated steatosis, the TG mice showed decreased expression of lipogenic genes, including Srebp1c, Acc1, Scd1, and Fas (Fig. 8E).

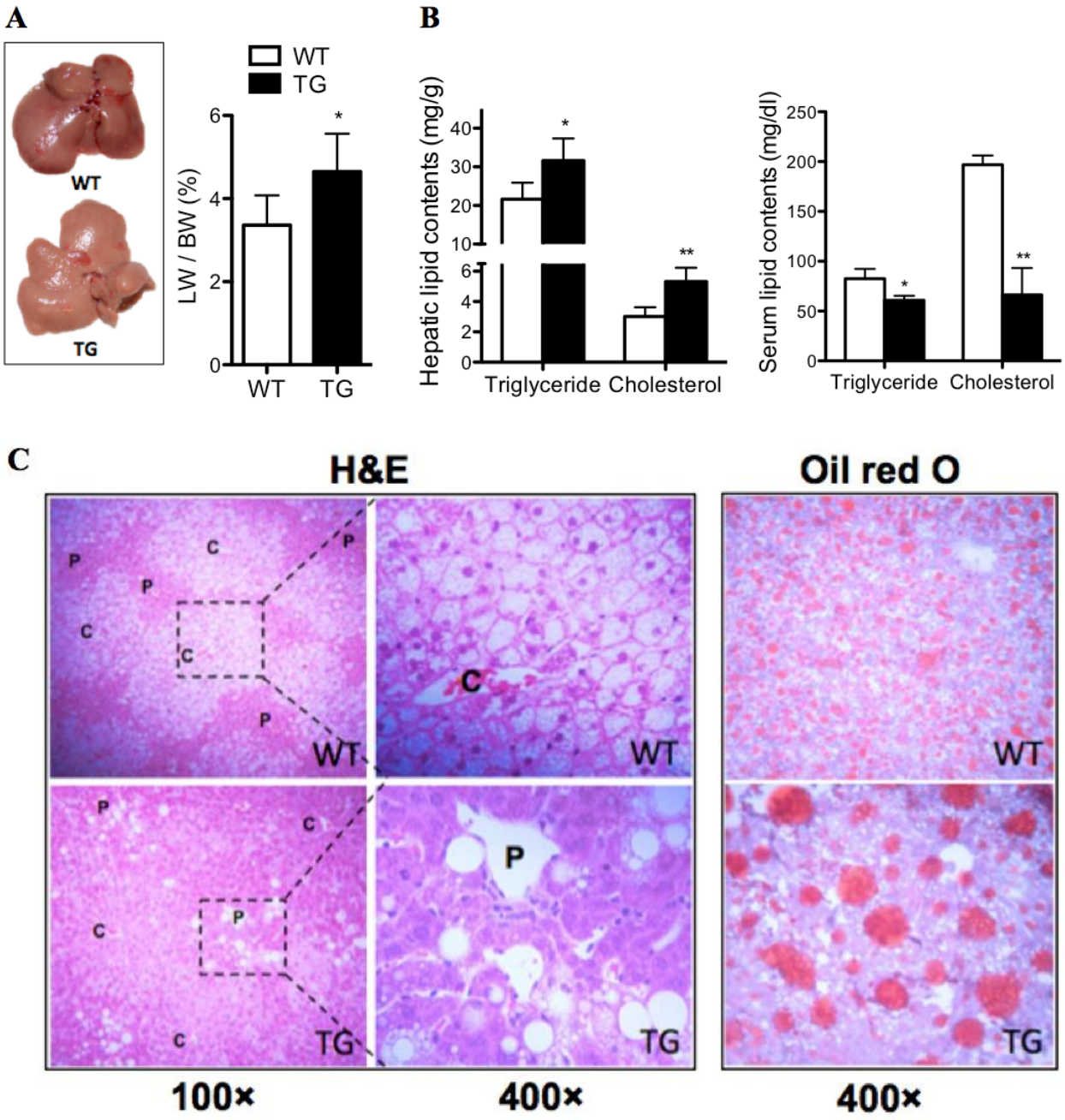

Figure 7. Activation of AHR exacerbated high-fat diet induced steatosis.
(A to C) WT and AHR transgenic (TG) mice were fed with HFD for 12 weeks. Shown are the gross appearance of the livers (left) and liver weight (LW) to body weight (BW) ratio (right) at the end of HFD feeding (A); hepatic (left) and serum (right) triglyceride and cholesterol contents measured at 500 nm (B); H&E staining (left, 100× and 400×) and Oil-red O staining (right, 400×) of the liver sections (C), C indicates central vein, and P indicates portal vein. N=5 for each group. *, $P<0.05$; **, $P<0.01$, TG vs. WT. Results are presented as means ± standard error of the mean (SEM).

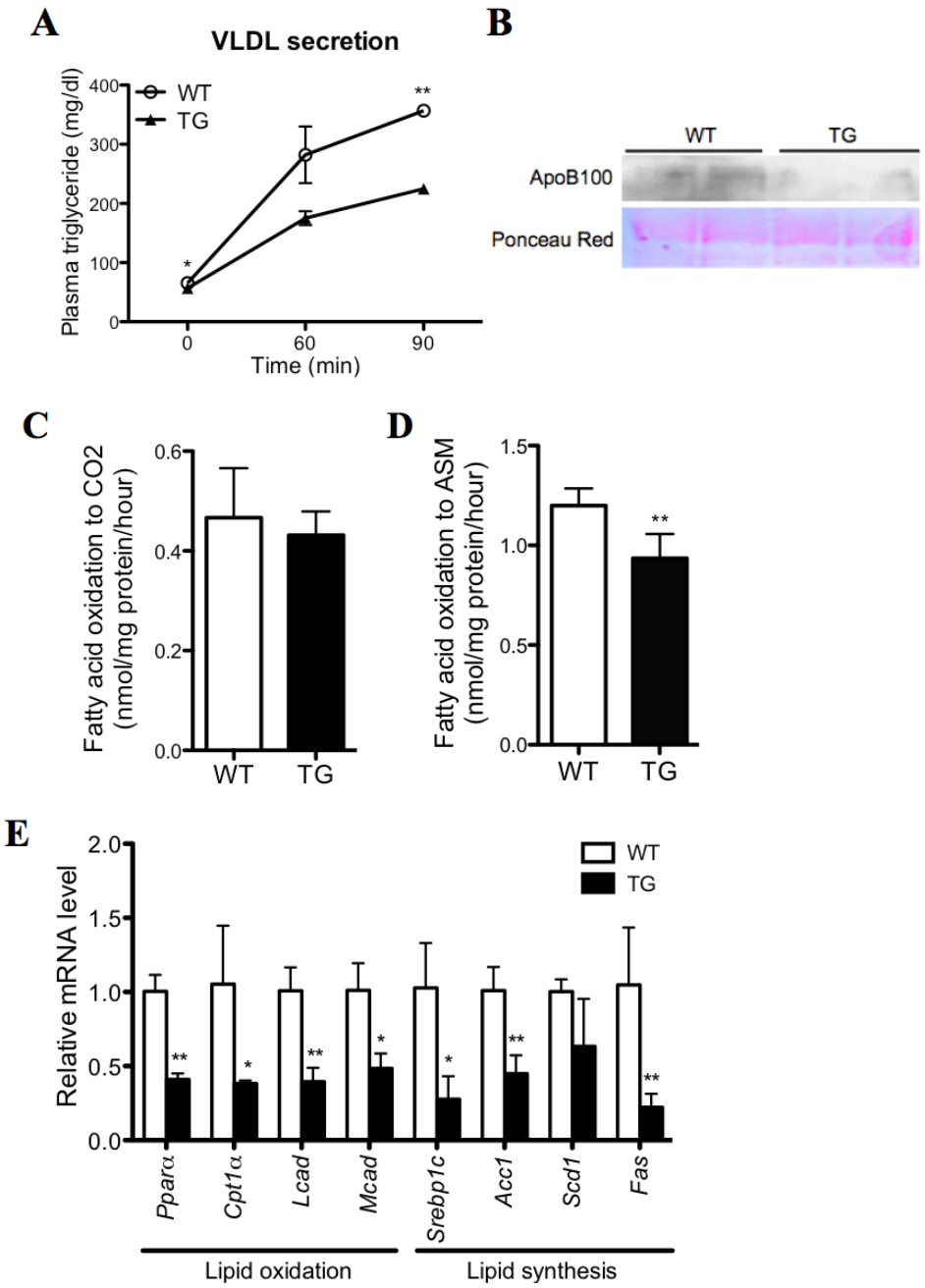

Figure 8. Decreased VLDL-triglyceride secretion and decreased fatty acid oxidation in TG mice.
(A) Mice were fasted for 4 h before receiving an intravenous injection of tyloxapol, a lipoprotein lipase inhibitor at 500 mg/kg body weight. Tail vein blood samples were collected at 0, 60, and 90 min after the tyloxapol injection, and plasma triglyceride levels were measured at 500 nm. (B) Western blotting showing a decreased ApoB100 protein level in the serum of fasted TG mice, and ponceau red staining for internal control. (C) Complete fatty acid oxidation to CO_2 and (D) incomplete fatty acid oxidation to acid soluble metabolites (ASM) in liver homogenates assessed by liquid scintillation counting of [^{14}C]-CO_2 and [^{14}C]-ASM, respectively. (E) mRNA expressions of lipid oxidation genes and lipogenic genes. N=5 for each group. *, P<0.05; **, P<0.01, TG vs. WT. Results are presented as means ± standard error of the mean (SEM).

2.5.4 AHR Transgenic Mice Were Protected from Diet-induced Obesity and Insulin Resistance

To our surprise, despite their exacerbated hepatosteatosis, the TG mice showed protection from diet-induced obesity and insulin resistance. Upon HFD feeding, the TG mice gained less body weight (Fig. 9A). At the end of the 12-week HFD feeding, TG mice were visibly leaner (Fig. 9B), and the lower body weight was accounted for largely by a reduction in the fat mass without affecting the lean mass (Fig. 9C). The difference in adiposity was not attributable to a reduction in food intake (Fig. 9D). The TG mice had lower fasting glucose (Fig. 10A) and insulin levels (Fig. 10B), as well as improved performance in glucose tolerance test (GTT) (Fig. 10C) and insulin tolerance test (ITT) (Fig. 10D), suggesting insulin hypersensitivity in these mice. However, the tissue sensitivity to insulin could not be directly assessed by GTT or ITT, and a hyperinsulinemic-euglycemic clamp may be further needed (91). These phenotypes seen in diet-induced mice were transgene dependent, because they were normalized in TG mice treated with DOX to silence the transgene expression (Fig. 13A-13C).

2.5.5 The Pleotropic Effects of AHR in Improving Metabolic Function

Although the AHR transgene was targeted to the liver, we observed metabolic benefits in multiple extrahepatic tissues, including adipose tissues and skeletal muscle. Obesity is associated with an increase in macrophage infiltration in adipose tissue (92). Consistent with their reduced size of visceral fat pad (Fig. 11A, left panel), the HFD-fed TG mice showed smaller adipocyte size and lower macrophage infiltration as shown by less crown-like structures (Fig. 11A, right

panel), which was supported by their decreased expression of macrophage marker genes F4/80 and CD68 (Fig. 11B).

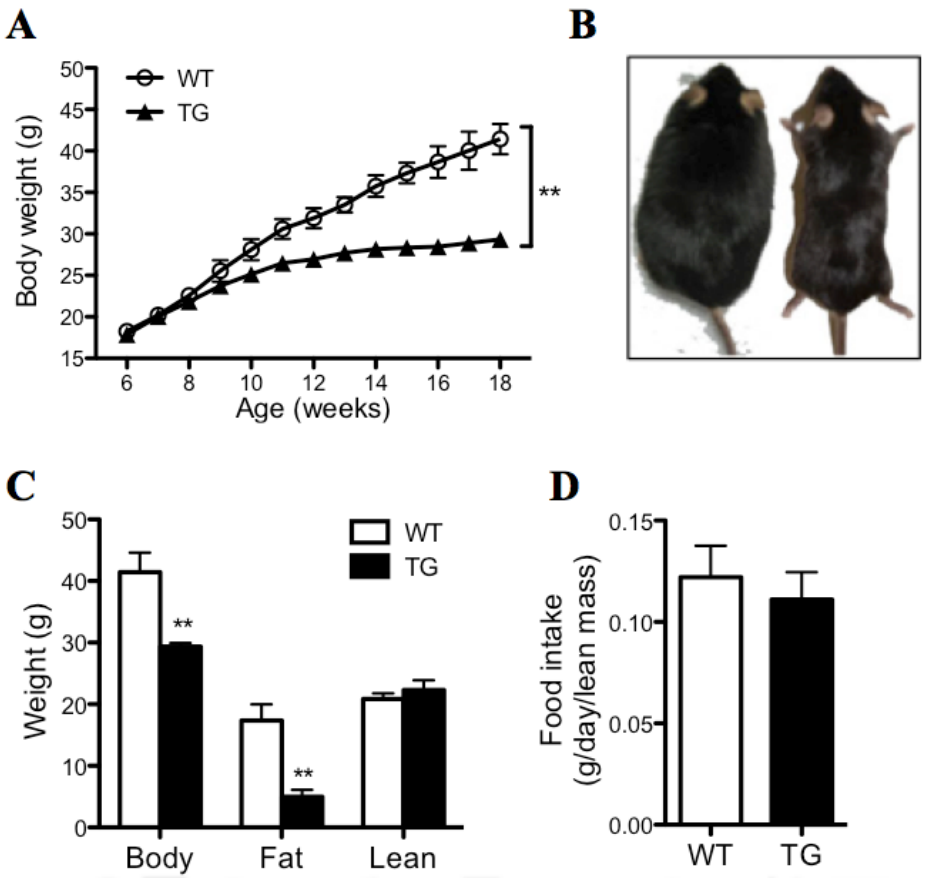

Figure 9. AHR transgenic mice were protected from diet-induced obesity.
WT and TG mice were fed with HFD for 12 weeks starting from 6 weeks old. (A) Body weights of mice during HFD challenge. (B) Appearance of WT and TG mice at the end of HFD feeding. (C) Body composition with fat and lean mass weights measured by EchoMRI. (D) Food intake measured between 10- and 12-week of HFD feeding. N=5 for each group. **, $P<0.01$, TG vs. WT. Results are presented as means ± standard error of the mean (SEM).

Reduction in fat mass without affecting food intake suggested an increase in energy expenditure. Indeed, both the oxygen consumption (Fig. 11C, left panel) and energy expenditure (Fig. 11C, right panel) were significantly higher in TG mice, which were normalized upon DOX treatment (Fig. 13D). There was also an increase in resting rectal temperature in TG mice (Fig. 11D), another indicator of increased energy expenditure and thermogenesis. The brown adipose

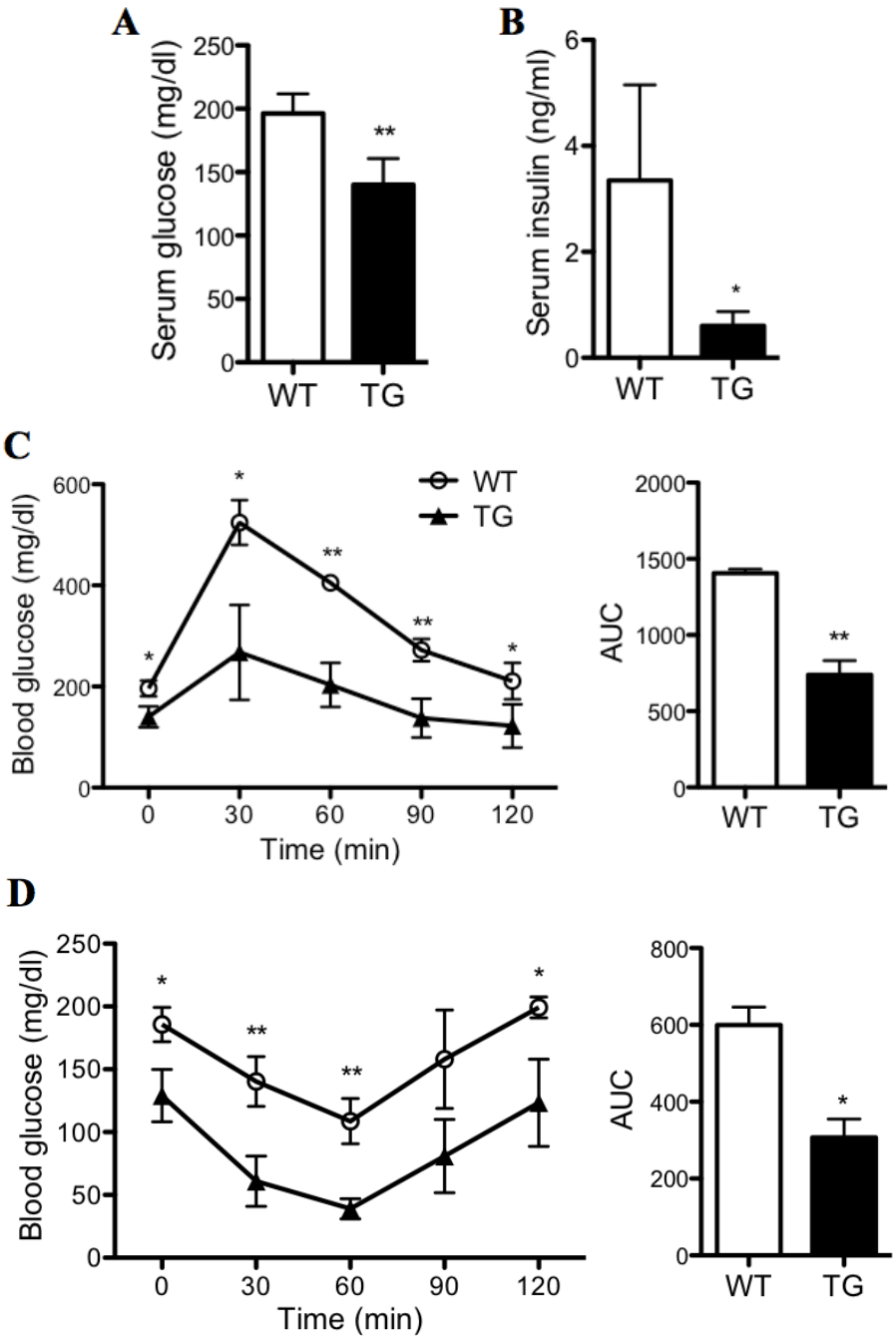

Figure 10. AHR transgenic mice were protected from diet-induced insulin resistance.
WT and TG mice were fed with HFD for 12 weeks starting from 6 weeks old. Mice were fasted overnight before measurements. (A) Fasting serum glucose levels were measured by the glucose meter. (B) Fasting serum insulin levels were measured by insulin-ELISA. (C to D) Glucose tolerance test (GTT) (C) and insulin tolerance test (ITT) (D) after overnight fasting. Area under curve (AUC) was calculated by the area between the curve and the x-axis. N=5 for each group. *, $P<0.05$; **, $P<0.01$, TG vs. WT. Results are presented as means ± standard error of the mean (SEM).

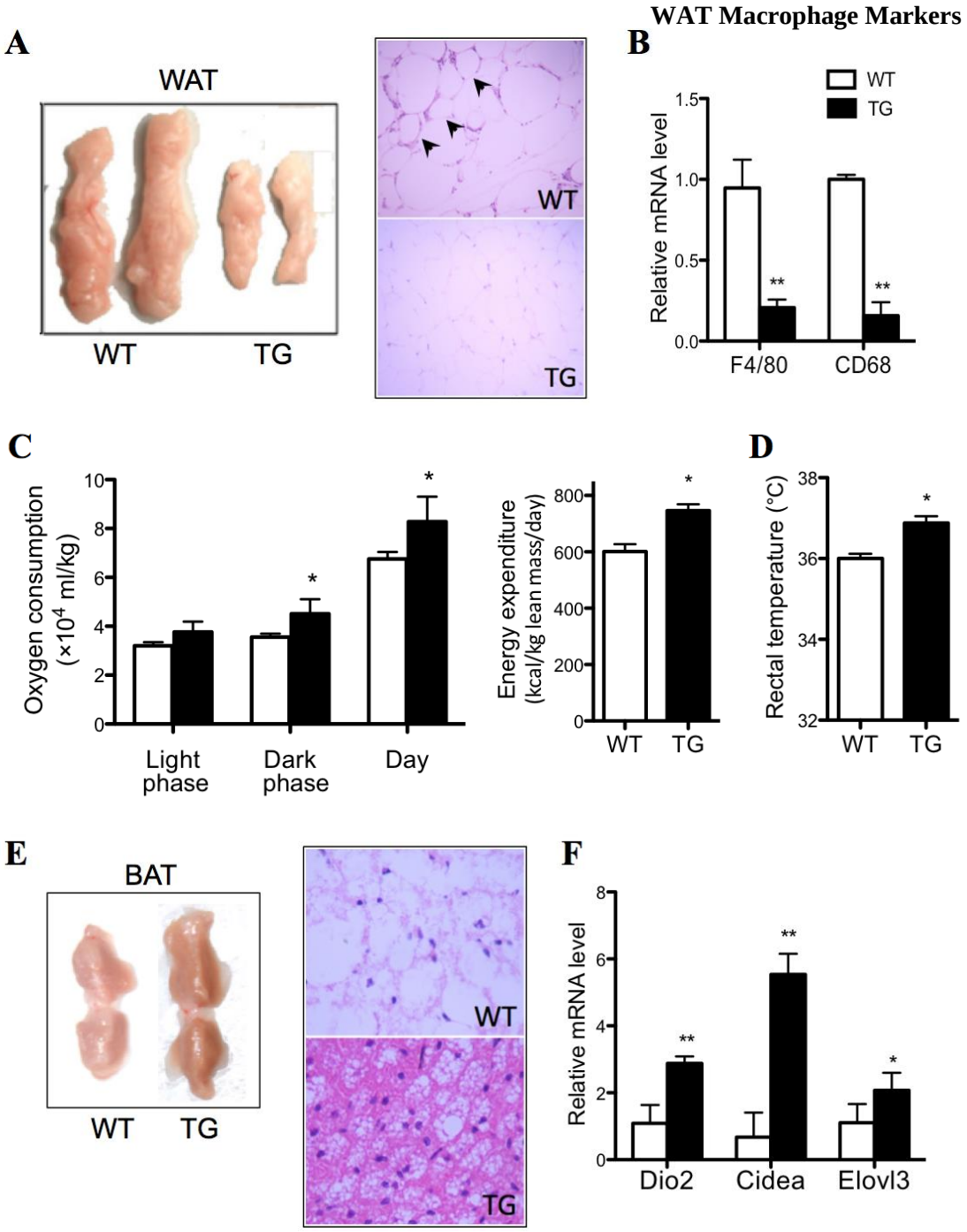

Figure 11. The pleotropic effects of AHR in improving metabolic function.
WT and TG mice were fed with HFD for 12 weeks starting from 6 weeks old, and tissues were harvested at the end of HFD feeding. (A) Representative appearance (left) and H&E staining (right, 400×) of visceral fat tissues. Arrowheads indicate the crown-like structures, which are characteristic of macrophage infiltration. (B) White adipose tissue (WAT) expression of macrophage markers. (C) Measurements of oxygen consumption (left) and energy expenditure (right) using the Oxymax Indirect Calorimetry System. (D) Rectal tempeature measured by thermometer. (E) Representative appearance (left) and H&E staining (right, 400×) of brown fat tissue (BAT). (F) BAT expression of thermogenic markers. N=5 for each group. *, $P<0.05$; **, $P<0.01$, TG vs. WT. Results are presented as means ± standard error of the mean (SEM).

tissue (BAT) plays an important role in thermogenesis. The TG BAT was obviously browner (Fig. 11E, left panel), which was supported by smaller adipocytes with smaller lipid droplets (Fig. 11E, right panel), and increased expression of BAT marker genes Dio2, Cidea and Elovl3 (Fig. 11F).

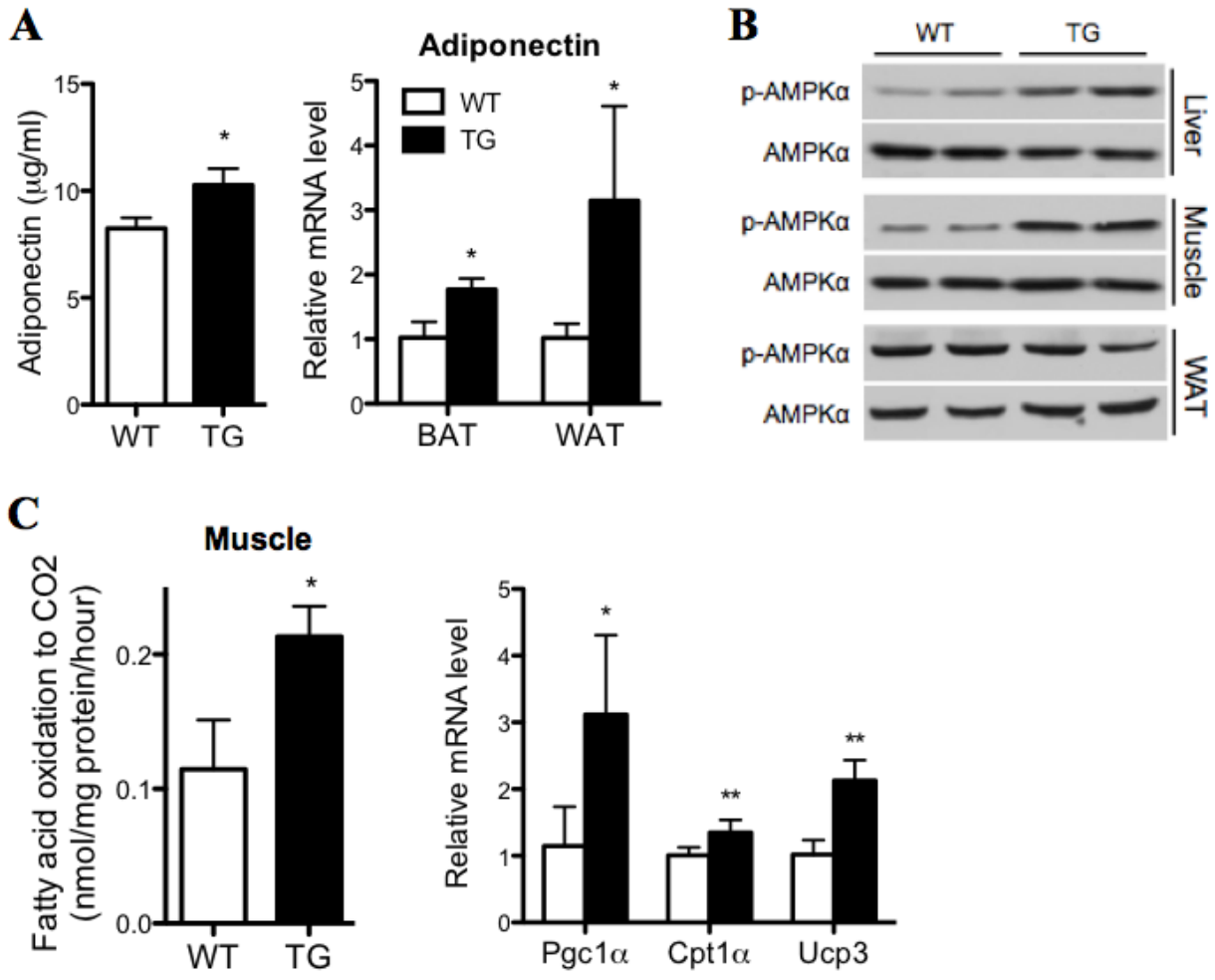

Figure 12. The pleotropic effects of AHR in improving metabolic function.
WT and TG mice were fed with HFD for 12 weeks starting from 6 weeks old, and tissues were harvested at the end of HFD feeding. (A) Serum adiponectin level measured by adiponectin-ELISA, and adipose expression of adiponectin. (B) Western blotting of p-AMPKα and total AMPKα in liver, muscle, and WAT. (C) Complete fatty acid oxidation to CO_2 in skeletal muscle homogenates (left) assessed by liquid scintillation counting of [^{14}C]-CO_2, and muscular expression of β-oxidation genes (right). N=5 for each group. *, P<0.05; **, P<0.01, TG vs. WT. Results are presented as means ± standard error of the mean (SEM).

We also observed an increased serum level and adipose expression of adiponectin (Fig. 12A), an adipokine known to have anti-inflammatory activity and improve insulin sensitivity (93). AMP-activated protein kinase (AMPK) is a key player in regulating energy metabolism (94). We observed an elevated AMPKα phosphorylation/activation in the liver and skeletal muscle, but not the white adipose tissue (WAT), of TG mice (Fig. 12B), which was normalized upon DOX treatment (Fig. 13E). AMPK activation is known to promote fatty acid oxidation in the skeletal muscle (95). Indeed, the complete fatty acid oxidation rate in TG muscle was significantly increased (Fig. 12C, left panel), which was associated with an increased expression of Pgc1α, Cpt1α and Ucp3 (Fig. 12C, right panel).

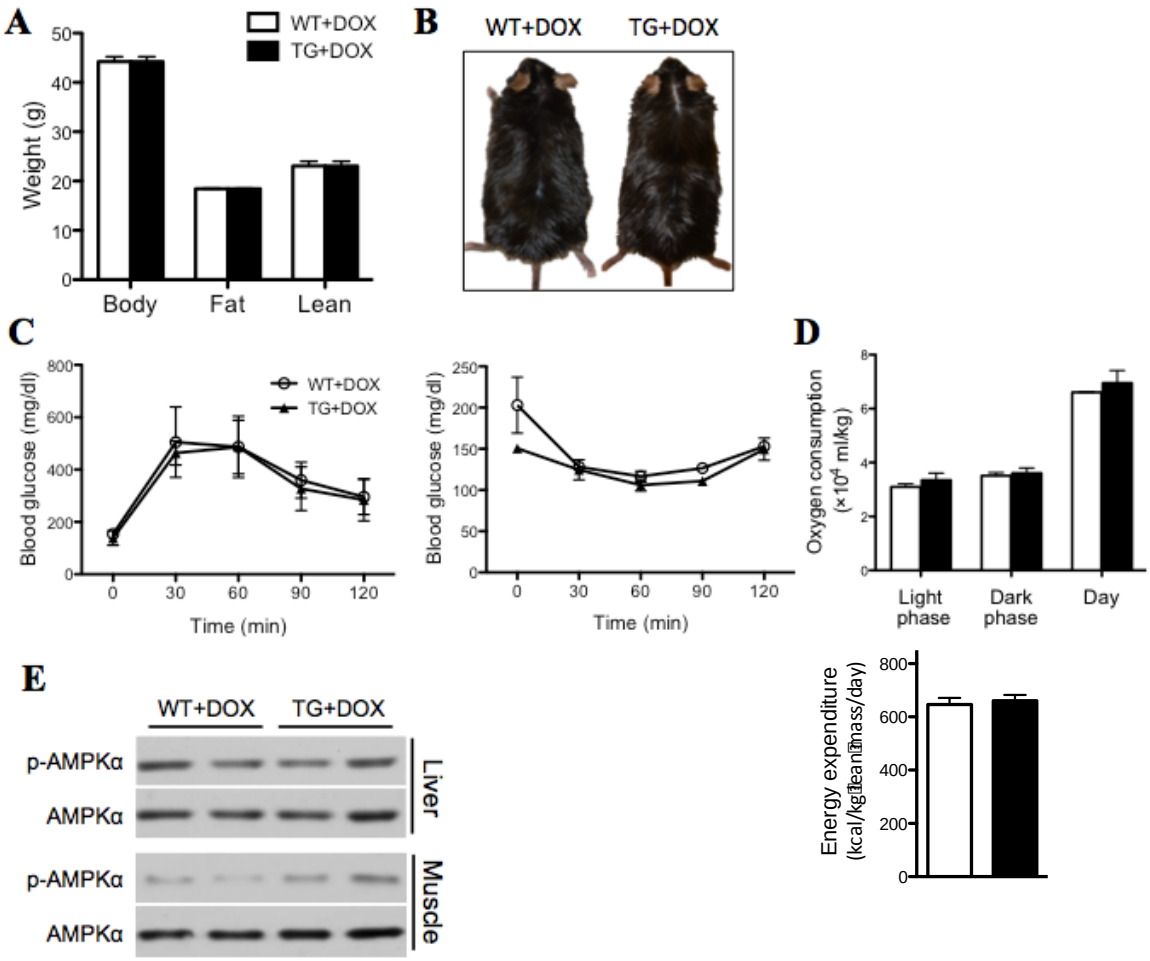

Figure 13. The metabolic benefits of the transgene were normalized upon DOX treatment.
WT and TG mice were fed with HFD for 12 weeks starting from 6 weeks old, and DOX (1mg/ml) was given in drinking water starting from 6 weeks old. Tissues were harvested at the end of HFD feeding. Body, fat mass, and lean mass weights (A) and appearance of mice (B) at the end of HFD feeding. (C) Glucose tolerance test (GTT) (left) and insulin tolerance test (ITT) (right) performed at 10-week HFD feeding after overnight fasting. (D) Oxygen consumption (top) and energy expenditure (bottom) measred using the Oxymax Indirect Calorimetry System. (E) Western blotting of hepatic and muscular p-AMPKα and total AMPKα. N=5 for each group. Results are presented as means ± standard error of the mean (SEM).

2.5.6 Activation of AHR Induced the Expression of FGF21

The pronounced dissociation of hepatosteatosis from insulin resistance and the pleotropic metabolic benefits observed in our TG mice prompted us to examine the underlying mechanism. We found that both the hepatic mRNA (Fig. 14A) and protein expression (Fig. 14B) and

circulating concentration (Fig. 14C) of FGF21, a metabolic peptide hormone secreted predominantly by hepatocytes (96), were significantly increased in both the chow-fed and HFD-fed TG mice. The FGF21 induction was liver-specific, because the induction was not seen in WAT and BAT (Fig. 14D). Both the serum level and hepatic expression of FGF21 in the TG mice were normalized upon DOX treatment (Fig. 15A, 15B, and 15C).

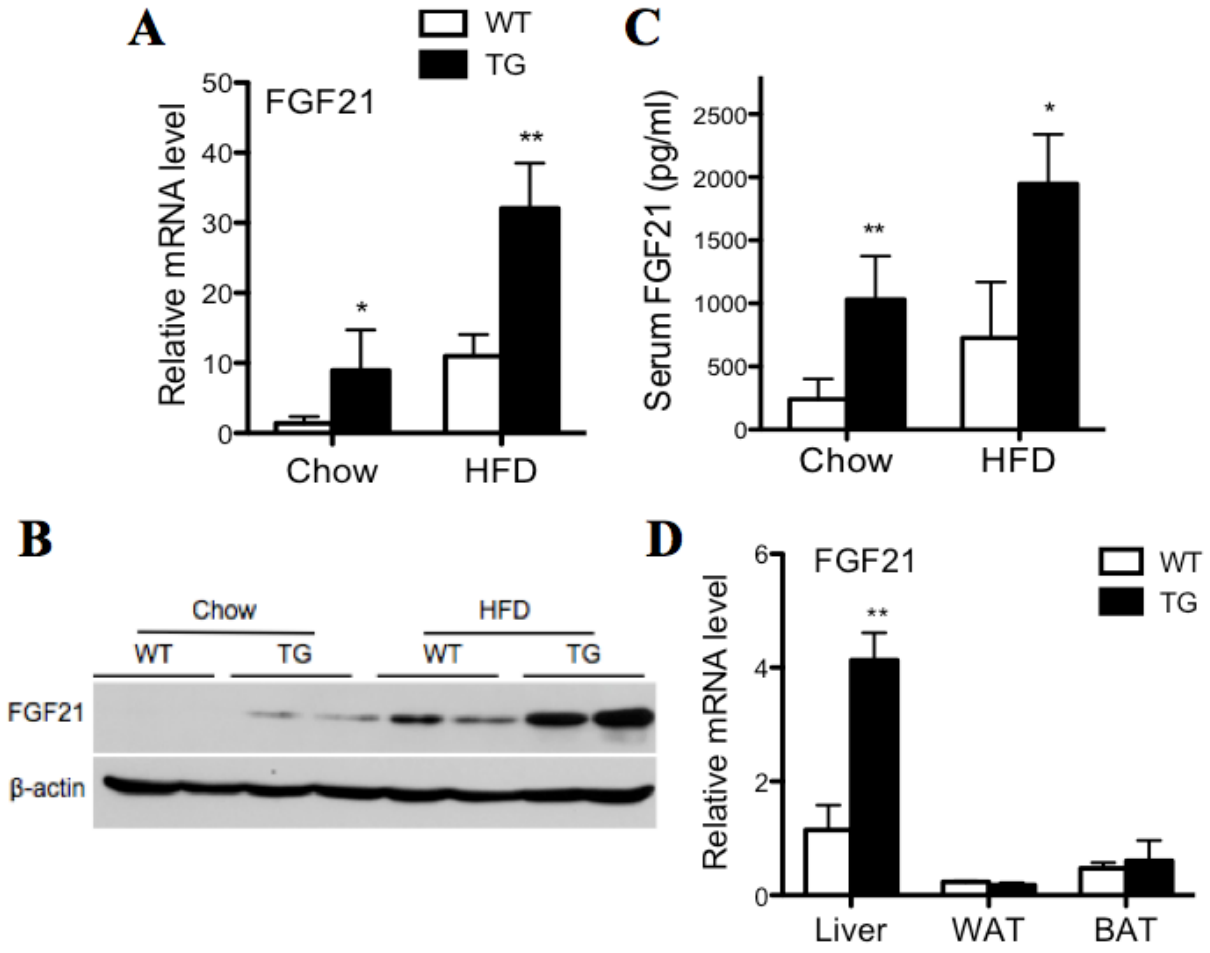

Figure 14. Activation of AHR induced the expression of FGF21.
Mice were fed with chow diet for 6 weeks, or HFD for 12 weeks starting at 6 weeks old. Tissues were harvested at the end of the HFD feeding. (A to C) Hepatic mRNA expression (A), Western blotting (B), and serum level (C) of FGF21 measured by FGF21-ELISA. (D) mRNA expression of FGF21 in tissues (liver, WAT, and BAT) of mice fed with HFD for 12 weeks. N=5 for each group. *, $P<0.05$; **, $P<0.01$, TG vs. WT. Results are presented as means ± standard error of the mean (SEM).

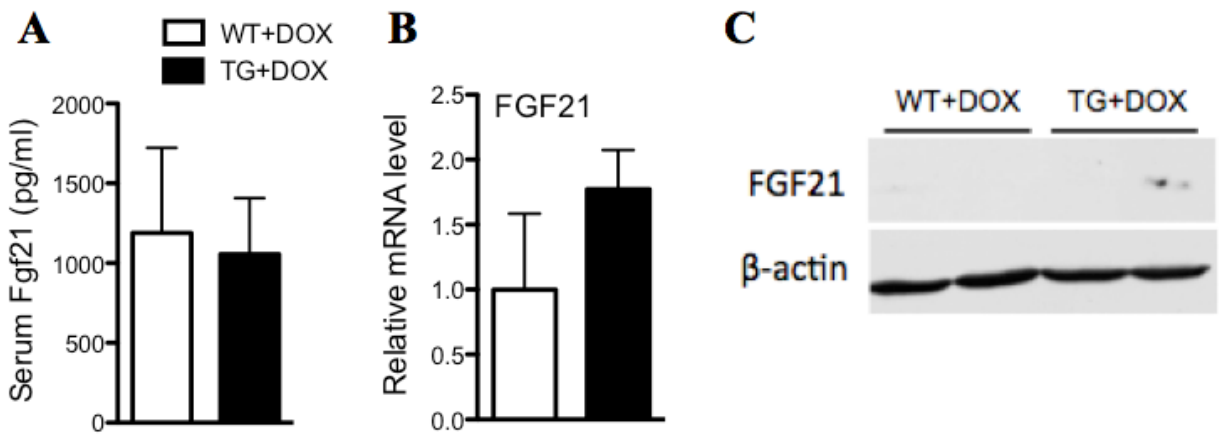

Figure 15. The AHR responsive induction of FGF21 was abolished upon DOX treatment.
WT and TG mice were fed with HFD for 12 weeks starting from 6 weeks old, and DOX (1mg/ml) was given in drinking water starting from 6 weeks old. Tissues were harvested at the end of HFD feeding. (A to C) Serum level (A), hepatic mRNA expression (B), and Western blotting (C) of FGF21. N=5 for each group. Results are presented as means ± standard error of the mean (SEM).

2.5.7 Knockdown of FGF21 Abolished the Metabolic Benefits of AHR

To understand the functional relevance of FGF21 induction, WT and TG mice were fed with HFD for 6 weeks before receiving an intravenous injection of adenovirus expressing short hairpin RNA targeting FGF21 (Ad-shFGF21) or the control LacZ gene (Ad-shLacZ) (83). The FGF21 knockdown was validated at mRNA, protein and circulating levels (Fig. 16A, 16B, and 16C). The lower body weight of TG mice was unchanged after FGF21 knockdown (Fig. 16D). We found that FGF21 knockdown abolished the transgenic effects in lowering fasting glucose levels (Fig. 16E) as well as improving glucose tolerance (Fig. 16F).

Upon FGF21 knockdown, the extrahepatic benefits of the transgene were also abolished. These included the decreased WAT macrophage infiltration (Fig. 17A) and decreased WAT expression of pro-inflammatory cytokines and macrophage marker genes (Fig. 17B), browning of the BAT (Fig. 17C) and increased expression of BAT marker genes (Fig. 17D), and increased

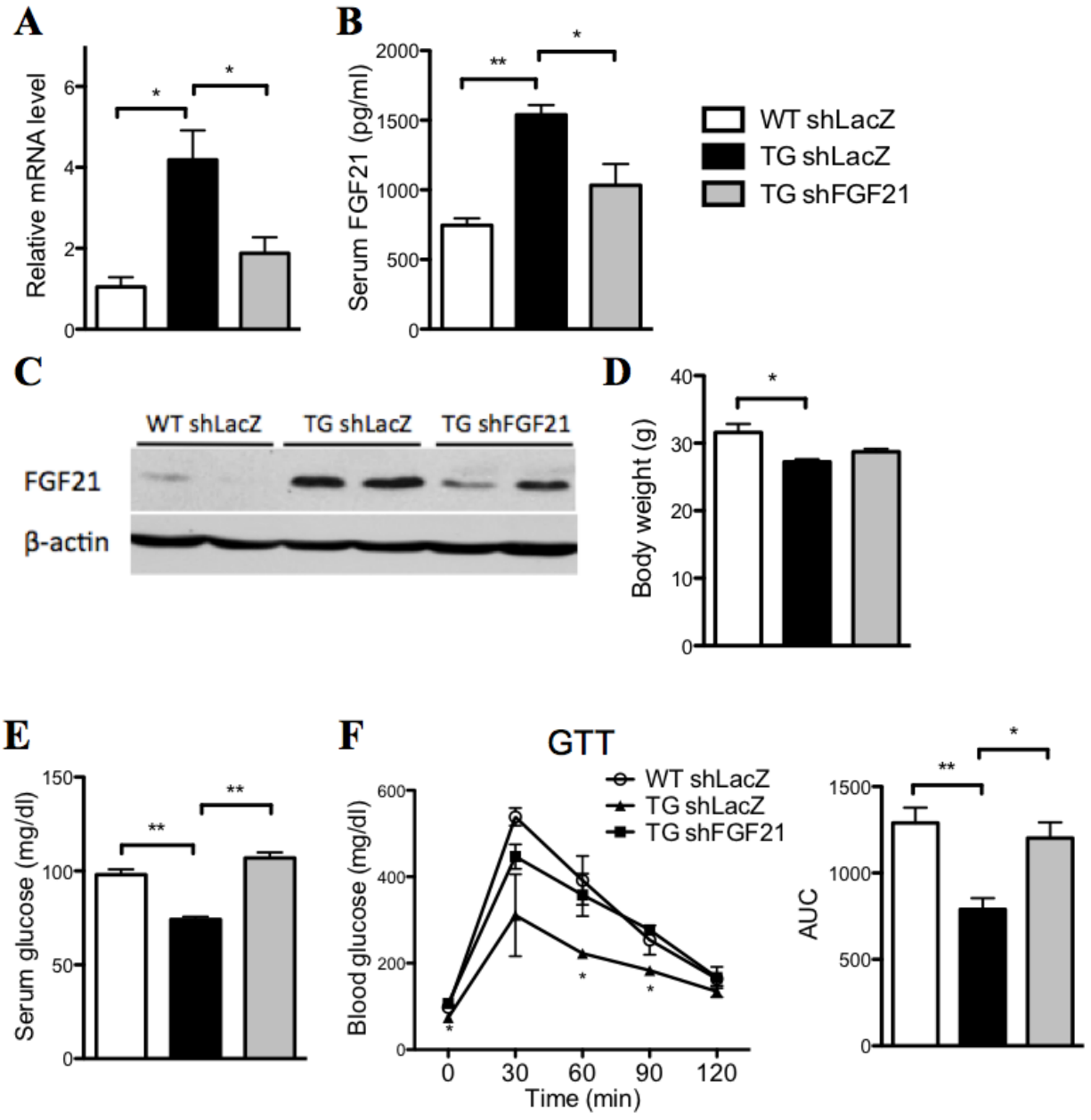

Figure 16. Knockdown of FGF21 abolished the metabolic benefits of AHR.
Mice were fed with HFD for 6 weeks before receiving intravenous injection of Ad-shFGF21 or Ad-shLacZ at 5×10^9 viral particle/gram of body weight for 2 weeks. Tissues were harvested 2 weeks after the viral injection. Shown are hepatic mRNA expression (A), serum level (B), and Western blotting (C) of FGF21; body weight (D) and fasting serum glucose levels (E) 2 weeks after the viral injection; (F) glucose tolerance test (GTT) was performed 1 week after the viral injection, and area under curve (AUC) was calculated by the area between the curve and the x-axis. N=5 for each group. *, $P<0.05$; **, $P<0.01$, TG shLacZ vs. WT shLacZ, or the comparisons are labled. Results are presented as means ± standard error of the mean (SEM).

serum level of adiponectin (Fig. 17E). In the skeletal muscle, the increased complete fatty acid oxidation (Fig. 17F) and the elevated AMPKα phosphorylation (Fig. 17G) were attenuated upon FGF21 knockdown.

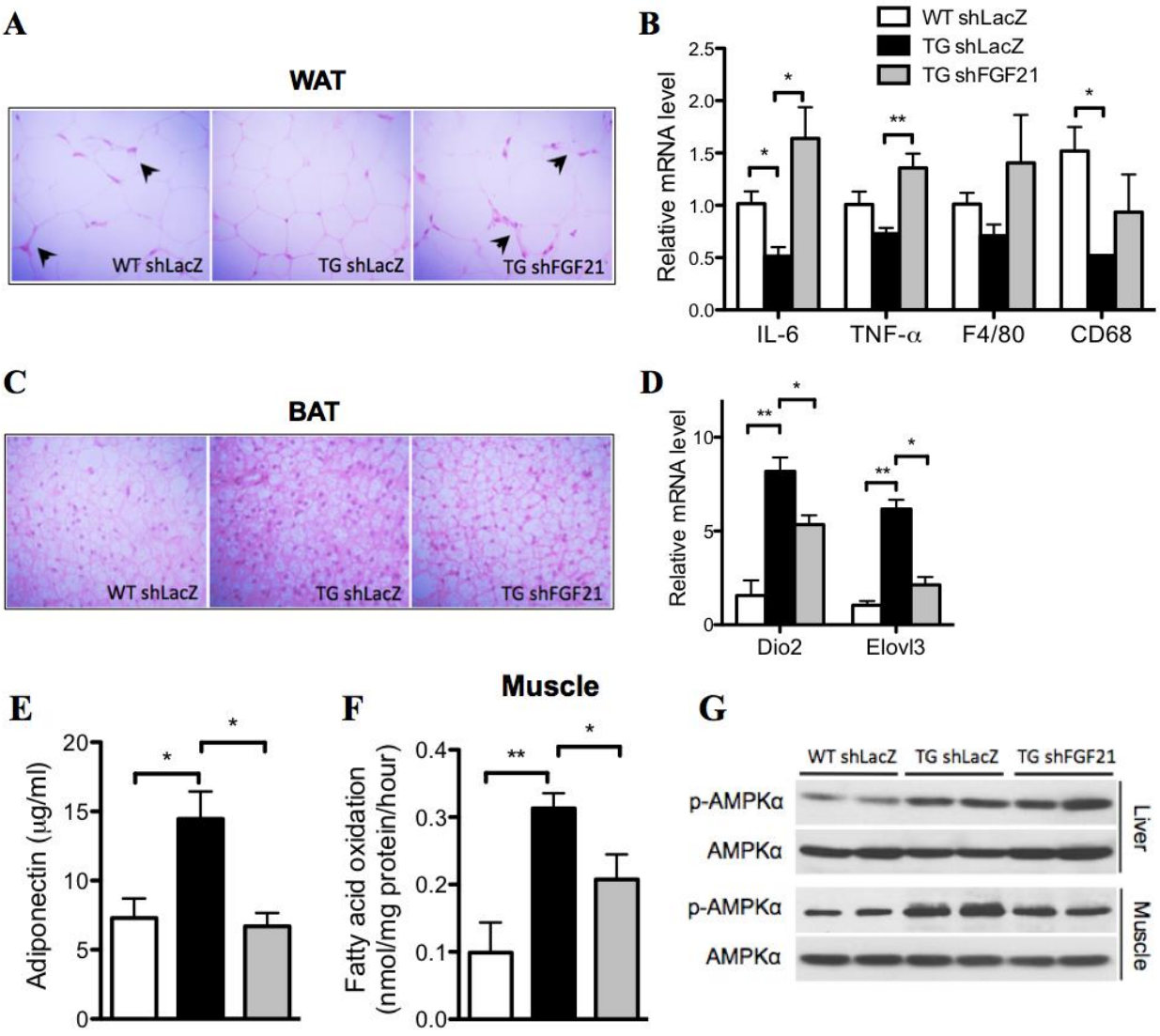

Figure 17. Knockdown of FGF21 abolished the metabolic benefits of AHR in extrahepatic tissues. Mice were fed with HFD for 6 weeks before receiving intravenous injection of Ad-shFGF21 or Ad-shLacZ at 5×10^9 viral particle/gram of body weight for 2 weeks. Tissues were harvested 2 weeks after the viral injection. (A and B) H&E staining (400×) (A) and expression of inflammatory marker genes (B) in WAT. Arrowheads indicate the crown-like structures. (C and D) H&E staining (400×) (C) and expression of thermogenic markers (D) in BAT. (E) Serum adiponectin levels measured by adiponectin-ELISA. (F) Complete fatty acid oxidation to CO_2 in skeletal muscle homogenates assessed by liquid scintillation counting of $[^{14}C]$-CO_2. (G) Western blotting of hepatic and muscular p-AMPKα and total AMPKα levels. N=5 for each group. *, $P<0.05$; **, $P<0.01$. Results are presented as means ± standard error of the mean (SEM).

2.5.8 FGF21 Knockdown Ameliorated Hepatosteatosis by AHR Activation

Interestingly, the large lipid droplets in HFD-fed TG livers were depleted upon FGF21 knockdown (Fig. 18A, left panel). FGF21 knockdown did not alter the repressed VLDL secretion in TG mice (Fig. 18A, right panel). The elevated hepatic triglyceride and cholesterol contents

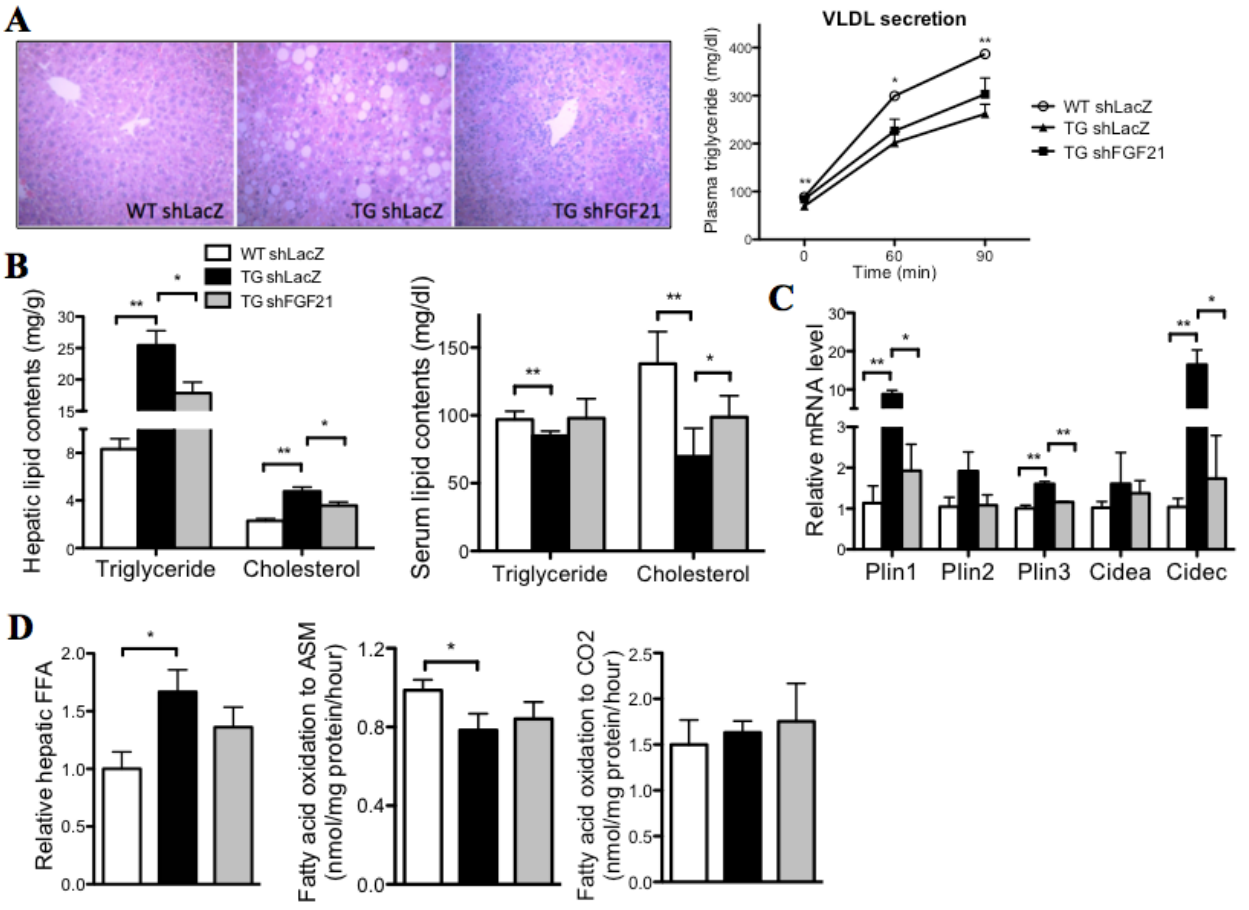

Figure 18. FGF21 knockdown ameliorated hepatosteatosis by AHR activation.
Mice were fed with HFD for 6 weeks before receiving intravenous injection of Ad-shFGF21 or Ad-shLacZ at 5×10^9 viral particle/gram of body weight for 2 weeks. Tissues were harvested 2 weeks after the viral injection. (A) H&E staining of liver tissues (left, 400×) and VLDL-triglyceride secretion rate measured by serum triglyceride levels at 500 nm at 0, 60, and 90 min after tyloxapol injection (right). (B) Hepatic (left) and serum (right) triglyceride and cholesterol contents. (C) Hepatic mRNA expression of lipid droplet associated genes. (D) Hepatic free fatty acid (FFA) contents measured by LC-MS method (left), complete hepatic fatty acid oxidation to CO_2 (middle), and incomplete hepatic fatty acid oxidation to acid soluble metabolites (ASM) (right) assessed by liquid scintillation counting of [^{14}C]-CO_2 and [^{14}C]-ASM, respectively. N=5 for each group. *, P<0.05; **, P<0.01, TG shLacZ vs. WT shLacZ, or the comparisons are labled. Results are presented as means ± standard error of the mean (SEM).

were decreased after FGF21 knockdown (Fig. 18B), which was associated with increased serum levels of triglycerides and cholesterol (Fig. 18B). Consistent with the decreased lipd droplet size, the induction of several lipid droplet-associated genes observed in shLacZ-infected TG mice, including Plin1, Plin3, and Cidec, was decreased in shFGF21-infected TG mice (Fig. 18C). The hepatic FFA concentrations (Fig. 18D, left panel) and fatty acid oxidation rate (Fig. 18D, right panel) in TG mice were not affected by FGF21 knockdown.

2.5.9 FGF21 Knockdown Exacerbated Liver Damage in CA-AHR Mice

Paradoxically, the depleted lipid droplets in shFGF21-infected TG livers was associated with hepatotoxicity as supported by increased hepatocyte degeneration and lymphocyte infiltration (Fig. 18A, left panel), increased expression of pro-inflammatory genes (Fig. 19A), increased serum IL-6 level (Fig. 19B), and increased serum ALT level (Fig. 19C). The hepatic concentrations of lipid intermediates diacylglycerol and ceramide, both of which are known to be lipotoxic (97, 98), were not affected in TG mice (data not shown).

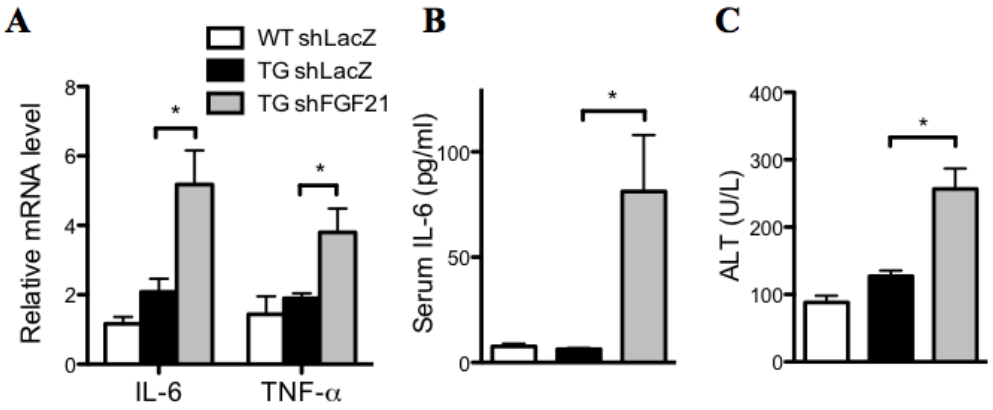

Figure 19. FGF21 knockdown exacerbated liver damage in CA-AHR mice.
Mice were fed with HFD for 6 weeks before receiving intravenous injection of Ad-shFGF21 or Ad-shLacZ at 5×10^9 viral particle/gram of body weight for 2 weeks. Tissues were harvested 2 weeks after the viral injection. (A) Hepatic mRNA expression of pro-inflammatory cytokines. (B) Serum level of IL-6 measured by IL-6-ELISA. (C) Serum ALT level. N=5 for each group. *, $P<0.05$. Results are presented as means ± standard error of the mean (SEM).

2.5.10 FGF21 is a Direct Transcriptional Target of AHR

The induction of FGF21 was also observed in WT mice acutely treated with TCDD, and this induction was abolished in AHRKO mice (Fig. 20A). These results, together with the FGF21 induction in TG mice, strongly suggested FGF21 as an AHR target gene. To directly test whether FGF21 is an AHR target gene, we cloned the human and mouse FGF21 gene promoters and evaluated their regulation by AHR. Inspection of the promoters revealed two putative dioxin responsive elements (DREs) in the hFGF21 gene promoter and one DRE in the mFGF21 gene promoter, whose bindings to the AHR-ARNT heterodimers or the CA-AHR-ARNT heterodimers were confirmed by EMSA (Fig. 20B). To confirm the recruitment of CA-AHR onto the hFGF21 gene promoter *in vivo*, we performed ChIP assay on cells transfected with Flag-CA-AHR. As shown in Fig. 20C, CA-AHR specifically recruited to the two DRE-franking regions, but not the control non-DRE region. The *in vivo* recruitment of CA-AHR onto the mFGF21 gene promoter was confirmed by ChIP assay in WT mice whose livers were hydrodynamically transfected with Flag-CA-AHR (Fig. 20D). The transactivation of the FGF21 gene promoters by AHR was evaluated by luciferase reporter gene assays. As shown in Fig. 20E, the 2-kb hFGF21 gene promoter was transactivated by CA-AHR or AHR in the presence of the AHR agonist 3-MC, whereas this activation was abolished when the region containing both DREs was deleted. A similar pattern of results was obtained when the mFGF21 gene promoter was evaluated (Fig. 20F).

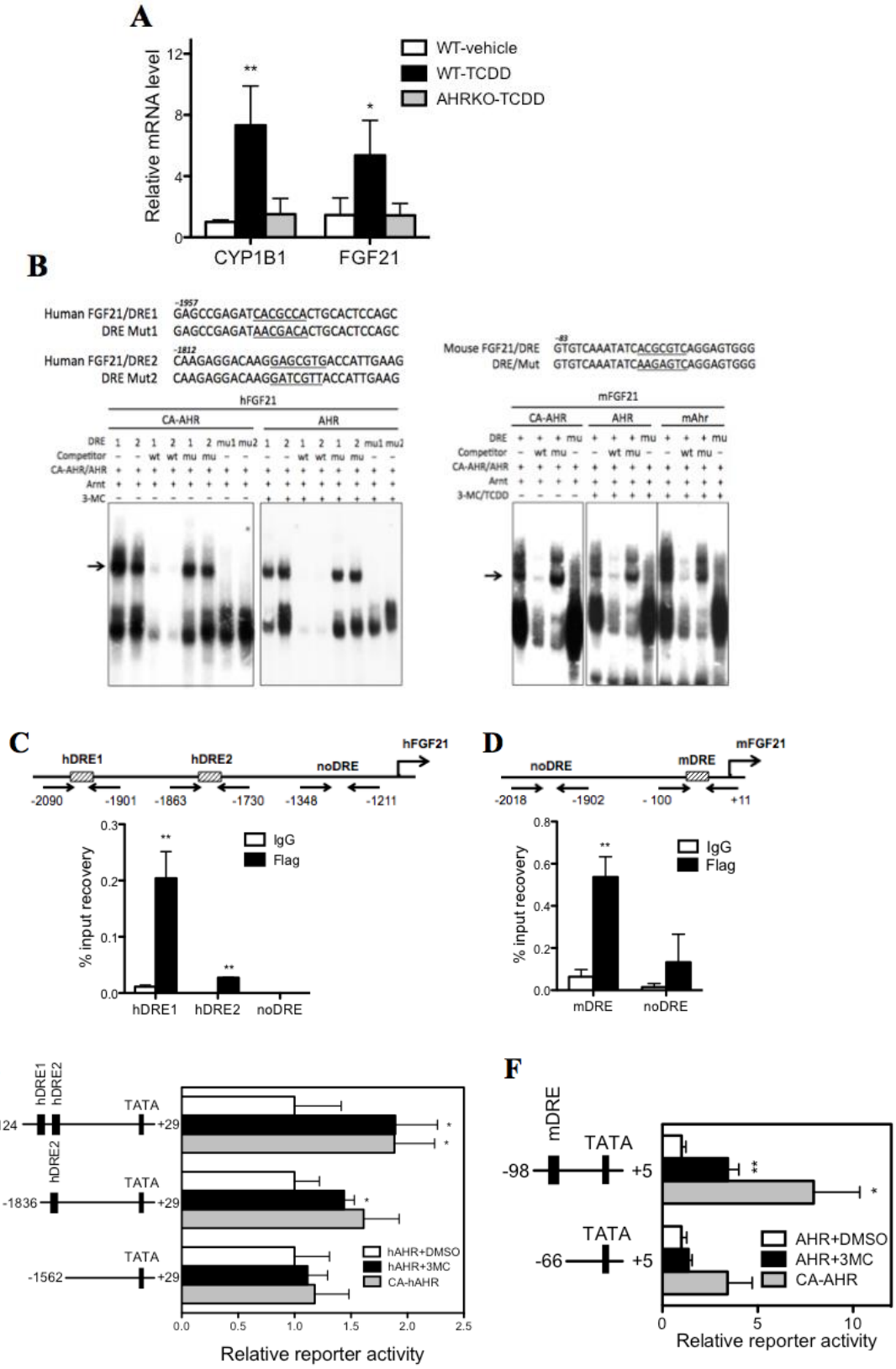
A
Relative mRNA level
WT-vehicle
WT-TCDD
AHRKO-TCDD
CYP1B1
FGF21
B
Human FGF21/DRE1 GAGCCGAGATCACGCCACTGCACTCCAGC
DRE Mut1 GAGCCGAGATAACGACACTGCACTCCAGC
Human FGF21/DRE2 CAAGAGGACAAGGAGCGTGACCATTGAAG
DRE Mut2 CAAGAGGACAAGGATCGTTACCATTGAAG
Mouse FGF21/DRE GTGTCAAATATCACGCGTCAGGAGTGGG
DRE/Mut GTGTCAAATATCAAGAGTCAGGAGTGGG
hFGF21
CA-AHR
AHR
mFGF21
mAhr
C
hDRE1
hDRE2
noDRE
hFGF21
% input recovery
IgG
Flag
D
noDRE
mDRE
mFGF21
E
hDRE1
hDRE2
TATA
hAHR+DMSO
hAHR+3MC
CA-hAHR
Relative reporter activity
F
mDRE
TATA
AHR+DMSO
AHR+3MC
CA-AHR
Relative reporter activity

Figure 20. FGF21 is a direct transcriptional target of AHR.
(A) Eight-week old WT and AHR knockout (AHRKO) mice were treated with a single dose of TCDD (30 μg/kg) and sacrificed 4 h later. The hepatic mRNA expression of CYP1B1 and FGF21. (B) The sequences of human and mouse FGF21 DREs and their mutant variants (top) and EMSA results (bottom). (C and D) ChIP assay in triplicate groups to show the recruitment of CA-AHR onto the human (C) and mouse (D) FGF21 promoters. 293 cells were transfected with pCMX-Flag-CA-AHR in (C) and WT mouse livers (N=5 for each group) were hydrodynamically transfected with pCMX-Flag-CA-AHR in (D). (E and F) Activation of the human (E) and mouse (F) FGF21 promoter reporter genes by AHR in the presence of 3-methylcholanthrene (3-MC), or by CA-AHR without an exogenously added ligand. HepG2 cells were co-transfected with indicated reporters and receptors. Transfected cells were treated with vehicle DMSO or 3-MC (4 μM) for 24 h before luciferase assay in triplicate groups. *, $P<0.05$; **, $P<0.01$. Results are presented as means ± standard error of the mean (SEM).

2.6 DISCUSSION

One of our most interesting findings in this study is the revelation of the AHR-FGF21 pathway and the implication of this regulation in conferring the metabolic benefit of AHR activation. FGF21, a peptide hormone and a potential therapeutic agent for diabetes, is known to have multiple metabolic benefits including reducing body weight and improving insulin sensitivity (85). We showed the induction of FGF21 was transgene specific, because silencing of the transgene normalized the induction and attenuated the metabolic benefit. We also showed, through the FGF21 knockdown, that FGF21 was required for the metabolic benefit of the transgene. The increased circulating level of FGF21 may have contributed to the pleotropic and extrahepatic benefits of the liver-specific AHR activation, such as those observed in the adipose tissues and skeletal muscle. The increased adipose expression and circulating level of adiponectin in TG mice were consistent with the notion that adiponectin mediates the systemic effects of FGF21 on energy metabolism and insulin sensitivity in skeletal muscle (87). The AMPKα phosphorylation in the liver and skeletal muscle of TG mice was increased, consistent with the report that FGF21 regulates energy homeostasis through the activation of AMPK (99).

Although FGF21 expression can be regulated by PPARα (83, 84), the hepatic expression of PPARα and its downstream target genes was down-regulated in TG mice, suggesting that PPARα was unlikely the mediator for the FGF21 induction in our mice.

Another intriguing finding is the dissociation between hepatosteatosis and insulin resistance in our TG mice. Although paradoxically, several recent studies suggested that hepatosteatosis and insulin resistance can be dissociated. In one such example, liver-specific knockout of the histone deacetylase 3 improved insulin sensitivity despite the hepatosteatosis (100). In another example, overexpressing the acyl-CoA:diacylglycerol acyltransferase 2 in the liver increased lipid accumulation without developing insulin resistance (101). One possibility that accounts for the dissociation is that insulin resistance may reflect inflammation rather than lipid accumulation in the liver (102). Indeed, there was no sign of increased inflammation in the TG liver, despite elevated triglyceride and cholesterol levels and FFA contents, suggesting that these lipids are sequestered in lipid droplets and thus prevented from causing lipotoxicity. In contrast, knockdown of FGF21 may have resulted in rupture of lipid droplets, leading to liver inflammation and toxicity, as well as the masking of insulin hypersensitivity. Our results suggested that in the context of AHR activation, FGF21 may have promoted lipid sequestration and storage into lipid droplets by up-regulating the expression of lipid droplet-associated genes (Fig. 18C), the mechanism of which remains to be understood. Decreased hepatic lipid contents were accompanied by increased serum triglyceride and cholesterol levels in FGF21-depleted TG mice, suggesting that liver fat is redistributed to the periphery.

The lack of increased hepatic fatty acid oxidation in HFD-fed TG mice seemed contradictory to the known function of FGF21 in promoting fatty acid oxidation and tricarboxylic acid cycle flux in the liver (103, 104). However, our TG mice also showed

decreased expression of PPARα and other fatty acid oxidation genes, which was consistent with those observed in transgenic mice expressing the constitutively activated mouse Ahr (49). The mechanism by which AHR supresses faty acid oxidation is unclear. Nevertheless, we reasoned the decreased incomplete oxidation and unchanged complete oxidation were the net result of the opposing effect of FGF21 and AHR on fatty acid oxidation. The absence of change in hepatic fatty acid oxidation after FGF21 knockdown also suggested a limited effect of FGF21 on hepatic fatty acid oxidaiton in our TG mice.

AHR was initially defined as a xenobiotic receptor that regulates drug metabolism. Subsequent observations, such as the developmental defects in AHR null mice (18, 105) and identification of endogenous AHR ligands (28, 106) have suggested equally important endobiotic functions of AHR. More recent studies suggested AHR also plays many other essential biological functions, such as functioning as an E3 ligase (107) and affecting the expansion of human hematopoietic stem cells (108). The typical pharmacological model of AHR activation using TCDD is often associated with toxicity that may affect the data interpretation, especially when the ligand has to be used chronically. Our TG mice offers a unique gain of function model to understand the endobiotic function of AHR without the concern of the toxicity.

Our findings that activation of AHR protected mice from diet-induced obesity and insulin resistance seems contradictory to the other two reports that AHR-null mice displayed enhanced insulin sensitivity and improved glucose tolerance in both normal chow diet- and high fat diet-fed conditions (65, 66). However, one explanation for this discrepancy is that the lack of AHR expression may not be equal to repression of AHR activity. In addition, the disadvantage of using genetic models is the likelihood of causing developmental issues, which may affect the metabolic function as well. Further studies using either AHR agonists or antagonists will better

evaluate the metabolic function of AHR *in vivo*.

FGF21 was demonstrated as a key regulator in the body's adaptation to fasting downstream of PPARα regulation (83, 84). However, fasting-induced FGF21 expression was unchanged in the AHR null mice (data not shown), indicating that the PPARα-FGF21 axis remains intact in the absence of AHR. Rather than physiological changes such as fasting, our study suggests that the AHR-FGF21 pathway is more responsive to exogenous insults. There are varied exogenous AHR ligands persistent in our environment with TCDD being the most potent. In our current study, TCDD is able to induce the expression of FGF21 in an AHR-dependent manor. Moreover, TCDD treatment in mice reproduced hepatic steatosis (49) and peripheral metabolic phenotype (109) as observed in our CA-AHR transgenic mice, revealing the consistency of the pharmacological and genetic manipulations. Furthermore, FGF21 was reported to be up-regulated during acute liver injury by exposure to acetaminophen (110) and/or chronic liver injury by HFD feeding (111), although it is unknown yet whether AHR is indispensable for FGF21 induction in these pathological models.

In summary, we showed that transgenic activation of AHR in the liver alleviated mice from HFD-induced obesity and insulin resistance despite having marked hepatosteatosis. The dissociation between fatty liver and insulin resistance likley has been mediated by the AHR-dependent activation of FGF21. We propose the endocrine hormone FGF21 as an important effector for the endobiotic function of AHR in lipid metabolism and energy homeostasis. Our results also argue that development of non-toxic AHR agonists may be a novel approach in managing metabolic syndrome.

3.0 CHAPTER III: FUNCTION OF AHR IN PROMOTING HEPATIC CARCINOGENESIS

3.1 THE ROLE OF AHR IN HEPATIC CARCINOGENESIS

3.1.1 AHR in Liver Carcinogenesis

TCDD is considered as both a complete epigenetic carcinogen and a potent tumor promoter (12). Rather than a genotoxic carcinogen, TCDD has proven to be particularly effective during the promotional stage of carcinogenesis in the two-stage initiation-promotion model (112). It is believed that although the binding of AHR by TCDD may not be sufficient for its carcinogenicity, it is necessary for its action. The effects of TCDD on liver carcinogenesis in rodents have been the focus for many years, in which a genotoxic carcinogen diethylnitrosamine (DEN) was applied to initiate genetic alterations followed by TCDD exposure. Using genetic murine models that express various AHR alleles, AHR has been suggested to play a key role in TCDD-induced liver tumor promotion. For example, mice that encode a receptor with low binding affinity for TCDD (Ahr^d) showed dramatically decreased liver tumor formation compared to mice with high binding affinity (Ahr^b) when exposed to both the initiation event (DEN) and the promotion event (TCDD) (113). Additionally, in mice expressing constitutively activated Ahr (CA-Ahr), the liver tumor prevalence and multiplicity were much higher than that

in wild-type mice after DEN exposure (114). However, generation of AHR deficient mice has shown increased tumor formation in DEN-initiated HCC model (no TCDD exposure), suggesting a tumor suppressing effect by AHR (115). This discrepancy might be explained by the fact that the lack of AHR expression may not be equated with repression of AHR activity, such as during the treatment of an existing tumor with an AHR antagonist (12). These observations would support testing whether TCDD can persistently promote liver tumor in AHR-null mice using the two-stage model. Overall, these findings support the conclusion that AHR activation enhances liver tumor formation and thus, antagonism of AHR activity by exogenous or endogenous AHR antagonists would be a logical way to consider AHR as a therapeutic target.

Inflammatory signaling was recently recognized as a major player in the mechanisms of liver tumor promotion (116). Particularly, absence of the receptors for TNFα/β and IL-1α a/β conferred resistance to the tumor promoting effects of TCDD characterized by much less number and size of liver tumors, suggesting that similar to the mechanisms of TCDD-induced acute hepatotoxicity, inflammatory signaling plays an important role in TCDD-induced liver tumor promotion in mice (113).

AHR may possess intrinsic functions in regulating cell cycle that are independent of its ligands. The cell cycle consists of five phases: G_0, G_1, S, G_2, and M. Earlier studies showed that AHR-defective Hepa1c1c7 cells displayed a prolonged doubling time compared with wild-type cells, which was due to delayed progress into G_1 phase (117). Knockdown of AHR in human HepG2 cells resulted in growth inhibition as well as decreased expression of cell cycle–related genes including cyclins D1 and E, cdk2, and cdk4 (118). On the other hand, AHR ligand treatment by TCDD was also shown to promote metastasis and cell migration through inducing metastasis marker anterior gradient 2 (AGR2) (119) and activating non-genomic focal adhesion

kinase (FAK)/Src pathway (120) in an AHR-dependent manner. However, TCDD was also reported to cause cell cycle arrest due to the crosstalk between AHR and the retinoblastoma (Rb) protein (121). Rb is a cell cycle-related phosphoprotein that complexes with E2F protein to repress E2F responsive genes, thereby inhibiting cell cycle entry from G1 into S phase. The direct AHR-Rb interaction was reported by both the yeast two-hybrid system and co-immunoprecipitation assays, and it participated in the transcriptional repression of the E2F-induced cell cycle progression (121-123).

The effect of AHR activation in HCC has also been linked through inhibiting apoptosis. In studies of the two-stage liver tumor promotion model, TCDD was shown to mediate clonal expansion of "initiated" preneoplastic hepatocytes by inhibiting apoptosis and bypassing AHR-mediated growth arrest (124). But other contradictory results indicated that TCDD induced apoptosis (125), which might be due to AHR-mediated oxidative stress generated by P450 enzyme induction (54). AHR-mediated metabolic conversion of its agonist BaP (a constituent of cigarette smoke) to the ultimate carcinogen benzo[α]pyrene-7,8-diol-9,10-epoxide (BPDE) lead to DNA adducts formation and mutagenesis. And the carcinogenic effects of BaP were AHR-dependent by the observation that the tumor formation was lost in mice lacking AHR (126) or decreased in mice lacking CYP1B1 (127). However, BPDE was also shown to induce apoptosis in HepG2 cells, which might be linked to the induction of the p38 MAPK (128).

3.1.2 Species Difference of AHR in Promoting Hepatic Carcinogenesis

The International Agency for Research on Cancer (IARC) has classified TCDD as a " Group I human carcinogen" (72), based on the carcinogenic effect of TCDD on experimental animals. However, this definition has been controversial for a long time due to insufficient and

inconsistent evidence of carcinogenicity in humans (129). In several follow-up epidemiologic studies on TCDD-exposed populations, the association between the increase of the total cancer incidence and TCDD exposure was much weaker and should be considered as inadequate rather than limited evidence of its carcinogenicity (129). And moreover, these studies were carried out by the same group and have not been confirmed by other investigators. This large inter-species variation severely limits generalizations from animals to humans.

Of note, there are marked species differences in the ligand-dependent activation of AHR, which is attributed to the sequence divergence in their ligand-binding domains. The human AHR has a 10-fold lower affinity for TCDD compared with the Ahr^b, which results in a much lower toxicity in human associated with TCDD exposure (130). Sequence analysis revealed a critical alteration in the ligand binding domain that is responsible for the variation in TCDD response between human and mouse: V381 in the hAHR versus A375 in the $mAhr^b$ (130). Moreover, there is only 58% similarity in the AHR C-terminal transactivation domain between human and mouse, suggesting that AHR may regulate a distinct subset of genes in response to activation (131). DNA microarray analysis of TCDD-treated hepatocytes from WT C57BL6/J mice and humanized AHR C57BL6/J mice showed dramatic species differences in AHR-regulated gene induction and repression (132). This structural difference underlines the importance of using humanized AHR transgenic mice to address the species specificity of AHR responses *in vivo*.

DEN treatment on transgenic mice expressing CA-Ahr clearly demonstrated the oncogenic potential of the activated mouse Ahr in promoting hepatic carcinogenesis (114). Since the animal evidence relating TCDD exposure to hepatic carcinogenesis is much stronger than that for humans, we do not know whether activation of human AHR itself is sufficient in

promoting hepatic carcinogenesis. Therefore, our research goal is to explore the function and molecular mechanisms of human AHR in the liver tumor promoting effect.

3.2 SPECIFIC AIMS

Having known that TCDD is a potent liver tumor promoter in mice, but it is not sufficient to activate the human AHR due to the species difference in their ligand binding affinity, we want to explore the role of human AHR in hepatic carcinogenesis. Gain-of function of mouse Ahr in CA-Ahr transgenic mice showed significantly more liver tumor formation, suggesting that genetic activation of mouse Ahr is also sufficient in promoting hepatic carcinogenesis. Therefore, our interest is to study whether and how genetic activation of human AHR plays a role in hepatic carcinogenesis using our CA-AHR transgenic mouse model.

Aim 1: To determine the tumor promoting effects of human AHR in the two-stage hepatic carcinogenic model using humanized CA-AHR transgenic mice.

Aim 2: To compare the tumor promoting effect between mouse and human AHR in hepatic carcinogenesis.

Aim 3: To explore the potential mechanisms underlying the tumor promoting effect by AHR activation.

3.3 METHODS

Mice

The generation of CA-AHR and CA-Ahr transgenic mice has been described in chapter 1 as well as in previous reports (49, 133). Two-stage liver tumor model will be established in both CA-AHR and CA-Ahr mice for a direct comparison. To generate the homozygous Gadd45b (growth arrest and DNA-damage-inducible beta)-/- (GK) mice that harbor a null allele for Gadd45b, Gadd45+/- mice in C57BL/6J background (stock number: 013101) from the Jackson Laboratory (Bar Harbor, ME) were self-crossed. Genotyping was performed by PCR using primers (10936: GCAACCCCAGTAACTTTGGA; 10937: CCTGCAGGAGAGAAGGAGTG; oIMR7996: CTT CCATTTGTCACGTCCTG) provided by the Jackson Laboratory. The complete deletion of Gadd45b was confirmed at the mRNA level by RT-PCR on RNA extracted from adult liver tissues. CA-AHR transgenic mice were crossbred with Gadd45b-/- mice to generate the CA-AHR/Gadd45b-/- (AGK) mice in C57BL/6J background, and to study the requirement of Gadd45b in the tumor promoting effect of AHR. AHR knockout (AHRKO) mice in C57BL/6 background were purchased from Taconic (Hudson, NY) to study the requirement of AHR in TCDD-induced Gadd45b transcription. WT male mice in CD-1 background were purchased from Charles River Laboratories for hydrodynamic overexpression of Gadd45b in the coactivation experiment.

Mice Treatment

In the two-stage initiation-promotion liver tumor model, 6-week-old male and female littermates from WT, CA-AHR, CA-Ahr, GK, and AGK mice (N=6-11 for each group) were injected intraperitoneally with a single dose of 90 μg/kg of body weight of DEN dissolved in saline and

sacrificed at 9 months after DEN injection. An equal volume of saline was injected to littermates as controls. For the gene regulation analysis, 10-week-old male C57BL/6J WT, AHRKO, and GK mice were treated by gavage with a dose of 10 μg/kg body weight of TCDD or 10 ml/kg body weight of corn oil once a day for 4 days before sacrifice. For hydrodynamic gene delivery study, 10-week-old male CD-1 WT mice were treated by a single gavage of 10 μg/kg body weight of TCDD or 10 ml/kg body weight of corn oil 7 days before the hydrodynamic transfection of pCMX-Flag-Gadd45b or pCMX-Flag empty construct into mouse livers.

Histology and immunohistochemistry

For H&E staining, liver tissues that bear tumors were fixed in 10% buffered formalin, embedded in paraffin, sectioned at 4 μm, and stained with hematoxylin and eosin. To detect Ki67 and Gadd45b proteins by immunohistochemistry, consecutive sections were deparaffinized and rehydrated. For antigen retrieval, tissue sections were immersed in the 10 mM citrate buffer (PH 6.0) at a sub-boiling temperature for 10 min followed by the treatment with 0.3% hydrogen peroxide for 30 min to inactive the endogenous peroxidase. To block the non-specific signal, sections were incubated with goat serum (1:200) at room temperature for 1 h, followed by incubation with the primary antibodies against Ki67 (1:200, ab15580, Abcam) or Gadd45b (1:200, ab197990, Abcam) at 4°C for overnight. Slides were then washed and incubated with a 1:200 diluted biotinylated anti-rabbit antibody at room temperature for 30 min. After incubation with the avidin-biotin-horseradish peroxidase complex (Vectastain ABC Peroxidase kit, Vector Laboratories) at room temperature for 30 min, slides were incubated with freshly prepared DAB substrate for 3-5 seconds and slightly counterstained with hematoxylin.

Serum Biochemical Analysis

Serum ALT and AST levels were measured by using commercial assay kits (Stanbio Laboratory, Boerne, TX).

Co-immunoprecipitation and Western Blotting Analysis

To study the interaction between AHR and Gadd45b proteins, 293T cells in 6-well plate were co-transfected with pCMX-HA-AHR and pCMX-Flag-Gadd45b plasmids, and treated with 3-MC for 24 hours. Cells were lysed in the NP-40 lysis buffer supplemented with proteinase inhibitors (1:200) and incubated with antibodies against HA-tag at 4°C for overnight, followed by incubation with protein G agarose beads at 4°C for 1 hour. Cells were then washed with the NP-40 lysis buffer and subjected to western blot analysis. Protein samples were resolved by SDS-PAGE gel, transferred to a polyvinylidene fluoride membrane, and blotted with antibodies. The primary antibodies used include those against HA-tag (cat# 26183, Pierce), Flag-tag (cat# F7425, Sigma), VP16 (cat# sc-7545, Santa Cruz), and Gal4-DBD (cat# sc-510, Santa Cruz).

Electrophoretic Mobility Shift Assay (EMSA), Chromatin Immunoprecipitation (ChIP) Assay, Transient Transfection and Luciferase Reporter Assay

EMSA was performed using ^{32}P-labeled oligonucleotides and receptor proteins prepared by the TNT method (88). ChIP assay for the Gadd45b promoter was performed in WT CD-1 mice (N=4 for each group) whose livers were transfected with the pCMX-Flag-CA-AHR plasmid or pCMX-Flag empty vector by a hydrodynamic gene delivery method for 8 h (88). Cells or liver lysates were immunoprecipitated with the anti-Flag or Anti-IgG antibody (Sigma) (88). The recovered DNA was assayed for enrichment of the Gadd45b promoter (-1286~ -1277) by RT-PCR. For

luciferase reporter assay, the Gadd45b reporter plasmids (-1332/+1, -1263/+1) were PCR-amplified. CV1 cells in triplicate groups were transfected with the reporter construct together with the AHR or CA-AHR expression vector in 48-well plates. For the coactivation analysis, Huh7 cells in triplicate groups in 48-well plates were transfected with pCMX-Flag-Gadd45b (50, 100, and 200 ng/well) and pCMX-AHR (50 ng/well) constructs, together with the pGud-reporter gene. When necessary, cells were treated with 3-MC (4 μM) for 24 h before luciferase assay. The transfection efficiency was normalized against the β-galactosidase activities from a co-transfected CMX-β-galactosidase vector.

Mammalian two-hybrid analysis

To access the direct AHR-Gadd45b interaction *in vivo*, fusion constructs containing the Gal4 DNA-binding domain (DBD) upstream of full-length or mutant Gadd45b (1-160, 1-125, 1-92, 93-160, and 126-160) (134), and the fusion vector containing the herpes simplex virus VP16 activation domain downstream of full-length Ahr were co-transfected into 293T cells in 48-well plates, along with a thymidine kinase luciferase reporter containing the Gal4 binding site (Tk-UAS (upstream activating sequence)). The pCMX-Gal4 and pCMX-VP empty plasmids were used as controls. The luciferase reporter activity of Tk-UAS in triplicate groups was normalized against the β-galactosidase activities from a co-transfected CMX-β-galactosidase vector.

Quantitative RT-PCR

Total RNA was extracted using TRIzol and subjected to reverse transcription with random hexamer primers and Superscript RT III enzyme (Invitrogen). SYBR Green-based qRT-PCR was performed with the ABI7500 System. Data were normalized against the cyclophilin control.

Statistical Analysis

When applicable, results are presented as means ± standard error of the mean (SEM). Statistical significance between the means of two groups was analyzed using an unpaired Student *t* test, and analysis of variance (ANOVA) for the comparison among the means of three or more groups. Differences were considered statistically significant at $P < 0.05$.

3.4 RESULTS

3.4.1 Activation of Human AHR Promoted DEN-initiated Liver Tumor

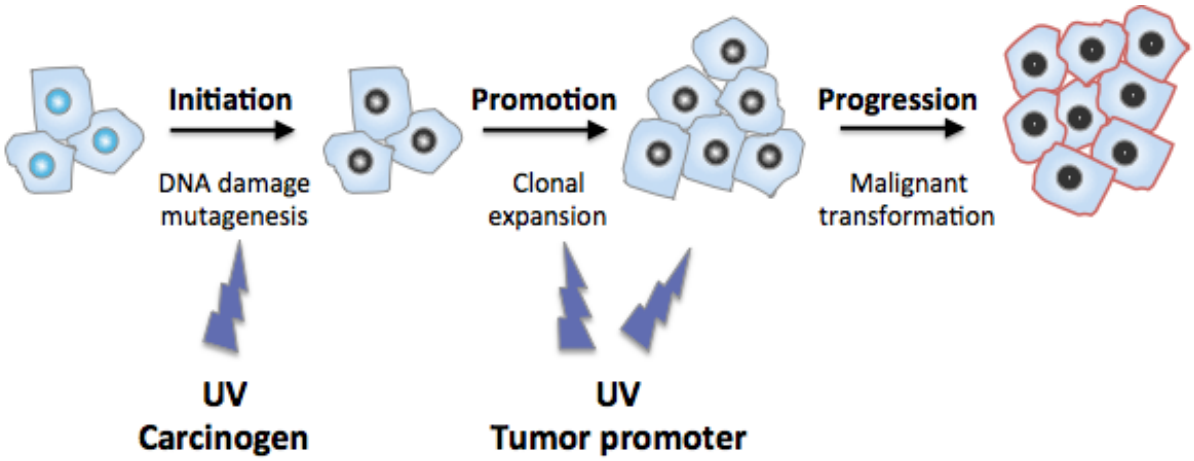

Figure 21. Schematic representation of the two-stage initiation-promotion liver tumor model.
In the two-stage model, a chemical carcinogen or UV irradiation acts as a tumor initiator, which causes genetic alterations such as DNA damage and mutagenesis. The clonal expansion and tumor progression require a tumor promoter such as UV irradiation and tumor promoter.

To study the human relevance of AHR in promoting liver tumors, we analyzed the susceptibility of mice expressing CA-AHR to DEN-initiated liver tumor development in the "Two-stage

initialization-promotion" model. Multistage carcinogenesis can be divided into three stages, termed initiation, promotion and progression (Fig. 21). Both genotoxic and non-genotoxic mechanisms contribute to the tumor development. Genotoxic events, including activation of oncogenes and/or loss of tumor suppressor genes, are the foundations of carcinogens. It can be induced by either endogenous or exogenous stimulus, such as DEN, which is a chemical carcinogen that induces the initiation of tumor cells through irreversible genetic alterations. The "initiated" cells may either be removed by apoptosis or be selected for expansion by a non-genotoxic stimulus, which may involve a variety of mechanisms including stimulation of regenerative cells by hormone-mediated growth stimulation or by actions of liver tumor promoters, such as phenobarbital- and dioxin-like chemicals (124).

Table 1. Liver tumors in DEN-treated male and female WT, CA-Ahr, and CA-AHR mice.

Gender	Genotype	LW/BW (%)	Number	Tumor incidence (%)	Multiplicity		
					1-3mm	3-7mm	>8mm
Male	WT	4.09±0.66	11	0 (0%)	0 (0)	0 (0)	0 (0)
	CA-Ahr	6.58±3.03*	9	8 (89%)	6.1 (55)	2 (18)	0.7 (6)
	CA-AHR	5.36±1.13**	10	10 (100%)	3.2 (32)	2.9 (29)	0.3 (3)
Female	WT	4.10±0.24	11	0 (0%)	0 (0)	0 (0)	0 (0)
	CA-Ahr	4.93±0.83**	6	2 (33%)	2 (12)	0.3 (2)	0.2 (1)
	CA-AHR	5.23±0.70**	10	3 (33%)	0.4 (4)	0.3 (3)	0.1 (1)

Livers were harvested 9 months after DEN exposure, and tumors on the liver surface were counted. Results are presented as means ± standard error of the mean (SEM). The number of mice in each group are shown in the table. The tumor incidence (%) repreesnts the ratio of the number of mice with tumors to the total number of mice in each group. The tumor multiplicity was calculated from the total tumor countings (denoted in the brakets) with varying tumor sizes divided by the total mouse numbers in each group. *, $P<0.05$; **, $P<0.01$. CA-Ahr vs. WT or CA-AHR vs. WT.

To directly compare the efficiency between human AHR and mouse Ahr in promoting hepatic carcinogenesis, two groups of CA-AHR and CA-Ahr transgenic mice in both genders were analyzed in this two-stage model. Wild-type age-matched littermates were included as controls. At the end of the experiment, the liver to body weight ratio in male CA-AHR and CA-Ahr mice were 5.36±1.13 and 6.06±1.81, respectively, compared to 4.09±0.66 in male WT mice (Table 1). There was 0% tumor in male WT mice and their livers look relatively normal (Fig. 22). Consistent with the previous study (114), the whole-body CA-Ahr transgenic male mice developed significantly enhanced liver tumors, as indicated by 89% of tumor incidence as well as increased tumor multiplicity and nodule size (Table 1). Surprisingly, we found that activation of human AHR also substantially promoted liver tumor, characterized by 100% of tumor incidence and enhanced nodule multiplicity and size (Table 1). Gross appearance showed one or multiple tumors on the surface of the CA-AHR mice livers, with the largest nodule more than 10mm in diameter (Table 1, Fig. 20). This observation suggested that direct activation of human AHR works at least as efficiently as mouse Ahr in promoting liver tumor formation in male mice.

Females are known to have much lower liver cancer risks, which is in agreement with the DEN-induced mouse liver tumor (116). Indeed, the female mice developed much lower tumor incidence (33% in both CA-AHR and CA-Ahr mice) and multiplicity. The liver weight to body weight ratio in female CA-AHR and CA-Ahr mice were 5.23±0.70 and 4.93±0.83, respectively, compared to 4.10±0.24 in WT mice. Among those mice with no tumors, hepatic cysts were commonly found on the liver surface (data not shown). In the following experiments, we mainly focused on studying the liver promoting effect of human AHR in male mice.

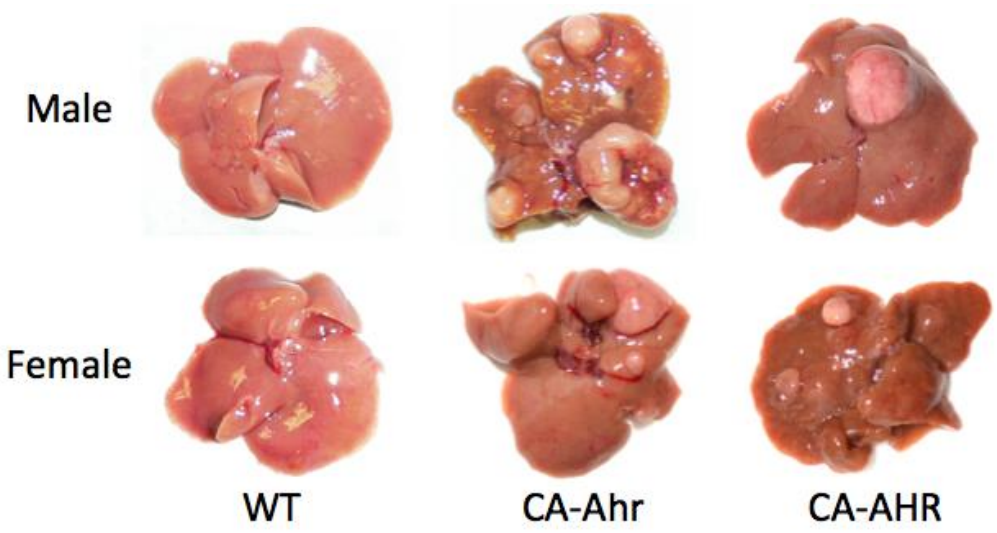

Figure 22. Representative gross tumor appearance of DEN-treated mice after 9 months.
Mice were i.p. injected with a single dose of 90 μg/kg DEN at 6-week-old. Shown are the representative images of the gross appearances of mice livers at 9 months after DEN challenge. N=6-11 for each group.

The tumors promoted by AHR activation were further analyzed under the microscope by H&E staining. Histologically, the liver architecture became trabecular and solid in both the CA-AHR and CA-Ahr mice, whereas WT mice displayed normal liver structure (Fig. 23A). Within the nodule area, hepatocytes displayed obvious degeneration and atypia, including enlarged and hyperchromatic nuclei, prominent nucleoli, and mitosis (indicated by arrows) (Fig. 23B), which are characteristic for hepatic carcinogenesis. The protein expression of Ki67 is strictly associated with cell proliferation, and the fraction of Ki67-positive tumor cells (the Ki67-labeling index) is often correlated with the clinical course of diseases such as carcinoma (135). Therefore, we stained the Ki67 protein in tumor regions by immunohistochemistry (Fig. 23C). A significantly increased fraction of Ki67-positive tumor cells were observed in both CA-Ahr livers (7.3%) and CA-AHR livers (12.5%), suggesting a higher proliferation rate.

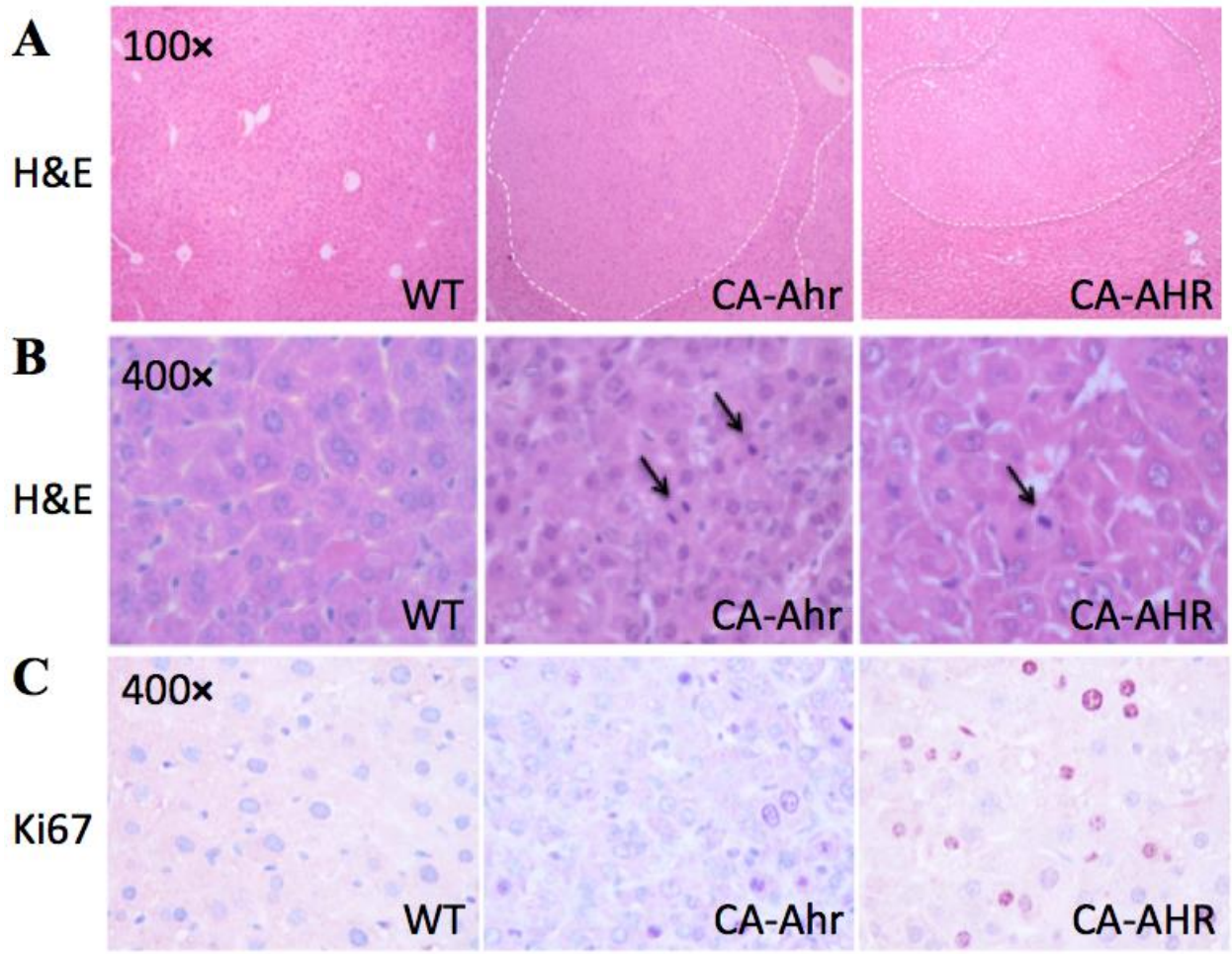

Figure 23. Activation of AHR induced mitosis and increased DNA proliferation.
Mice were i.p. injected with a single dose of 90 μg/kg DEN at 6-week-old, and liver tissues were harvested after 9 months. Shown are representative images from liver tumor sections by H&E staining (100×) with dotted lines denoting the nodule areas (A), H&E staining (400×) with arrows indicating cells that are undergoing mitosis (B), and immunohistochemistry (400×) stained with the proliferation marker Ki67 (C). N=6-11 for each group.

3.4.2 Activation of Human AHR Increased Inflammation and Impaired Liver Function after DEN Treatment

This intriguing finding strongly suggested the carcinogenic effect of AHR activation in humans. A connection between chronic inflammation and hepatic carcinogenesis has long been proposed. Inflammatory cells and cytokines generated in tumor microenvironment are a major contributing

factor to tumor growth, progression, and immunosuppression, and deletion or inhibition of inflammatory cytokines inhibits development of experimental cancer (136). Like many tumor promoters and nongenotoxic carcinogens, inflammatory cytokines play an important role in TCDD-mediated liver tumor promoting events (113). To determine whether activation of human AHR plays a role in increasing inflammatory cytokine expressions as observed by others in DEN-treated mice (116), we measured the mRNA expressions of IL-6 and TNF-α in the whole liver. TNF-α was significantly upregulated in the livers of DEN-exposed CA-AHR mice than in WT mice, but not IL-6 (Fig. 24A), suggesting that AHR activation may promote proinflammation through increasing the expression of TNF-α after DEN treatment. In the inflamed liver, TNF-α is a major effector that binds to the receptors TNFR1 and TNFR2 and triggers the transcriptional activation of NF-κB, which is known as a tumor promoter in inflammatory-associated cancer (137). The observation that Ahr activation facilitated oxidative stress together with the fact that oxidative stress can lead to chronic inflammation (138) also suggested the link between AHR activation and inflammation. Common liver functional tests, including measurements of serum ALT and AST levels, may be used to predict hepatic carcinogenesis risk in general population with unknown risk (139). Both ALT and AST levels were significantly increased in mice of both genotypes compared to WT mice (Figure 24B), indicating impaired liver function by AHR activation after DEN treatment.

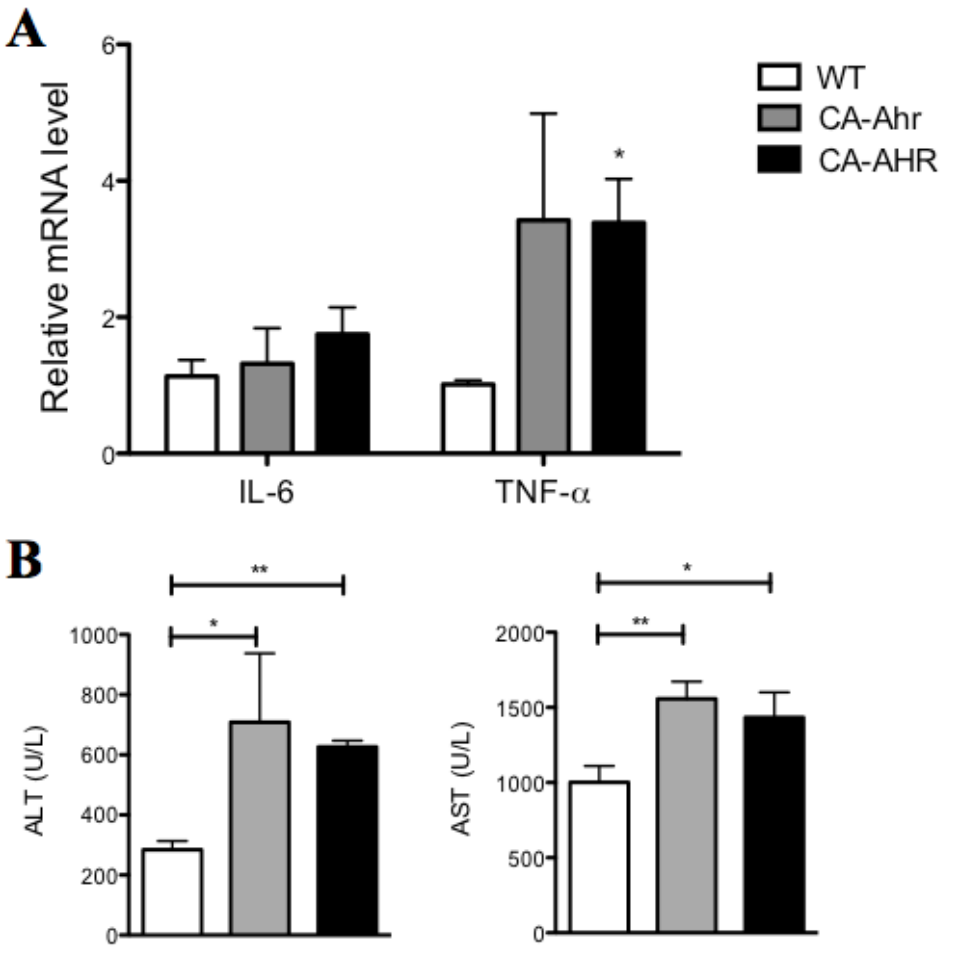

Figure 24. Activation of AHR induced TNF-α expression and increased liver injury after DEN treatment.

Mice were i.p. injected with a single dose of 90 μg/kg DEN at 6-week-old and sacrificed after 9 months. Livers and serum were collected at the end of the experiment. (A) Hepatic expression of IL-6 and TNF-α. (B) Serum concentrations of ALT and AST. N=6-11 for each group. *, $P<0.05$; **, $P<0.01$. CA-AHR vs. WT, or the comparisons are labled. Results are presented as means ± standard error of the mean (SEM).

3.4.3 Growth Arrest and DNA-Damage-Inducible beta (Gadd45b) is Induced by AHR Activation

Comparison of the gene expression profiles has provided important insights in identifying the genes that are associated with clinicopathologic features of hepatic carcinogenesis. Of particular, dysregulation of cell proliferation is a fundamental aspect of cancer, and this can be caused by alternations in cell cycle genes such as Cyclin D, Cyclin E, and cyclin-dependent kinase (Cdk) families including Cdk1, Cdk2, Cdk4, and Cdk6 (140). Among these cell cycle genes, Cyclin D1 and Cdk1 were upregulated by AHR activation in DEN-exposed mice (Fig. 25A). Moreover, the proto-oncogene c-Myc encodes a transcription factor that regulates cell proliferation, growth and apoptosis (141). Dysregulated expression of c-Myc is one of the most common abnormalities in malignant transformation (142). We found that c-Myc expression was significantly higher in CA-AHR mice with a 5.5-fold induction compared to WT mice (Fig. 25A). These results indicated the malignancy in CA-AHR mice liver, which was also suggested by previous histological identification.

Of note, we found that the expression of the growth arrest and DNA-damage-inducible beta (Gadd45b), a signal molecule inducible to external stress and UV irradiation, was highly induced upon AHR activation after DEN exposure (Fig. 25A). Interestingly, Gadd45b was reported to promote liver regeneration after partial hepatectomy (143), and its dysregulated expression has been observed in multiple types of solid tumors (144, 145). To examine the expression profile and the localization of the Gadd45b protein in CA-AHR mice livers that bear tumors, we collected their liver tissues from tumors and tumor-surrounding areas and measured their mRNA and protein levels. We found significantly increased hepatic Gadd45b mRNA in both tumor and non-tumor tissues from CA-AHR mice compared to that in WT mice (Fig. 25B).

Also, Gadd45b protein was highly expressed in hepatocytes from both tumor and non-tumor areas, and its expression was detected in both cytoplasm and nucleus (Fig. 25C).

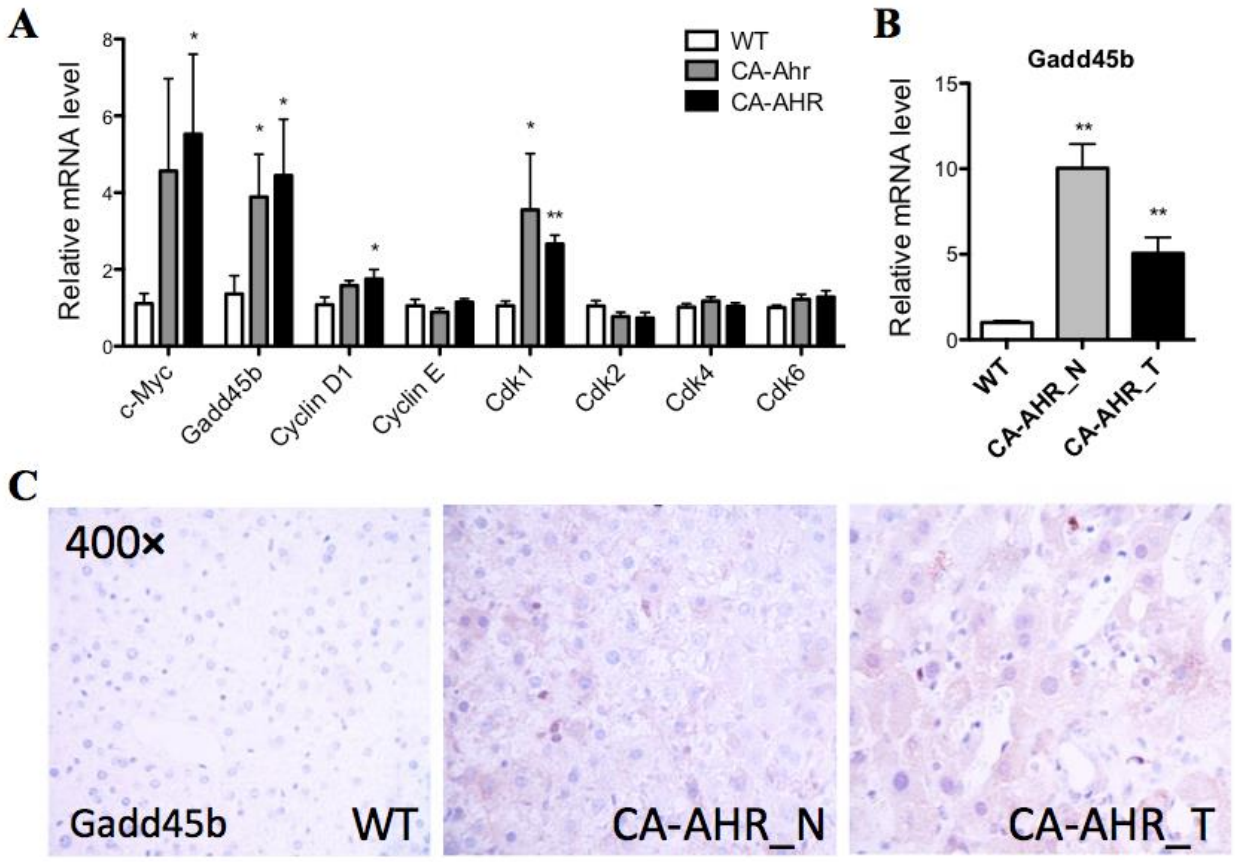

Figure 25. AHR activation induced expression of Gadd45b.
Mice were i.p. injected with a single dose of 90 μg/kg DEN at 6-week-old and sacrificed after 9 months. Tumor bearing liver tissues and the surrounding non-tumor tissues were collected. (A) Expressions of Gadd45b, c-Myc, and cell cycle related genes in DEN-exposed mice livers. (B and C) are mRNA Expression (B) and immunohistochemistry (C) of Gadd45b in liver tissues from tumor-surrounding (N) and tumor (T) areas in CA-AHR mice and WT mice. N=6-11 for each group. *, $P<0.05$; **, $P<0.01$. Results are presented as means ± standard error of the mean (SEM).

3.4.4 Gadd45b is An AHR Target Gene

After observing the dramatic induction of hepatic Gadd45b in DEN-exposed CA-AHR mice, we want to know if this induction is AHR responsive. The mRNA expression profile in the non-challenged 6-week-old CA-AHR mice showed dramatic increase of Gadd45b compared to WT mice, whereas other oncogenes (including c-Myc, Cyclin D1, and Cdk1) that are upregulated by AHR activation in the tumor settings remained unchanged (Fig. 26A). These results suggested that the induction of c-Myc, Cyclin D1, and Cdk1 might be a secondary effect due to the tumor microenvironment, whereas Gadd45b upregulation is likely to be an AHR-dependent effect. Indeed, the induction of Gadd45b was also observed in WT mice acutely treated with TCDD, but this induction was abolished in AHRKO mice (Fig. 26B). Although TCDD treatment seemed to induce expression of c-Myc, this increase is still present in AHRKO mice, indicating the c-Myc upregulation by TCDD may involve AHR-independent mechanisms (Fig. 26B). Moreover, by treating human primary hepatocytes with the human AHR ligand 3-MC, Gadd45b expression was significantly induced (Fig. 26C). These results, together with the Gadd45b induction in CA-AHR mice, strongly suggested Gadd45b as an AHR responsive gene.

To directly test whether Gadd45b is an AHR target gene, we cloned the Gadd45b gene promoter and evaluated its regulation by AHR. Inspection of the Gadd45b promoter revealed three putative DREs (Fig. 27A). EMSA confirmed that only the DRE1 was bound by the AHR-ARNT heterodimer or the CA-AHR-ARNT heterodimer (Fig. 27B). To confirm the recruitment of CA-AHR onto the Gadd45b gene promoter *in vivo*, we performed ChIP assay on cells transfected with Flag-CA-AHR. As shown in Fig. 27C, CA-AHR was significantly recruited to the DRE1-franking region on Gadd45b gene promoter. The transactivation of the Gadd45b gene promoter by AHR was also evaluated by luciferase reporter assays (Fig. 27D). The 1.33-kb

Gadd45b gene promoter was transactivated by CA-AHR or AHR in the presence of the AHR agonist 3-MC, whereas this activation was partially abolished when the region containing DRE1 was deleted (Fig. 27D).

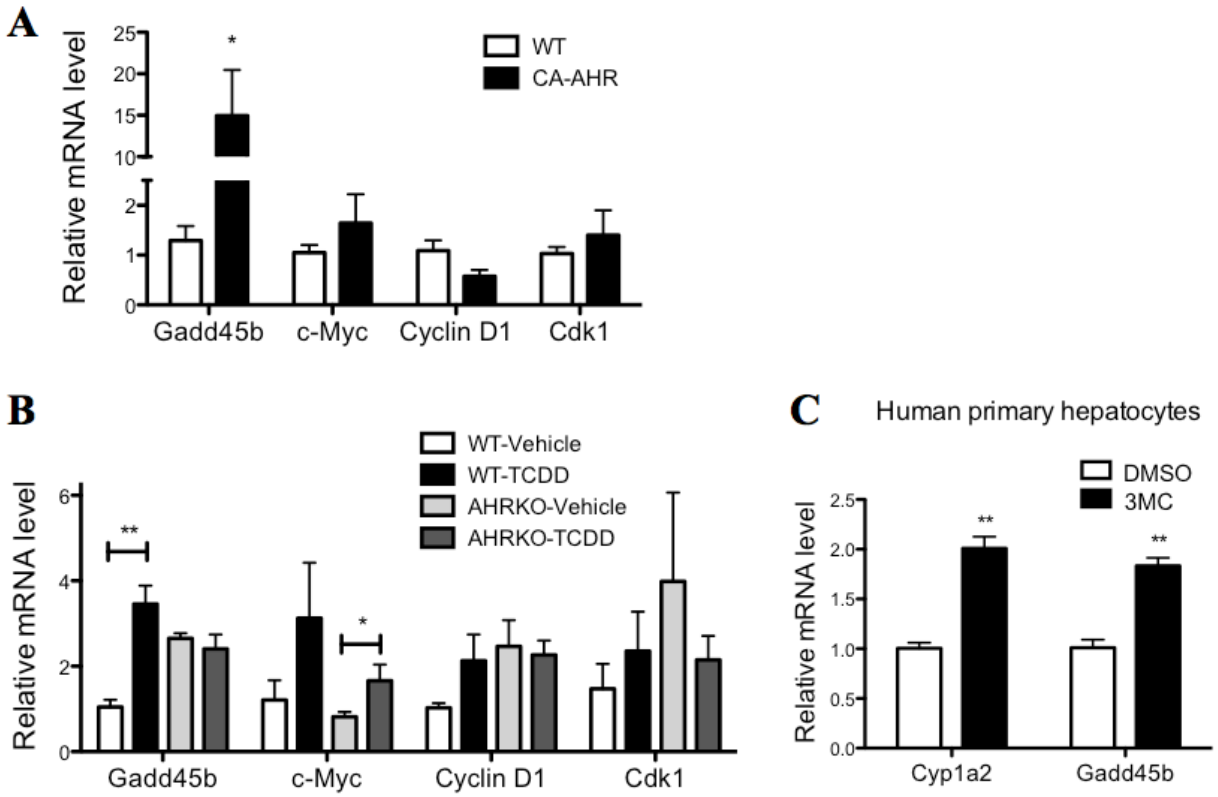

Figure 26. AHR activation induced expression of Gadd45b in an AHR-dependent manner.
(A) Expressions of Gadd45b, c-Myc, Cyclin D1, and Cdk1 in 6-week-old WT and CA-AHR mice livers (N=5 for each group). (B) 8-week old WT and AHRKO male mice (N=5 for each group) were i.p. injected with TCDD (10μg/kg) or coin oil for a consecutive 4 days before tissue harvesting. Expressions of Gadd45b, c-Myc, Cyclin D1, and Cdk1 were determined in livers. (C) Human primary hepatocytes were isolated from human livers and treated with DMSO or 3-MC (4 μM) for 24 hours before harvesting. Expressions of Cyp1a2 and Gadd45b were analyzed in triplicate groups. *, $P<0.05$; **, $P<0.01$. Results are presented as means ± standard error of the mean (SEM).

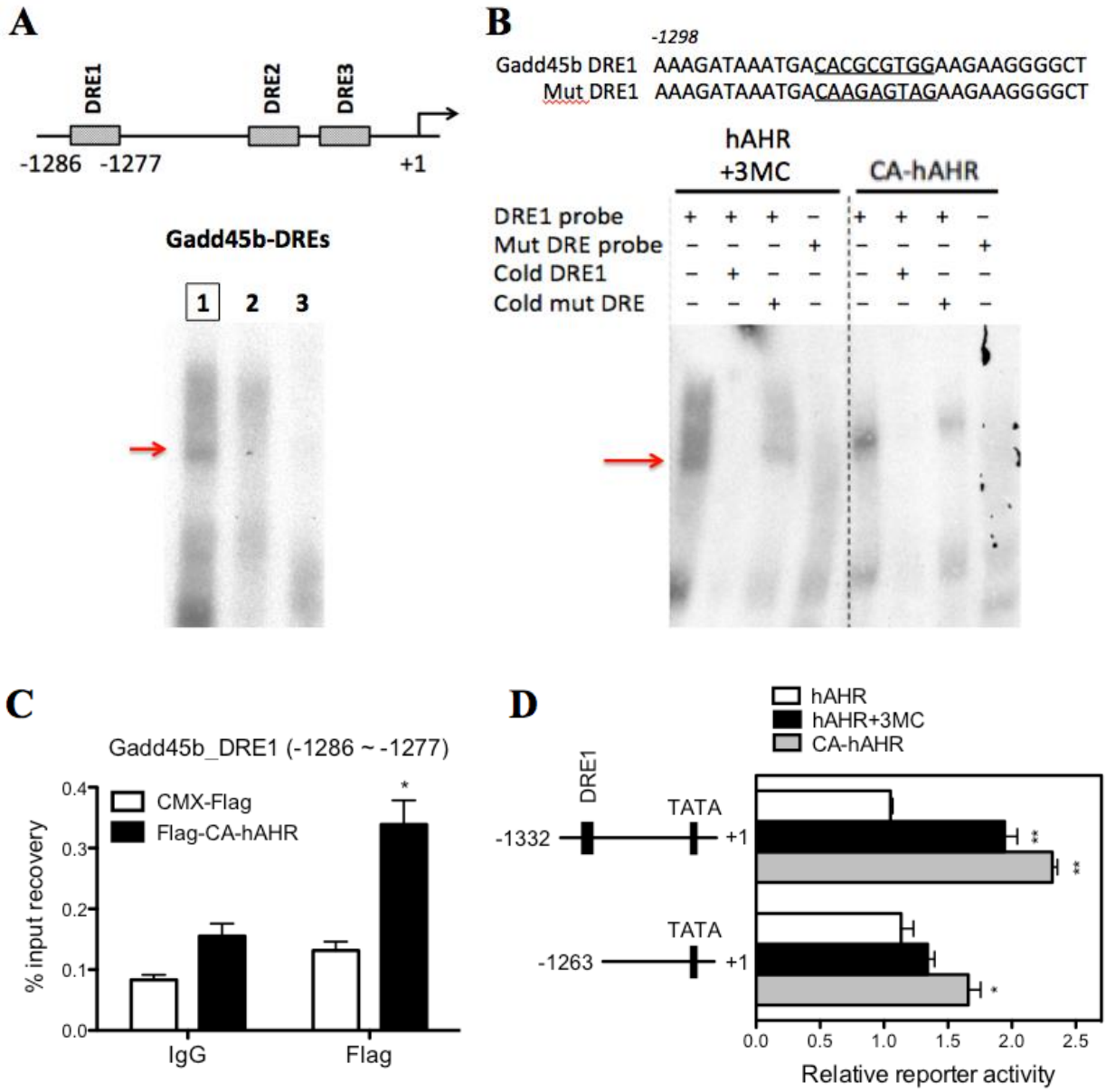

Figure 27. Gadd45b is a direct transcriptional target of AHR.
(A) Representation of DREs on Gadd45b promoter. (B) The sequence of Gadd45b DRE1 and the mutant variant (top) and EMSA result (bottom). (C) ChIP assay to show the recruitment of CA-AHR onto the Gadd45b promoters. WT CD-1 mice (N=4 for each group) livers were hydrodynamically transfected with pCMX-Flag empty construct or pCMX-Flag-CA-AHR expressing construct. (D) Activation of the Gadd45b promoter reporter gene by AHR in the presence of 3-MC, or by CA-AHR without an exogenously added ligand. CV1 cells were co-transfected with indicated reporters and receptors. Transfected cells were treated with vehicle DMSO or 3-MC (4 μM) for 24 h before luciferase assay in triplicate groups. *, $P<0.05$; **, $P<0.01$. Results are presented as means ± standard error of the mean (SEM).

3.4.5 Gadd45b Coactivates AHR-mediated Transcription

Despite its transcriptional regulation by AHR, Gadd45b was reported to contain two LXXLL (where L is leucine and X is any amino acid) signature motifs and act as a coactivator of several nuclear receptors (146). Of note, Gadd45b directly binds to the xenobiotic receptor constitutive androstane receptor (CAR) and facilitates its transcription activity (134, 147). As a member of the bHLH/PAS family of transcription factor, AHR recruits several coactivators (such as SRC-1 and p300/CBP) and enhances its own transcriptional activity (148). To explore whether Gadd45b has a coactivation effect on AHR transcription activity, we co-transfected Gadd45b and AHR expression plasmids with the AHR reporter construct pGud-Luc in human hepatoma Huh7 cells. Gadd45b dose-dependently induced the reporter activity of pGud-Luc with or without TCDD treatment, and this coactivation effect was even more pronounced in AHR-transfected cells (Fig. 28A). Moreover, hydrodynamic overexpression of Gadd45b in mice liver induced hepatic mRNA expressions of CYP1A1 and NRF2, both of which are typical AHR target genes (Fig. 28B). In mice that received TCDD treatment, Gadd45b exerted a stronger coactivation effect by upregulating expression of AHR targets including CYP1A2, CYP1B1, Tiparp, and NRF2 (Fig. 28B). To determine whether Gadd45b is required for AHR activity, we treated WT and Gadd45b knockout (GK) mice with TCDD. We found that AHR target genes remained highly induced by TCDD even after Gadd45b was deleted (Fig. 28C), suggesting that other coactivators of AHR, such as SRC-1, NCoA-2, and p/CIP (149) might account for the persistent AHR transcription activity in the absence of Gadd45b. These observations suggested that Gadd45b is capable of facilitating AHR-mediated transcription activity, but may not be solely necessary.

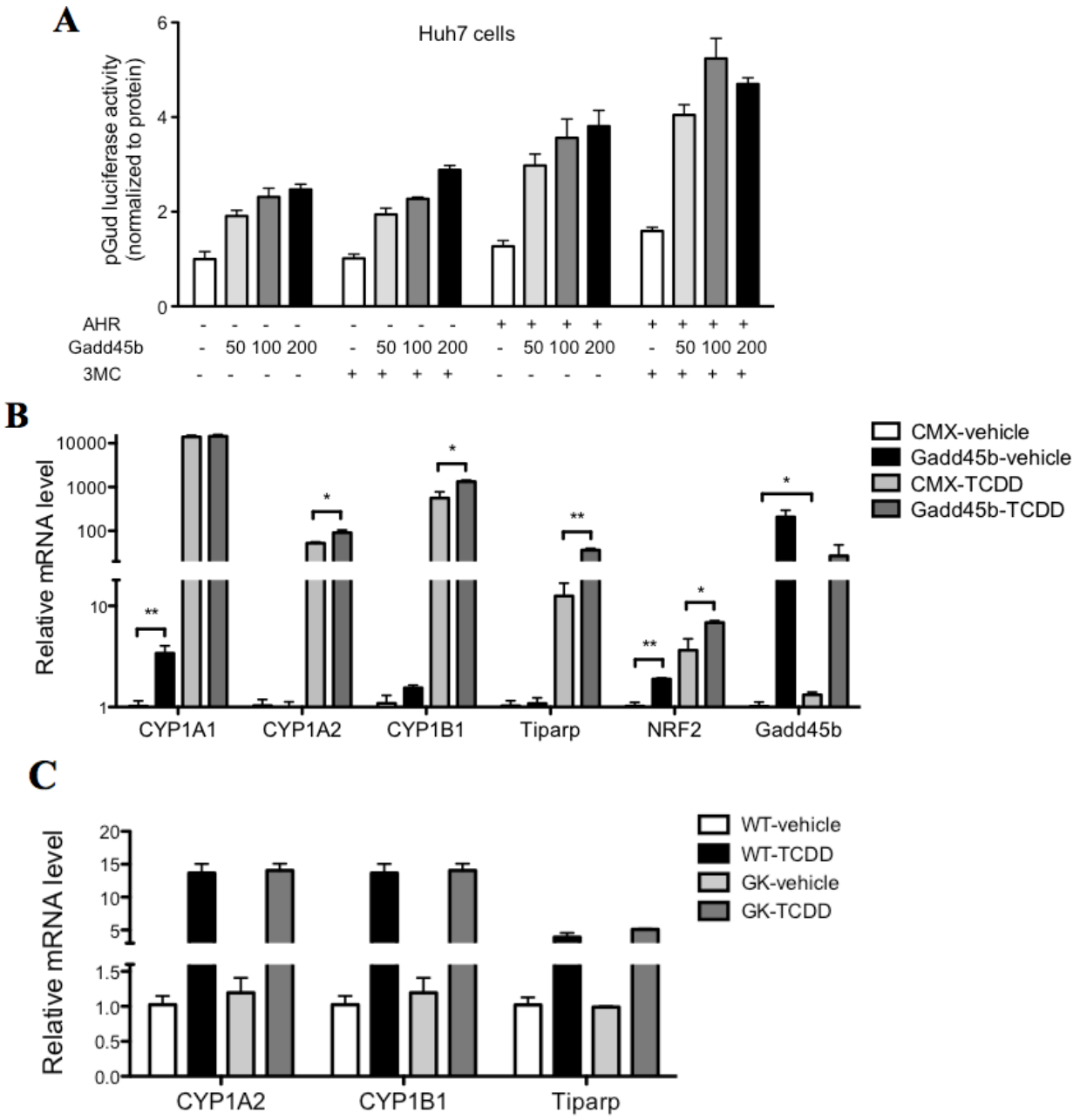

Figure 28. Gadd45b coactivates AHR-mediated transcription.
(A) Luciferase activity of the AHR reporter pGud-Luc. Huh7 cells were cotransfected with Flag-Gadd45b, pCMX-AHR, and pGud-luciferase reporter gene and were subsequently treated with DMSO and TCDD (10 nM) for 24 h. Luciferase activity was measured in triplicate groups. (B) mRNA levels of AHR target genes in CD-1 male mice (N=5 for each group) livers overexpressed with pCMX-Flag or Flag-Gadd45b construct and treated with TCDD (10 μg/kg) for 24 h. (C) Hepatic mRNA levels of AHR target genes in WT and Gadd45b knockout (GK) mice (N=5 for each group) treated with corn oil and TCDD (10 μg/kg) for 24 h. *, $P<0.05$; **, $P<0.01$. Results are presented as means ± standard error of the mean (SEM).

The co-immunoprecipitation analysis demonstrated direct binding of HA-tagged AHR and Flag-tagged Gadd45b, and 3-MC further enhanced the interaction (Fig. 29A). To explore the mechanism of their interaction, we utilized the Gal4-VP16 system, in which Gadd45b was fused to the Gal4-DBD construct (Gal4-Gadd45b) and Ahr was fused to the VP16-AD construct (Ahr-VP). The fusion constructs were transfected with the Gal4 reporter gene thymidine kinase-upstreatm activation sequence (Tk-UAS) in 293T cells. As shown in Fig. 29B, co-transfection of Ahr-VP and Gal4-Gadd45b significantly activated the UAS-mediated transcription, whereas deletion of the 93-160 domain in Gadd45b abolished this activity. These observations indicated that the 93-160 domain in the Gadd45b was required for the Ahr-Gadd45b interaction.

Having observed the transcriptional regulation of Gadd45b by AHR and the coactivation effect of AHR by Gadd45b, we crossbred the CA-AHR mice with GK mice to generate the AHR transgenic mice with the deletion of Gadd45b (AGK). The functional relevance of the AHR-Gadd45b induction in AHR-promoted liver tumor will be explored in the future study.

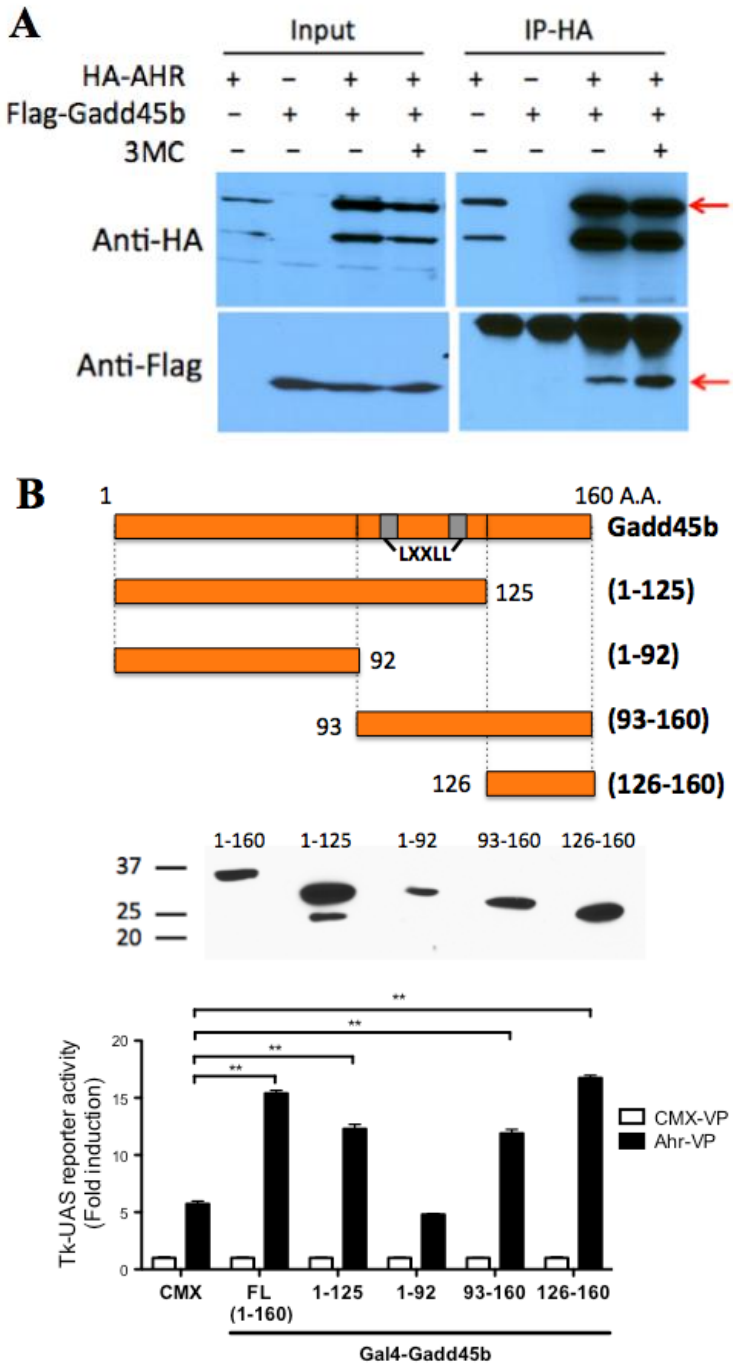

Figure 29. Physical interaction of AHR and Gadd45b.
(A) Physical interaction of HA-AHR and Flag-Gadd45b in 293T cells by co-immunoprecipitation. HA-AHR and Flag-Gadd45b plasmids (0.4 μg/well for each) were co-transfected in 6-well 293T cells, and cell lysates from three wells were combined for co-IP. (B) Mapping of the Ahr binding domain on Gadd45b. Shown are the representation (top) and western blot (middle) of Gal4-Gadd45b constructs using antibody against Gal4-DBD, and Tk-UAS reporter activity in 293T cells transfected with the Ahr-VP construct and truncated Gal4-Gadd45b constructs (bottom) in triplicate groups. *, $P<0.05$; **, $P<0.01$. Results are presented as means ± standard error of the mean (SEM).

3.5 DISCUSSION

The interpretation of the carcinogenic effect of AHR from animal studies into humans is confounded by many different components. First, the primary structure of the AHR protein shares limited similarity between human and mouse, conferring distinct ligand binding affinity and the variety of the transcriptional activity. Second, humans are relatively resistant to the toxic effects by the class of dioxin chemicals represented by TCDD. Additionally, the epidemiological evidence regarding carcinogenesis by TCDD has been considered inadequate and limited (129). Given the known fact that constitutive activation of the mouse Ahr receptor was able to promote liver cancer development, in this study, we attempted to identify the *in vivo* carcinogenic potential of the human AHR in a humanized mouse model to better evaluate the receptor mediated human cancer risk assessment.

For this purpose, we overexpressed the CA-AHR in the mouse background, which allowed the constitutive activation of human AHR with no requirement for human AHR agonists. This strategy offers a major focus on the AHR receptor rather than different ligand efficiency. Surprisingly, in comparison to mice that overexpressed the CA-Ahr, activated human AHR also promoted hepatic carcinogenesis in the DEN-initiated two-stage model, and the liver tumor promoting efficiency is almost comparable between human and mouse receptor. This seems contradictory to the previous report that replacement of the mouse Ahr gene with human AHR cDNA conferred mice less sensitive to TCDD-induced toxic effects such as fetal teratogenesis (150). This might be largely due to the distinct affinities of mouse and human receptor to TCDD. Our model excluded the potential confounder due to inadequate activation of human AHR by mouse Ahr agonists such as TCDD. Limited level of the human AHR protein

might also account for the attenuated responsiveness of hAHR knock-in mice to TCDD (150). There are concerns in humanized AHR mice that the human receptor may not recruit coactivators as efficiently as the mouse counterpart (150). But our results that human and mouse AHR exerted almost equal carcinogenic effect suggested that the coactivator recruitment might be varying during different molecular events. At least in the liver tumor promoting process CA-AHR was relatively efficient. It is also plausible that the constitutively activated constructs work differently from the wild-type constructs in their efficacy of recruiting coactivators.

A connection between cell apoptosis and cancer has long been proposed. Whether a hepatocyte proliferates or dies in response to a genotoxic stress such as DEN will dictate cell fate during carcinogenesis. Gadd45b is an anti-apoptotic factor that directly binds to MKK7 and inhibits MKK7-dependent phosphorylation of JNK1/2, thereby repressing JNK-mediated apoptosis (143). Gadd45b belongs to the small-molecule (~18 kDa) Gadd45 family of inducible proteins that play important roles in diverse biological processes including stress response, survival, senescence, and apoptosis (151). Notably, a possible role of Gadd45b in hepatocarcinogenesis and hepatocyte proliferation has been suggested by establishing Gadd45b as a constitutive androgen receptor (CAR)-responsive gene (134). CAR, a xenobiotic nuclear receptor, was also reported to be a nongenotoxic tumor promoter that mediates the carcinogenic effect of phenobarbital in hepatic carcinogenic development in mice. Interestingly, we found that Gadd45b was highly induced in the DEN-challenged CA-AHR mice, suggesting its potential role as an AHR responsive gene as well.

We hypothesized that Gadd45b should exhibit AHR-dependent induction long before the liver developed tumors, suggestive by its upregulation in 6-week-old CA-AHR mice as well as in mice acutely treated with TCDD. In contrast, we searched a panel of AHR-regulated molecules

that may be involved in the promotion of hepatic carcinogenesis, such as c-Myc, Cyclin D1, and Cdk1, and we found that they are only induced in the tumor-developing livers, but not in the short-term induced models. Therefore, here we have further explored the Gadd45b as a candidate of AHR-regulated gene. The AHR-Gadd45b regulation was also suggested in human primary hepatocytes treated with the human AHR agonist 3MC, along with the validated DRE on the promoter of Gadd45b in both *in vitro* and *in vivo*.

In addition, Gadd45 proteins were reported to act as transcriptional coactivators of several nuclear receptor transcription factors (146). The transcription of CAR target genes activated by 1,4-Bis[2-(3,5-dichloropyridyloxy)]benzene (TCPOBOP) was attenuated in Gadd45-/- mice, despite their intact proliferative responses (134). This coactivation effect of CAR transcription by Gadd45b was achieved by their direct binding, and TCPOBOP recruited both proteins onto the regulatory element of the CAR target gene Cyp2B10 (134). Another xenobiotic receptor, pregnane X receptor (PXR), was also reported to stimulate Gadd45b expression and then interacts with the protein after it is expressed (152). Similarly, we found that Gadd45b acted as a coactivator of AHR, by showing a dose-dependent coactivation effect of Gadd45b in the luciferase activity of AHR reporter gene. Also, transfection of Gadd45b into mouse liver further enhanced TCDD-induced AHR transcription by increasing its target gene expression. The coactivation effect of Gadd45b was also suggested by the presence of 2 LXXLL signature motifs, at amino acid 98 and 117 (134). However, deletion of the LXXLL motifs did not block its binding to AHR, an effect also found for its interaction with CAR (134). But lacking the half C-terminal (93-160) domain resulted in no interaction, suggesting that both the LXXLL motifs and the 126-160 region are required for its interaction with AHR.

Our results indicated that the AHR-Gadd45b induction might serve as a feed-forward

mechanism, by which the synthesis of a coactivator Gadd45b facilitates AHR-mediated transcription. The unchanged response of TCDD-induced AHR target gene expression in Gadd45b-/- mice could be explained by compensation of other classical AHR coactivators. However, the intrinsic biological functions of Gadd45b in stress response and apoptosis led us to think that lacking Gadd45b might alter AHR-caused cellular events in the DEN-initiated carcinogenic settings. Further studies using AHR transgenic mice lacking the Gadd45b will better depict the role of the AHR-Gadd45b axis in liver tumor promoting events.

4.0 CHAPTER IV: SUMMARY AND PERSPECTIVES

In the first part of this thesis work, my results have revealed the role of human AHR in fatty liver and energy metabolism as summarized in Fig. 30. Despite the notion that exposure to dioxins results in metabolic abnormalities, the transcriptional mechanisms by which AHR affects metabolic homeostasis have not been well understood. In our current model, hepatic activation of AHR can upregulate the expression of the endocrine hormone FGF21, which can be released into circulation and act on extra-hepatic tissues to exert metabolic benefits despite having fatty liver. The direct metabolic benefits of FGF21 in adipose tissue are through the FGFR1-βKlotho pathway. We propose that FGF21-induced adiponectin production and secretion mediates the improved metabolic functions in adipose tissue and skeletal muscle of transgenic mice as well.

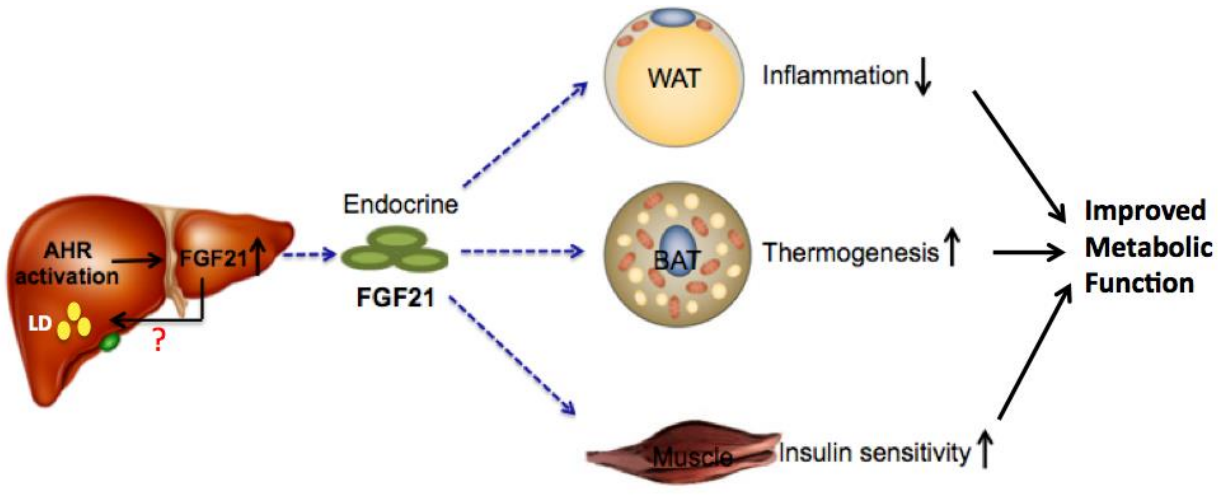

Figure 30. Model of the AHR-FGF21 axis in lipid and energy metabolism.

Of note, the AHR-FGF21 regulation in the liver seems to be responsible for the hepatic lipid droplet formation, and the underlying mechanisms need further study.

For future studies, whether pharmacological activation of AHR relieves the pre-existing obesity and insulin resistance needs to be examined. Our data has suggested that AHR activation protects mice from diet-induced obesity and type 2 diabetes, which support the beneficial role of AHR in the anti-diabetic effect. On the other hand, studies using AHR null mice also revealed an improved phenotype in type 2 diabetes and insulin resistance, suggesting the detrimental role of AHR in the diabetic effect. However, both studies have the shortage about the genetic model, which is one does not know whether the effects are due to developmental issues or whether they occur early in the diabetic process. Additionally, the constitutive activation of AHR or lack of the AHR expression makes it difficult to translate into physiological conditions, which may limit the data interpretation. Since many endogenous and less-toxic AHR agonists and antagonists have been developed, it's interesting to investigate how these ligands may potentially affect energy metabolism through AHR activation or repression. It's equally interesting to evaluate whether metabolic alteration by AHR agonists are opposite to that by AHR antagonists.

My current study is mainly focused on the hepatic role of AHR activation, and assumes the phenotypes observed in extra-hepatic tissues are FGF21-dependent. However, AHR is also highly expressed in a variety of other organs, such as lung, intestine, heart, muscle, etc., in which AHR signaling may also contribute to the metabolic homeostasis. Generation of other tissue-specific AHR transgenic mice may help better delineate the contribution of AHR signaling in each organ to the overall energy metabolism.

In the second part of this thesis work, my results revealed that genetic activation of human AHR promoted DEN-initiated liver tumor formation, which is summarized in Fig. 31. The carcinogenic effect of TCDD in humans is considered inadequate and limited compared to that in rodents, which is largely due to its much weaker ligand binding affinity to human AHR. Here we focused on the carcinogenic potential of human AHR receptor itself by overexpressing the constitutively-activated human AHR in mouse liver and we found transgenic activation of AHR was, as efficiently as its mouse counterpart, in promoting hepatic carcinogenesis. Of note, AHR activation upregulates the expression of Gadd45b, a stress inducer with anti-apoptotic effect and was found abnormally expressed during carcinogenesis. On the other hand, the induction of Gadd45b facilitates AHR transcription activity, which may serve as a feed-forward mechanism to potentiate the tumor promoting effect of AHR. Future studies are necessary to determine whether the activation of Gadd45 is required for the tumor promoting effect of AHR by generating CA-AHR transgenic mice in the Gadd45b null background.

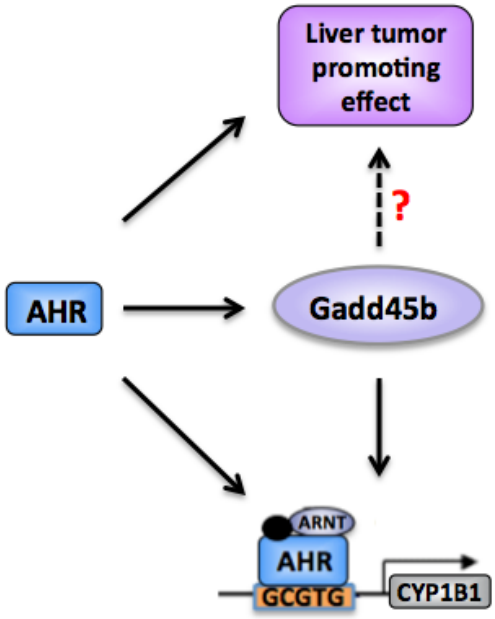

Figure 31. Model of AHR-Gadd45b regulation in hepatic carcinogenesis.

Our data has suggested that human AHR activation works as efficiently as mouse counterpart in promoting hepatic carcinogenesis when comparing the liver-specific CA-AHR transgenic mice to the CA-Ahr transgenic mice. One limitation of the humanized CA-AHR transgenic mouse model is that the human receptor might recruit coactivators and corepressors differently in the human body compared to that in the mouse background. The lack of ligand binding domain in the CA-AHR construct might also lead to differential coregulator recruitment compared to the wild type receptor, which will limit the data interpretation.

Although AHR was first identified as a xenobiotic receptor that mediates dioxin toxicity, emerging evidence suggests equally important roles of this receptor in various endobiotic functions. Specifically, the roles of AHR in livers were found to be very diverse, with some beneficial and some detrimental effects. Gain-of-function of hepatic AHR by TCDD treatment or transgenic mice caused liver fibrosis and hepatic carcinogenesis. On the other hand, loss-of-function of hepatic AHR leads to similar outcomes. In addition, the paradoxical observations that AHR has an anti-inflammatory effect in LPS-treated macrophages, whereas it mediates the pro-inflammatory effect of TCDD in hepatocytes underlines the liver-specific AHR signaling in the generation of distinct physiological outcomes. Further studies are needed to determine the cell-specific function of AHR in different cell types within the liver as well as other organs in various physiological and pathophysiological conditions.

The diverse functions of AHR raise many challenges in developing AHR as a potential therapeutic target. To achieve a precise targeting of AHR, cell-specific targeting by conjunction of targeting moieties such as antibodies and short peptides that can be recognized by specific cells may be required. More importantly, better selective AHR ligands that can specifically target the beneficial components with minimal toxicity are needed. One strategy is to develop selective

AHR modulators that can differently alter AHR-responsive genes through differential coactivator and corepressor recruitment. However, whether or not different ligands can mediate differential coregulator recruitment warrants further investigation. Growing interest has been focused on developing weak AHR agonists that have moderate affinity for AHR but would not exhibit the toxicity of a full agonist, such as TCDD. These selective AHR agonists will exhibit antagonistic effect on AHR activity in the presence of a full agonist, but the efficacy of these ligands with regard to different physiological settings needs to be evaluated. However, we must be aware that, whether it is the use of agonists or antagonists, an efficacious AHR ligand might not fulfill a "one size fits all" role in treating different types of diseases.

Altogether, my thesis work has highlighted the important, although conflicting and counterintuitive, aspects of the role of AHR in energy metabolism and hepatic carcinogenesis. The humanized AHR transgenic mouse model would serve as a favorable approach for future studies *in vivo*. It is hoped that AHR can be developed as a therapeutic target in human diseases.

APPENDIX A

SEQUENCES OF REAL-TIME PCR PRIMERS

Gene	Primer Sequences	
	Forward	**Reverse**
CYP1A1	GTGCATCGGAGAGACCATTG	GGTAGGAGTCATATCCACCTT
CYP1A2	GCAGTGGAAAGACCCCTTTG	CCTTCTCGCTCTGGGTCTTG
CYP1B1	CTCCAGAGCTTCTCCCAGAT	TGGACTGTCTGCACTAAGGC
IL-6	CCACGGCCTTCCCTACTTC	TGGGAGTGGTATCCTCTGTGAA
VEGF	TACTGCTGTACCTCCACCTCCACCATG	TCACTTCATGGGACTTCTGCTCT
TNF-a	AAGCCTGTAGCCCACGTCGTA	AGGTACAACCCATCGGCTGG
F4/80	GCTGTGAGATTGTGGAAGCA	ATGGCCAAGGCAAGACATAC
CD68	CCAATTCAGGGTGGAAGAAA	CTCGGGCTCTGATGTAGGTC
PPARa	TGTCGAATATGTGGGGACAA	AATCTTGCAGCTCCGATCAC
CPT-1a	GCTGCTTCCCCTCACAAGTTCC	GCTTTGGCTGCCTGTGTCAGTATGC
Lcad	TCAATGGAAGCAAGGTGTTCA	GCCACGACGATCACGAGA
Mcad	TTGAGTTGACGGAACAGCAG	CCCCAAAGAATTTGCTTCAA
Srebp-1c	CCCTGTGTGTACTGGCCTTT	TTGCGATGTCTCCAGAAGTG
ACC-1	GCCTCTTCCTGACAAACGAG	TGACTGCCGAAACATCTCTG
SCD-1	TTCTTACACGACCACCACCA	CCGAAGAGGCAGGTGTAGAG
Fas	CCCTTGATGAAGAGGGATCA	ACTCCACAGGTGGGAACAAG
Dio2	GATGCTCCCAATTCCAGTGT	TGAACCAAAGTTGACCACCA
Cidea	AGGCCGTGTTAAGGAATCTG	CCCAGTACTCGGAGCATGTA
Elovl3	CTTTGCCATCTACACGGATG	TGTCTCCCAGTTCAACAACC
Adiponectin	GCACTGGCAAGTTCTACTGCAACA	AGAGAACGGCCTTGTCCTTCTTGA
PGC1a	GACTCAGTGTCACCACCGAAA	TGAACGAGAGCGCATCCT
UCP3	ATGAGTTTTGCCTCCATTCG	GGCGTATCATGGCTTGAAAT
FGF21	CTGGGGGTCTACCAAGCATA	CACCCAGGATTTGAATGACC
Plin1	CTCTGGGAAGCATCGAGAAG	GCATGGTGTGTCGAGAAAGA
Plin2	CATTTCTCAGCTCCACTCCA	GTAGCCGATGCTTCTCTTCC
Plin3	CTCAAGCTGCTATGGAGGAACC	CATACGTGGAACTGATAAGAGGCA
Cidec	ATCAGAACAGCGCAAGAAGA	CAGCTTGTACAGGTCGAAGG
C-Myc	TGACCTAACTCGAGGAGGAGCTGGAA	AAGTTTGAGGCAGTTAAAATTATG
Gadd45b	GCCCGAGACCTGCACTGCCT	CCATTGGTTATTGCCTCTGCTCTCTT

Cyclin D1	TGAGAACAAGCAGACCATCC	TGAACTTCACATCTGTGGCA
Cyclin E	AATTGGGGCAATAGAGAAGAGGT	TGGAGCTTATAGACTTCGCACA
Cdk1	TTGGAGAAGGTACTTACGGTGTGGTG	CCAGGAGGGATGGAGTCCAGGT
Cdk2	CCGGCTCGACACTGAGACTGAAG	GAGGAATGCCCGTGAGAGCAGA
Cdk4	TGCTACTGGAAATGCTGACC	TCCTTGTGCAGGTAGGAGTG
Cdk6	GGCCCTTACCTCGGTGGTCGTC	GGCCACGTCCCTAGGCCAGTCT
Tiparp	CCAGCTCCAGCTCCAACTAC	CTGTAAGAACGGCATCAGCA
Nrf2	CACATTCCCAAACAAGATGC	CTGAACTTTCAGCGTGGCT
Cyclophilin	TGGAGAGCACCAAGACAGACA	TGGAGAGCACCAAGACAGACA

BIBLIOGRAPHY

1. Nebert, D.W. 1991. Proposed role of drug-metabolizing enzymes: regulation of steady state levels of the ligands that effect growth, homeostasis, differentiation, and neuroendocrine functions. *Molecular endocrinology* 5:1203-1214.
2. Guengerich, F.P. 2001. Common and uncommon cytochrome P450 reactions related to metabolism and chemical toxicity. *Chem Res Toxicol* 14:611-650.
3. Nebert, D.W., and Gonzalez, F.J. 1987. P450 genes: structure, evolution, and regulation. *Annual review of biochemistry* 56:945-993.
4. McCarver, D.G., and Hines, R.N. 2002. The ontogeny of human drug-metabolizing enzymes: phase II conjugation enzymes and regulatory mechanisms. *J Pharmacol Exp Ther* 300:361-366.
5. Ayrton, A., and Morgan, P. 2008. Role of transport proteins in drug discovery and development: a pharmaceutical perspective. *Xenobiotica* 38:676-708.
6. Handschin, C., and Meyer, U.A. 2003. Induction of drug metabolism: the role of nuclear receptors. *Pharmacol Rev* 55:649-673.
7. Waxman, D.J., and Azaroff, L. 1992. Phenobarbital induction of cytochrome P-450 gene expression. *Biochem J* 281 (Pt 3):577-592.
8. Hankinson, O. 1995. The aryl hydrocarbon receptor complex. *Annu Rev Pharmacol Toxicol* 35:307-340.
9. Poland, A., Glover, E., and Kende, A.S. 1976. Stereospecific, high affinity binding of 2,3,7,8-tetrachlorodibenzo-p-dioxin by hepatic cytosol. Evidence that the binding species is receptor for induction of aryl hydrocarbon hydroxylase. *J Biol Chem* 251:4936-4946.
10. Hoffman, E.C., Reyes, H., Chu, F.F., Sander, F., Conley, L.H., Brooks, B.A., and Hankinson, O. 1991. Cloning of a factor required for activity of the Ah (dioxin) receptor. *Science* 252:954-958.
11. Stockinger, B., Di Meglio, P., Gialitakis, M., and Duarte, J.H. 2014. The aryl hydrocarbon receptor: multitasking in the immune system. *Annual review of immunology* 32:403-432.
12. Murray, I.A., Patterson, A.D., and Perdew, G.H. 2014. Aryl hydrocarbon receptor ligands in cancer: friend and foe. *Nature reviews. Cancer* 14:801-814.
13. Diani-Moore, S., Ram, P., Li, X., Mondal, P., Youn, D.Y., Sauve, A.A., and Rifkind, A.B. 2010. Identification of the aryl hydrocarbon receptor target gene TiPARP as a mediator of suppression of hepatic gluconeogenesis by 2,3,7,8-tetrachlorodibenzo-p-

dioxin and of nicotinamide as a corrective agent for this effect. *J Biol Chem* 285:38801-38810.

14. Sato, S., Shirakawa, H., Tomita, S., Ohsaki, Y., Haketa, K., Tooi, O., Santo, N., Tohkin, M., Furukawa, Y., Gonzalez, F.J., et al. 2008. Low-dose dioxins alter gene expression related to cholesterol biosynthesis, lipogenesis, and glucose metabolism through the aryl hydrocarbon receptor-mediated pathway in mouse liver. *Toxicol Appl Pharmacol* 229:10-19.
15. Denison, M.S., and Nagy, S.R. 2003. Activation of the aryl hydrocarbon receptor by structurally diverse exogenous and endogenous chemicals. *Annu Rev Pharmacol Toxicol* 43:309-334.
16. Fernandez-Salguero, P., Pineau, T., Hilbert, D.M., McPhail, T., Lee, S.S., Kimura, S., Nebert, D.W., Rudikoff, S., Ward, J.M., and Gonzalez, F.J. 1995. Immune system impairment and hepatic fibrosis in mice lacking the dioxin-binding Ah receptor. *Science* 268:722-726.
17. Lahvis, G.P., Lindell, S.L., Thomas, R.S., McCuskey, R.S., Murphy, C., Glover, E., Bentz, M., Southard, J., and Bradfield, C.A. 2000. Portosystemic shunting and persistent fetal vascular structures in aryl hydrocarbon receptor-deficient mice. *Proc Natl Acad Sci U S A* 97:10442-10447.
18. Schmidt, J.V., Su, G.H., Reddy, J.K., Simon, M.C., and Bradfield, C.A. 1996. Characterization of a murine Ahr null allele: involvement of the Ah receptor in hepatic growth and development. *Proc Natl Acad Sci U S A* 93:6731-6736.
19. Denison, M.S., Soshilov, A.A., He, G., DeGroot, D.E., and Zhao, B. 2011. Exactly the same but different: promiscuity and diversity in the molecular mechanisms of action of the aryl hydrocarbon (dioxin) receptor. *Toxicol Sci* 124:1-22.
20. Singh, S.S., Hord, N.G., and Perdew, G.H. 1996. Characterization of the activated form of the aryl hydrocarbon receptor in the nucleus of HeLa cells in the absence of exogenous ligand. *Arch Biochem Biophys* 329:47-55.
21. Chang, C.Y., and Puga, A. 1998. Constitutive activation of the aromatic hydrocarbon receptor. *Mol Cell Biol* 18:525-535.
22. Wincent, E., Amini, N., Luecke, S., Glatt, H., Bergman, J., Crescenzi, C., Rannug, A., and Rannug, U. 2009. The suggested physiologic aryl hydrocarbon receptor activator and cytochrome P4501 substrate 6-formylindolo[3,2-b]carbazole is present in humans. *J Biol Chem* 284:2690-2696.
23. Jin, U.H., Lee, S.O., Sridharan, G., Lee, K., Davidson, L.A., Jayaraman, A., Chapkin, R.S., Alaniz, R., and Safe, S. 2014. Microbiome-derived tryptophan metabolites and their aryl hydrocarbon receptor-dependent agonist and antagonist activities. *Mol Pharmacol* 85:777-788.
24. Zelante, T., Iannitti, R.G., Cunha, C., De Luca, A., Giovannini, G., Pieraccini, G., Zecchi, R., D'Angelo, C., Massi-Benedetti, C., Fallarino, F., et al. 2013. Tryptophan catabolites from microbiota engage aryl hydrocarbon receptor and balance mucosal reactivity via interleukin-22. *Immunity* 39:372-385.
25. Opitz, C.A., Litzenburger, U.M., Sahm, F., Ott, M., Tritschler, I., Trump, S., Schumacher, T., Jestaedt, L., Schrenk, D., Weller, M., et al. 2011. An endogenous tumour-promoting ligand of the human aryl hydrocarbon receptor. *Nature* 478:197-203.
26. Chiaro, C.R., Morales, J.L., Prabhu, K.S., and Perdew, G.H. 2008. Leukotriene A4 metabolites are endogenous ligands for the Ah receptor. *Biochemistry* 47:8445-8455.

27. Chiaro, C.R., Patel, R.D., and Perdew, G.H. 2008. 12(R)-Hydroxy-5(Z),8(Z),10(E),14(Z)-eicosatetraenoic acid [12(R)-HETE], an arachidonic acid derivative, is an activator of the aryl hydrocarbon receptor. *Mol Pharmacol* 74:1649-1656.
28. Beischlag, T.V., Luis Morales, J., Hollingshead, B.D., and Perdew, G.H. 2008. The aryl hydrocarbon receptor complex and the control of gene expression. *Crit Rev Eukaryot Gene Expr* 18:207-250.
29. Pollenz, R.S. 2002. The mechanism of AH receptor protein down-regulation (degradation) and its impact on AH receptor-mediated gene regulation. *Chem Biol Interact* 141:41-61.
30. Gonzalez, F.J., and Fernandez-Salguero, P. 1998. The aryl hydrocarbon receptor: studies using the AHR-null mice. *Drug metabolism and disposition: the biological fate of chemicals* 26:1194-1198.
31. Bunger, M.K., Moran, S.M., Glover, E., Thomae, T.L., Lahvis, G.P., Lin, B.C., and Bradfield, C.A. 2003. Resistance to 2,3,7,8-tetrachlorodibenzo-p-dioxin toxicity and abnormal liver development in mice carrying a mutation in the nuclear localization sequence of the aryl hydrocarbon receptor. *J Biol Chem* 278:17767-17774.
32. Bunger, M.K., Glover, E., Moran, S.M., Walisser, J.A., Lahvis, G.P., Hsu, E.L., and Bradfield, C.A. 2008. Abnormal liver development and resistance to 2,3,7,8-tetrachlorodibenzo-p-dioxin toxicity in mice carrying a mutation in the DNA-binding domain of the aryl hydrocarbon receptor. *Toxicol Sci* 106:83-92.
33. Safe, S., and Wormke, M. 2003. Inhibitory aryl hydrocarbon receptor-estrogen receptor alpha cross-talk and mechanisms of action. *Chem Res Toxicol* 16:807-816.
34. Cohen, J.C., Horton, J.D., and Hobbs, H.H. 2011. Human fatty liver disease: old questions and new insights. *Science* 332:1519-1523.
35. Nguyen, P., Leray, V., Diez, M., Serisier, S., Le Bloc'h, J., Siliart, B., and Dumon, H. 2008. Liver lipid metabolism. *Journal of animal physiology and animal nutrition* 92:272-283.
36. Utzschneider, K.M., and Kahn, S.E. 2006. Review: The role of insulin resistance in nonalcoholic fatty liver disease. *The Journal of clinical endocrinology and metabolism* 91:4753-4761.
37. Tilg, H., and Moschen, A.R. 2008. Inflammatory mechanisms in the regulation of insulin resistance. *Molecular medicine* 14:222-231.
38. Potter, C.L., Menahan, L.A., and Peterson, R.E. 1986. Relationship of alterations in energy metabolism to hypophagia in rats treated with 2,3,7,8-tetrachlorodibenzo-p-dioxin. *Fundam Appl Toxicol* 6:89-97.
39. Albro, P.W., Corbett, J.T., Harris, M., and Lawson, L.D. 1978. Effects of 2,3,7,8-tetrachlorodibenzo-p-dioxin on lipid profiles in tissue of the Fischer rat. *Chem Biol Interact* 23:315-330.
40. Kohli, K.K., Gupta, B.N., Albro, P.W., Mukhtar, H., and McKinney, J.D. 1979. Biochemical effects of pure isomers of hexachlorobiphenyl: fatty livers and cell structure. *Chem Biol Interact* 25:139-156.
41. Jones, G., and Greig, J.B. 1975. Pathological changes in the liver of mice given 2,3,7,8-tetrachlorodibenzo-p-dioxin. *Experientia* 31:1315-1317.

42. Lee, C.C., Yao, Y.J., Chen, H.L., Guo, Y.L., and Su, H.J. 2006. Fatty liver and hepatic function for residents with markedly high serum PCDD/Fs levels in Taiwan. *Journal of toxicology and environmental health. Part A* 69:367-380.
43. Hinton, D.E., Glaumann, H., and Trump, B.F. 1978. Studies on the cellular toxicity of polychlorinated biphenyls (PCBs). I. Effect of PCBs on microsomal enzymes and on synthesis and turnover of microsomal and cytoplasmic lipids of rat liver- a morphological and biochemical study. *Virchows Arch B Cell Pathol* 27:279-306.
44. Gorski, J.R., Weber, L.W., and Rozman, K. 1988. Tissue-specific alterations of de novo fatty acid synthesis in 2,3,7,8-tetrachlorodibenzo-p-dioxin (TCDD)-treated rats. *Arch Toxicol* 62:146-151.
45. Lakshman, M.R., Ghosh, P., and Chirtel, S.J. 1991. Mechanism of action of 2,3,7,8-tetrachlorodibenzo-p-dioxin on intermediary metabolism in the rat. *J Pharmacol Exp Ther* 258:317-319.
46. Tanos, R., Murray, I.A., Smith, P.B., Patterson, A., and Perdew, G.H. 2012. Role of the Ah receptor in homeostatic control of fatty acid synthesis in the liver. *Toxicol Sci* 129:372-379.
47. Lakshman, M.R., Campbell, B.S., Chirtel, S.J., and Ekarohita, N. 1988. Effects of 2,3,7,8-tetrachlorodibenzo-p-dioxin (TCDD) on de novo fatty acid and cholesterol synthesis in the rat. *Lipids* 23:904-906.
48. Fletcher, N., Wahlstrom, D., Lundberg, R., Nilsson, C.B., Nilsson, K.C., Stockling, K., Hellmold, H., and Hakansson, H. 2005. 2,3,7,8-Tetrachlorodibenzo-p-dioxin (TCDD) alters the mRNA expression of critical genes associated with cholesterol metabolism, bile acid biosynthesis, and bile transport in rat liver: a microarray study. *Toxicol Appl Pharmacol* 207:1-24.
49. Lee, J.H., Wada, T., Febbraio, M., He, J., Matsubara, T., Lee, M.J., Gonzalez, F.J., and Xie, W. 2010. A novel role for the dioxin receptor in fatty acid metabolism and hepatic steatosis. *Gastroenterology* 139:653-663.
50. Kawano, Y., Nishiumi, S., Tanaka, S., Nobutani, K., Miki, A., Yano, Y., Seo, Y., Kutsumi, H., Ashida, H., Azuma, T., et al. 2010. Activation of the aryl hydrocarbon receptor induces hepatic steatosis via the upregulation of fatty acid transport. *Arch Biochem Biophys* 504:221-227.
51. Tilg, H., and Moschen, A.R. 2010. Evolution of inflammation in nonalcoholic fatty liver disease: the multiple parallel hits hypothesis. *Hepatology* 52:1836-1846.
52. He, J., Hu, B., Shi, X., Weidert, E.R., Lu, P., Xu, M., Huang, M., Kelley, E.E., and Xie, W. 2013. Activation of the aryl hydrocarbon receptor sensitizes mice to nonalcoholic steatohepatitis by deactivating mitochondrial sirtuin deacetylase Sirt3. *Mol Cell Biol* 33:2047-2055.
53. Lu, H., Cui, W., and Klaassen, C.D. 2011. Nrf2 protects against 2,3,7,8-tetrachlorodibenzo-p-dioxin (TCDD)-induced oxidative injury and steatohepatitis. *Toxicol Appl Pharmacol* 256:122-135.
54. Nebert, D.W., Roe, A.L., Dieter, M.Z., Solis, W.A., Yang, Y., and Dalton, T.P. 2000. Role of the aromatic hydrocarbon receptor and [Ah] gene battery in the oxidative stress response, cell cycle control, and apoptosis. *Biochem Pharmacol* 59:65-85.
55. Remillard, R.B., and Bunce, N.J. 2002. Linking dioxins to diabetes: epidemiology and biologic plausibility. *Environ Health Perspect* 110:853-858.

56. Henriksen, G.L., Ketchum, N.S., Michalek, J.E., and Swaby, J.A. 1997. Serum dioxin and diabetes mellitus in veterans of Operation Ranch Hand. *Epidemiology* 8:252-258.
57. Matsumura, F. 1995. Mechanism of action of dioxin-type chemicals, pesticides, and other xenobiotics affecting nutritional indexes. *Am J Clin Nutr* 61:695S-701S.
58. Enan, E., Liu, P.C., and Matsumura, F. 1992. 2,3,7,8-Tetrachlorodibenzo-p-dioxin causes reduction of glucose transporting activities in the plasma membranes of adipose tissue and pancreas from the guinea pig. *J Biol Chem* 267:19785-19791.
59. Enan, E., Liu, P.C., and Matsumura, F. 1992. TCDD (2,3,7,8-tetrachlorodibenzo-P-dioxin) causes reduction in glucose uptake through glucose transporters on the plasma membrane of the guinea pig adipocyte. *J Environ Sci Health B* 27:495-510.
60. Kern, P.A., Dicker-Brown, A., Said, S.T., Kennedy, R., and Fonseca, V.A. 2002. The stimulation of tumor necrosis factor and inhibition of glucose transport and lipoprotein lipase in adipose cells by 2,3,7,8-tetrachlorodibenzo-p-dioxin. *Metabolism* 51:65-68.
61. Liu, P.C., and Matsumura, F. 1995. Differential effects of 2,3,7,8-tetrachlorodibenzo-p-dioxin on the "adipose- type" and "brain-type" glucose transporters in mice. *Mol Pharmacol* 47:65-73.
62. Weber, L.W., Lebofsky, M., Stahl, B.U., Gorski, J.R., Muzi, G., and Rozman, K. 1991. Reduced activities of key enzymes of gluconeogenesis as possible cause of acute toxicity of 2,3,7,8-tetrachlorodibenzo-p-dioxin (TCDD) in rats. *Toxicology* 66:133-144.
63. Cranmer, M., Louie, S., Kennedy, R.H., Kern, P.A., and Fonseca, V.A. 2000. Exposure to 2,3,7,8-tetrachlorodibenzo-p-dioxin (TCDD) is associated with hyperinsulinemia and insulin resistance. *Toxicol Sci* 56:431-436.
64. Ebner, K., Brewster, D.W., and Matsumura, F. 1988. Effects of 2,3,7,8-tetrachlorodibenzo-p-dioxin on serum insulin and glucose levels in the rabbit. *J Environ Sci Health B* 23:427-438.
65. Xu, C.X., Wang, C., Zhang, Z.M., Jaeger, C.D., Krager, S.L., Bottum, K.M., Liu, J., Liao, D.F., and Tischkau, S.A. 2015. Aryl hydrocarbon receptor deficiency protects mice from diet-induced adiposity and metabolic disorders through increased energy expenditure. *International Journal of Obesity* 39:1300-1309.
66. Wang, C., Xu, C.X., Krager, S.L., Bottum, K.M., Liao, D.F., and Tischkau, S.A. 2011. Aryl hydrocarbon receptor deficiency enhances insulin sensitivity and reduces PPAR-alpha pathway activity in mice. *Environmental Health Perspectives* 119:1739-1744.
67. Reisz-Porszasz, S., Probst, M.R., Fukunaga, B.N., and Hankinson, O. 1994. Identification of functional domains of the aryl hydrocarbon receptor nuclear translocator protein (ARNT). *Mol Cell Biol* 14:6075-6086.
68. Gunton, J.E., Kulkarni, R.N., Yim, S., Okada, T., Hawthorne, W.J., Tseng, Y.H., Roberson, R.S., Ricordi, C., O'Connell, P.J., Gonzalez, F.J., et al. 2005. Loss of ARNT/HIF1beta mediates altered gene expression and pancreatic-islet dysfunction in human type 2 diabetes. *Cell* 122:337-349.
69. Wang, X.L., Suzuki, R., Lee, K., Tran, T., Gunton, J.E., Saha, A.K., Patti, M.E., Goldfine, A., Ruderman, N.B., Gonzalez, F.J., et al. 2009. Ablation of ARNT/HIF1beta in liver alters gluconeogenesis, lipogenic gene expression, and serum ketones. *Cell Metab* 9:428-439.
70. Haidari, M., Leung, N., Mahbub, F., Uffelman, K.D., Kohen-Avramoglu, R., Lewis, G.F., and Adeli, K. 2002. Fasting and postprandial overproduction of intestinally derived lipoproteins in an animal model of insulin resistance. Evidence that chronic fructose

feeding in the hamster is accompanied by enhanced intestinal de novo lipogenesis and ApoB48-containing lipoprotein overproduction. *J Biol Chem* 277:31646-31655.

71. Federico, L.M., Naples, M., Taylor, D., and Adeli, K. 2006. Intestinal insulin resistance and aberrant production of apolipoprotein B48 lipoproteins in an animal model of insulin resistance and metabolic dyslipidemia: evidence for activation of protein tyrosine phosphatase-1B, extracellular signal-related kinase, and sterol regulatory element-binding protein-1c in the fructose-fed hamster intestine. *Diabetes* 55:1316-1326.
72. 1997. IARC Working Group on the Evaluation of Carcinogenic Risks to Humans: Polychlorinated Dibenzo-Para-Dioxins and Polychlorinated Dibenzofurans. Lyon, France, 4-11 February 1997. *IARC Monogr Eval Carcinog Risks Hum* 69:1-631.
73. Geusau, A., Abraham, K., Geissler, K., Sator, M.O., Stingl, G., and Tschachler, E. 2001. Severe 2,3,7,8-tetrachlorodibenzo-p-dioxin (TCDD) intoxication: clinical and laboratory effects. *Environ Health Perspect* 109:865-869.
74. Martin, J.V. 1984. Lipid abnormalities in workers exposed to dioxin. *Br J Ind Med* 41:254-256.
75. Pelclova, D., Fenclova, Z., Preiss, J., Prochazka, B., Spacil, J., Dubska, Z., Okrouhlik, B., Lukas, E., and Urban, P. 2002. Lipid metabolism and neuropsychological follow-up study of workers exposed to 2,3,7,8- tetrachlordibenzo- p-dioxin. *Int Arch Occup Environ Health* 75 Suppl:S60-66.
76. Brewster, D.W., Bombick, D.W., and Matsumura, F. 1988. Rabbit serum hypertriglyceridemia after administration of 2,3,7,8-tetrachlorodibenzo-p-dioxin (TCDD). *J Toxicol Environ Health* 25:495-507.
77. Minami, K., Nakajima, M., Fujiki, Y., Katoh, M., Gonzalez, F.J., and Yokoi, T. 2008. Regulation of insulin-like growth factor binding protein-1 and lipoprotein lipase by the aryl hydrocarbon receptor. *J Toxicol Sci* 33:405-413.
78. Swift, L.L., Gasiewicz, T.A., Dunn, G.D., Soule, P.D., and Neal, R.A. 1981. Characterization of the hyperlipidemia in guinea pigs induced by 2,3,7,8-tetrachlorodibenzo-p-dioxin. *Toxicol Appl Pharmacol* 59:489-499.
79. Brewster, D.W., and Matsumura, F. 1984. TCDD (2,3,7,8-tetrachlorodibenzo-p-dioxin) reduces lipoprotein lipase activity in the adipose tissue of the guinea pig. *Biochem Biophys Res Commun* 122:810-817.
80. Bombick, D.W., Matsumura, F., and Madhukar, B.V. 1984. TCDD (2,3,7,8-tetrachlorodibenzo-p-dioxin) causes reduction in the low density lipoprotein (LDL) receptor activities in the hepatic plasma membrane of the guinea pig and rat. *Biochem Biophys Res Commun* 118:548-554.
81. Cheng, X., Vispute, S.G., Liu, J., Cheng, C., Kharitonenkov, A., and Klaassen, C.D. 2014. Fibroblast growth factor (Fgf) 21 is a novel target gene of the aryl hydrocarbon receptor (AhR). *Toxicol Appl Pharmacol* 278:65-71.
82. Kliewer, S.A., and Mangelsdorf, D.J. 2010. Fibroblast growth factor 21: from pharmacology to physiology. *Am J Clin Nutr* 91:254S-257S.
83. Badman, M.K., Pissios, P., Kennedy, A.R., Koukos, G., Flier, J.S., and Maratos-Flier, E. 2007. Hepatic fibroblast growth factor 21 is regulated by PPARalpha and is a key mediator of hepatic lipid metabolism in ketotic states. *Cell Metab* 5:426-437.
84. Inagaki, T., Dutchak, P., Zhao, G., Ding, X., Gautron, L., Parameswara, V., Li, Y., Goetz, R., Mohammadi, M., Esser, V., et al. 2007. Endocrine regulation of the fasting response by PPARalpha-mediated induction of fibroblast growth factor 21. *Cell Metab* 5:415-425.

85. Kharitonenkov, A., Shiyanova, T.L., Koester, A., Ford, A.M., Micanovic, R., Galbreath, E.J., Sandusky, G.E., Hammond, L.J., Moyers, J.S., Owens, R.A., et al. 2005. FGF-21 as a novel metabolic regulator. *J Clin Invest* 115:1627-1635.
86. Ding, X., Boney-Montoya, J., Owen, B.M., Bookout, A.L., Coate, K.C., Mangelsdorf, D.J., and Kliewer, S.A. 2012. betaKlotho is required for fibroblast growth factor 21 effects on growth and metabolism. *Cell Metab* 16:387-393.
87. Lin, Z., Tian, H., Lam, K.S., Lin, S., Hoo, R.C., Konishi, M., Itoh, N., Wang, Y., Bornstein, S.R., Xu, A., et al. 2013. Adiponectin mediates the metabolic effects of FGF21 on glucose homeostasis and insulin sensitivity in mice. *Cell Metab* 17:779-789.
88. Zhou, J., Zhai, Y., Mu, Y., Gong, H., Uppal, H., Toma, D., Ren, S., Evans, R.M., and Xie, W. 2006. A novel pregnane X receptor-mediated and sterol regulatory element-binding protein-independent lipogenic pathway. *J Biol Chem* 281:15013-15020.
89. Gao, J., He, J., Zhai, Y., Wada, T., and Xie, W. 2009. The constitutive androstane receptor is an anti-obesity nuclear receptor that improves insulin sensitivity. *J Biol Chem* 284:25984-25992.
90. McGuire, J., Okamoto, K., Whitelaw, M.L., Tanaka, H., and Poellinger, L. 2001. Definition of a dioxin receptor mutant that is a constitutive activator of transcription: delineation of overlapping repression and ligand binding functions within the PAS domain. *J Biol Chem* 276:41841-41849.
91. DeFronzo, R.A., Tobin, J.D., and Andres, R. 1979. Glucose clamp technique: a method for quantifying insulin secretion and resistance. *The American journal of physiology* 237:E214-223.
92. Heilbronn, L.K., and Campbell, L.V. 2008. Adipose tissue macrophages, low grade inflammation and insulin resistance in human obesity. *Current pharmaceutical design* 14:1225-1230.
93. Maeda, N., Shimomura, I., Kishida, K., Nishizawa, H., Matsuda, M., Nagaretani, H., Furuyama, N., Kondo, H., Takahashi, M., Arita, Y., et al. 2002. Diet-induced insulin resistance in mice lacking adiponectin/ACRP30. *Nat Med* 8:731-737.
94. Zhang, B.B., Zhou, G., and Li, C. 2009. AMPK: an emerging drug target for diabetes and the metabolic syndrome. *Cell Metab* 9:407-416.
95. Yamauchi, T., Kamon, J., Minokoshi, Y., Ito, Y., Waki, H., Uchida, S., Yamashita, S., Noda, M., Kita, S., Ueki, K., et al. 2002. Adiponectin stimulates glucose utilization and fatty-acid oxidation by activating AMP-activated protein kinase. *Nat Med* 8:1288-1295.
96. Itoh, N. 2014. FGF21 as a Hepatokine, Adipokine, and Myokine in Metabolism and Diseases. *Frontiers in endocrinology* 5:107.
97. Erion, D.M., and Shulman, G.I. 2010. Diacylglycerol-mediated insulin resistance. *Nat Med* 16:400-402.
98. Summers, S.A. 2006. Ceramides in insulin resistance and lipotoxicity. *Prog Lipid Res* 45:42-72.
99. Chau, M.D., Gao, J., Yang, Q., Wu, Z., and Gromada, J. 2010. Fibroblast growth factor 21 regulates energy metabolism by activating the AMPK-SIRT1-PGC-1alpha pathway. *Proc Natl Acad Sci U S A* 107:12553-12558.
100. Sun, Z., Miller, R.A., Patel, R.T., Chen, J., Dhir, R., Wang, H., Zhang, D., Graham, M.J., Unterman, T.G., Shulman, G.I., et al. 2012. Hepatic Hdac3 promotes gluconeogenesis by repressing lipid synthesis and sequestration. *Nat Med* 18:934-942.

101. Monetti, M., Levin, M.C., Watt, M.J., Sajan, M.P., Marmor, S., Hubbard, B.K., Stevens, R.D., Bain, J.R., Newgard, C.B., Farese, R.V., Sr., et al. 2007. Dissociation of hepatic steatosis and insulin resistance in mice overexpressing DGAT in the liver. *Cell Metab* 6:69-78.
102. Arkan, M.C., Hevener, A.L., Greten, F.R., Maeda, S., Li, Z.W., Long, J.M., Wynshaw-Boris, A., Poli, G., Olefsky, J., and Karin, M. 2005. IKK-beta links inflammation to obesity-induced insulin resistance. *Nat Med* 11:191-198.
103. Potthoff, M.J., Inagaki, T., Satapati, S., Ding, X., He, T., Goetz, R., Mohammadi, M., Finck, B.N., Mangelsdorf, D.J., Kliewer, S.A., et al. 2009. FGF21 induces PGC-1alpha and regulates carbohydrate and fatty acid metabolism during the adaptive starvation response. *Proc Natl Acad Sci U S A* 106:10853-10858.
104. Fisher, F.M., Chui, P.C., Nasser, I.A., Popov, Y., Cunniff, J.C., Lundasen, T., Kharitonenkov, A., Schuppan, D., Flier, J.S., and Maratos-Flier, E. 2014. Fibroblast growth factor 21 limits lipotoxicity by promoting hepatic fatty acid activation in mice on methionine and choline-deficient diets. *Gastroenterology* 147:1073-1083 e1076.
105. Fernandez-Salguero, P.M., Hilbert, D.M., Rudikoff, S., Ward, J.M., and Gonzalez, F.J. 1996. Aryl-hydrocarbon receptor-deficient mice are resistant to 2,3,7,8-tetrachlorodibenzo-p-dioxin-induced toxicity. *Toxicol Appl Pharmacol* 140:173-179.
106. Nguyen, L.P., and Bradfield, C.A. 2008. The search for endogenous activators of the aryl hydrocarbon receptor. *Chem Res Toxicol* 21:102-116.
107. Ohtake, F., Baba, A., Takada, I., Okada, M., Iwasaki, K., Miki, H., Takahashi, S., Kouzmenko, A., Nohara, K., Chiba, T., et al. 2007. Dioxin receptor is a ligand-dependent E3 ubiquitin ligase. *Nature* 446:562-566.
108. Boitano, A.E., Wang, J., Romeo, R., Bouchez, L.C., Parker, A.E., Sutton, S.E., Walker, J.R., Flaveny, C.A., Perdew, G.H., Denison, M.S., et al. 2010. Aryl hydrocarbon receptor antagonists promote the expansion of human hematopoietic stem cells. *Science* 329:1345-1348.
109. Linden, J., Lensu, S., and Pohjanvirta, R. 2014. Effect of 2,3,7,8-tetrachlorodibenzo-p-dioxin (TCDD) on hormones of energy balance in a TCDD-sensitive and a TCDD-resistant rat strain. *International journal of molecular sciences* 15:13938-13966.
110. Ye, D., Wang, Y., Li, H., Jia, W., Man, K., Lo, C.M., Lam, K.S., and Xu, A. 2014. Fibroblast growth factor 21 protects against acetaminophen-induced hepatotoxicity by potentiating peroxisome proliferator-activated receptor coactivator protein-1alpha-mediated antioxidant capacity in mice. *Hepatology* 60:977-989.
111. Fisher, F.M., Chui, P.C., Antonellis, P.J., Bina, H.A., Kharitonenkov, A., Flier, J.S., and Maratos-Flier, E. 2010. Obesity is a fibroblast growth factor 21 (FGF21)-resistant state. *Diabetes* 59:2781-2789.
112. Safe, S., Lee, S.O., and Jin, U.H. 2013. Role of the aryl hydrocarbon receptor in carcinogenesis and potential as a drug target. *Toxicol Sci* 135:1-16.
113. Kennedy, G.D., Nukaya, M., Moran, S.M., Glover, E., Weinberg, S., Balbo, S., Hecht, S.S., Pitot, H.C., Drinkwater, N.R., and Bradfield, C.A. 2014. Liver tumor promotion by 2,3,7,8-tetrachlorodibenzo-p-dioxin is dependent on the aryl hydrocarbon receptor and TNF/IL-1 receptors. *Toxicol Sci* 140:135-143.
114. Moennikes, O., Loeppen, S., Buchmann, A., Andersson, P., Ittrich, C., Poellinger, L., and Schwarz, M. 2004. A constitutively active dioxin/aryl hydrocarbon receptor promotes hepatocarcinogenesis in mice. *Cancer Res* 64:4707-4710.

115. Fan, Y., Boivin, G.P., Knudsen, E.S., Nebert, D.W., Xia, Y., and Puga, A. 2010. The aryl hydrocarbon receptor functions as a tumor suppressor of liver carcinogenesis. *Cancer Res* 70:212-220.
116. Naugler, W.E., Sakurai, T., Kim, S., Maeda, S., Kim, K., Elsharkawy, A.M., and Karin, M. 2007. Gender disparity in liver cancer due to sex differences in MyD88-dependent IL-6 production. *Science* 317:121-124.
117. Ma, Q., and Whitlock, J.P., Jr. 1996. The aromatic hydrocarbon receptor modulates the Hepa 1c1c7 cell cycle and differentiated state independently of dioxin. *Mol Cell Biol* 16:2144-2150.
118. Abdelrahim, M., Smith, R., 3rd, and Safe, S. 2003. Aryl hydrocarbon receptor gene silencing with small inhibitory RNA differentially modulates Ah-responsiveness in MCF-7 and HepG2 cancer cells. *Mol Pharmacol* 63:1373-1381.
119. Ambolet-Camoit, A., Bui, L.C., Pierre, S., Chevallier, A., Marchand, A., Coumoul, X., Garlatti, M., Andreau, K., Barouki, R., and Aggerbeck, M. 2010. 2,3,7,8-tetrachlorodibenzo-p-dioxin counteracts the p53 response to a genotoxicant by upregulating expression of the metastasis marker agr2 in the hepatocarcinoma cell line HepG2. *Toxicol Sci* 115:501-512.
120. Tomkiewicz, C., Herry, L., Bui, L.C., Metayer, C., Bourdeloux, M., Barouki, R., and Coumoul, X. 2013. The aryl hydrocarbon receptor regulates focal adhesion sites through a non-genomic FAK/Src pathway. *Oncogene* 32:1811-1820.
121. Puga, A., Barnes, S.J., Dalton, T.P., Chang, C., Knudsen, E.S., and Maier, M.A. 2000. Aromatic hydrocarbon receptor interaction with the retinoblastoma protein potentiates repression of E2F-dependent transcription and cell cycle arrest. *J Biol Chem* 275:2943-2950.
122. Huang, G., and Elferink, C.J. 2005. Multiple mechanisms are involved in Ah receptor-mediated cell cycle arrest. *Mol Pharmacol* 67:88-96.
123. Puga, A., Ma, C., and Marlowe, J.L. 2009. The aryl hydrocarbon receptor cross-talks with multiple signal transduction pathways. *Biochem Pharmacol* 77:713-722.
124. Bock, K.W., and Kohle, C. 2005. Ah receptor- and TCDD-mediated liver tumor promotion: clonal selection and expansion of cells evading growth arrest and apoptosis. *Biochem Pharmacol* 69:1403-1408.
125. Marlowe, J.L., and Puga, A. 2005. Aryl hydrocarbon receptor, cell cycle regulation, toxicity, and tumorigenesis. *J Cell Biochem* 96:1174-1184.
126. Shimizu, Y., Nakatsuru, Y., Ichinose, M., Takahashi, Y., Kume, H., Mimura, J., Fujii-Kuriyama, Y., and Ishikawa, T. 2000. Benzo[a]pyrene carcinogenicity is lost in mice lacking the aryl hydrocarbon receptor. *Proc Natl Acad Sci U S A* 97:779-782.
127. Shimada, T., and Fujii-Kuriyama, Y. 2004. Metabolic activation of polycyclic aromatic hydrocarbons to carcinogens by cytochromes P450 1A1 and 1B1. *Cancer Sci* 95:1-6.
128. Chen, S., Nguyen, N., Tamura, K., Karin, M., and Tukey, R.H. 2003. The role of the Ah receptor and p38 in benzo[a]pyrene-7,8-dihydrodiol and benzo[a]pyrene-7,8-dihydrodiol-9,10-epoxide-induced apoptosis. *J Biol Chem* 278:19526-19533.
129. Cole, P., Trichopoulos, D., Pastides, H., Starr, T., and Mandel, J.S. 2003. Dioxin and cancer: a critical review. *Regulatory toxicology and pharmacology : RTP* 38:378-388.
130. Ema, M., Ohe, N., Suzuki, M., Mimura, J., Sogawa, K., Ikawa, S., and Fujii-Kuriyama, Y. 1994. Dioxin binding activities of polymorphic forms of mouse and human arylhydrocarbon receptors. *J Biol Chem* 269:27337-27343.

131. Flaveny, C.A., and Perdew, G.H. 2009. Transgenic Humanized AHR Mouse Reveals Differences between Human and Mouse AHR Ligand Selectivity. *Molecular and cellular pharmacology* 1:119-123.
132. Flaveny, C.A., Murray, I.A., and Perdew, G.H. 2010. Differential gene regulation by the human and mouse aryl hydrocarbon receptor. *Toxicol Sci* 114:217-225.
133. Lu, P., Yan, J., Liu, K., Garbacz, W.G., Wang, P., Xu, M., Ma, X., and Xie, W. 2015. Activation of aryl hydrocarbon receptor dissociates fatty liver from insulin resistance by inducing fibroblast growth factor 21. *Hepatology* 61:1908-1919.
134. Tian, J., Huang, H., Hoffman, B., Liebermann, D.A., Ledda-Columbano, G.M., Columbano, A., and Locker, J. 2011. Gadd45beta is an inducible coactivator of transcription that facilitates rapid liver growth in mice. *J Clin Invest* 121:4491-4502.
135. Scholzen, T., and Gerdes, J. 2000. The Ki-67 protein: from the known and the unknown. *Journal of cellular physiology* 182:311-322.
136. Balkwill, F., and Mantovani, A. 2001. Inflammation and cancer: back to Virchow? *Lancet* 357:539-545.
137. Pikarsky, E., Porat, R.M., Stein, I., Abramovitch, R., Amit, S., Kasem, S., Gutkovich-Pyest, E., Urieli-Shoval, S., Galun, E., and Ben-Neriah, Y. 2004. NF-kappaB functions as a tumour promoter in inflammation-associated cancer. *Nature* 431:461-466.
138. Reuter, S., Gupta, S.C., Chaturvedi, M.M., and Aggarwal, B.B. 2010. Oxidative stress, inflammation, and cancer: how are they linked? *Free radical biology & medicine* 49:1603-1616.
139. Wen, C.P., Lin, J., Yang, Y.C., Tsai, M.K., Tsao, C.K., Etzel, C., Huang, M., Hsu, C.Y., Ye, Y., Mishra, L., et al. 2012. Hepatocellular carcinoma risk prediction model for the general population: the predictive power of transaminases. *Journal of the National Cancer Institute* 104:1599-1611.
140. Deshpande, A., Sicinski, P., and Hinds, P.W. 2005. Cyclins and cdks in development and cancer: a perspective. *Oncogene* 24:2909-2915.
141. Levens, D. 2002. Disentangling the MYC web. *Proc Natl Acad Sci U S A* 99:5757-5759.
142. Cole, M.D., and McMahon, S.B. 1999. The Myc oncoprotein: a critical evaluation of transactivation and target gene regulation. *Oncogene* 18:2916-2924.
143. Papa, S., Zazzeroni, F., Fu, Y.X., Bubici, C., Alvarez, K., Dean, K., Christiansen, P.A., Anders, R.A., and Franzoso, G. 2008. Gadd45beta promotes hepatocyte survival during liver regeneration in mice by modulating JNK signaling. *J Clin Invest* 118:1911-1923.
144. Wang, L., Xiao, X., Li, D., Chi, Y., Wei, P., Wang, Y., Ni, S., Tan, C., Zhou, X., and Du, X. 2012. Abnormal expression of GADD45B in human colorectal carcinoma. *Journal of translational medicine* 10:215.
145. Qiu, W., Zhou, B., Zou, H., Liu, X., Chu, P.G., Lopez, R., Shih, J., Chung, C., and Yen, Y. 2004. Hypermethylation of growth arrest DNA damage-inducible gene 45 beta promoter in human hepatocellular carcinoma. *Am J Pathol* 165:1689-1699.
146. Yi, Y.W., Kim, D., Jung, N., Hong, S.S., Lee, H.S., and Bae, I. 2000. Gadd45 family proteins are coactivators of nuclear hormone receptors. *Biochem Biophys Res Commun* 272:193-198.
147. Yamamoto, Y., and Negishi, M. 2008. The antiapoptotic factor growth arrest and DNA-damage-inducible 45 beta regulates the nuclear receptor constitutive active/androstane receptor-mediated transcription. *Drug metabolism and disposition: the biological fate of chemicals* 36:1189-1193.

148. Hankinson, O. 2005. Role of coactivators in transcriptional activation by the aryl hydrocarbon receptor. *Arch Biochem Biophys* 433:379-386.
149. Beischlag, T.V., Wang, S., Rose, D.W., Torchia, J., Reisz-Porszasz, S., Muhammad, K., Nelson, W.E., Probst, M.R., Rosenfeld, M.G., and Hankinson, O. 2002. Recruitment of the NCoA/SRC-1/p160 family of transcriptional coactivators by the aryl hydrocarbon receptor/aryl hydrocarbon receptor nuclear translocator complex. *Mol Cell Biol* 22:4319-4333.
150. Moriguchi, T., Motohashi, H., Hosoya, T., Nakajima, O., Takahashi, S., Ohsako, S., Aoki, Y., Nishimura, N., Tohyama, C., Fujii-Kuriyama, Y., et al. 2003. Distinct response to dioxin in an arylhydrocarbon receptor (AHR)-humanized mouse. *Proc Natl Acad Sci U S A* 100:5652-5657.
151. Sheikh, M.S., Hollander, M.C., and Fornance, A.J., Jr. 2000. Role of Gadd45 in apoptosis. *Biochem Pharmacol* 59:43-45.
152. Kodama, S., and Negishi, M. 2011. Pregnane X receptor PXR activates the GADD45beta gene, eliciting the p38 MAPK signal and cell migration. *J Biol Chem* 286:3570-3578.